Modelling Hydrogen in Power Systems

Optimisation for Investment and Operational Models

Yavuz Cinek

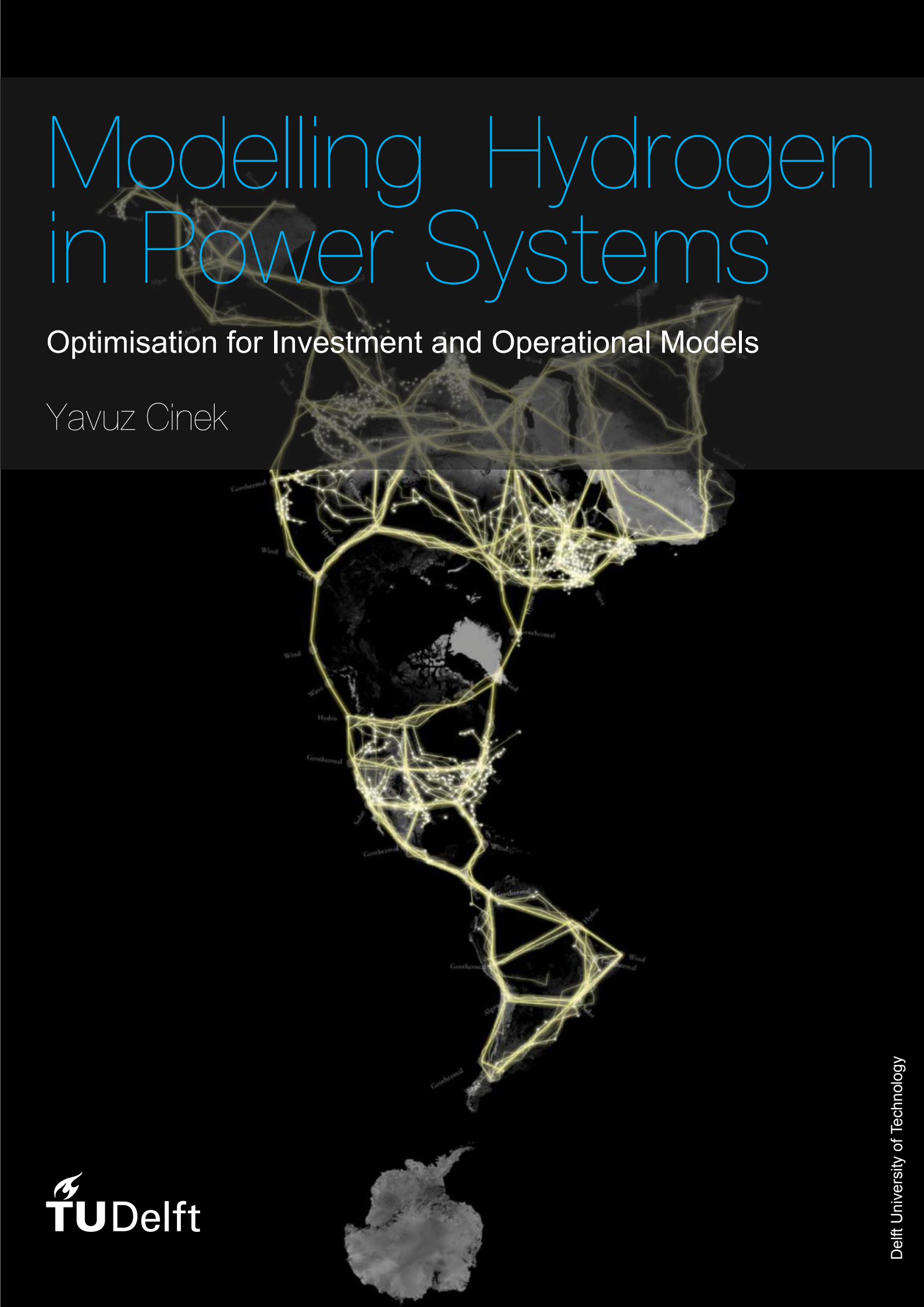

TU Delft

Delft University of Technology

The cover photo is an adoption from 'The Energy Report' composed by WWF - AMO - Ecofys (2011) and resembles an artistic impression of a future *'World Energy Grid'*.

Modelling Hydrogen in Power Systems

Optimisation for Investment and Operational Models

by

Yavuz Cinek

to obtain the degree of Master of Science in Sustainable Energy Technology
at Delft University of Technology,
to be defended publicly on Friday August 26th, 2022 at 10:30 AM.

Student number:	4205804		
Project duration:	01 June 2021 – 26 August 2022		
Thesis committee:	Prof. dr. P. Palensky	TU Delft - IEPG	Chair of Committee
	Dr. G. Morales-España	TNO	Daily supervisor
	Dr. M. Cvetković	TU Delft - IEPG	Supervisor
	Dr. H. Ziar	TU Delft - PVMD	External Committee Member

TU Delft TNO

Preface

With fossil fuels expected to deplete soon, polar ice melting faster than any predictions uphold and our tiny home in The Netherlands under sea level, it is always in your face. Following any news outlets, opening the television or having a conversation with friends and family only adds a top of it, our craving for a 'transition'. More specifically the transition towards a new 'green' way of generating and consuming energy: the energy transition!

With this research, performed for both TNO and the Technical University of Delft, I was able to contribute to the energy transition. It was one of the biggest challenges of my life, working on an academic project on my own, and trying to put forward a new and innovative branch of research. In the meantime having started my full-time job, it resulted in many lessons learned and challenges overcome.

My dream since childhood is to be an engineer! I always wanted to contribute to societal problems with an engineering mindset: analysing and solving problems. With the completion of my Master's Thesis, the crown of a long journey of studies in Delft, the confidence to say I have the required 'engineering mindset' is finally there!

Therefore, I want to take this opportunity to thank first and foremost my supervisors: Dr. Germán Morales-España from TNO and Dr. Miloš Cvetković from TUD for their support during the whole Thesis period and for making this dream become reality. Especially Germán, who has supported me on so many occasions and helped me get through the unsolvable! Thank you very much for all those meetings and support! Although not involved as a supervisor, but always open for guidance and feedback during the process, I want to thank ir. Hernandez-Serna and Dr. Janssen. Furthermore, I want to thank prof. Palensky and Dr. Ziar for their feedback during the final stretch of the research.

This journey was not made possible without my friends and family who have always supported me, in all possible kinds of ways. I hope I have made them proud by obtaining this Master's degree, paying back for all the love and support. Therefore, I want to thank my mother Fatma, father Ercan, and brothers and sisters Neşe, Nuray, Yunus and Yusuf Ahmet Selim. But also much gratitude and appreciation towards my dear friend Volkan, my parents-in-law Betül and Yaşar, and all the other relatives, family and close friends whom I want to thank!

Without her, especially during the whole thesis journey, it would not be possible. Always backing me, motivating me and helping wherever she could, I want to thank from the bottom of my heart, my wife Yasemin Simge Cinek-Şavlı for her unconditional love.

Yavuz Cinek
Delft, August 31, 2022

Abstract

The energy transition is one of the major challenges of the 21st century, impacting the way energy is generated, conserved and consumed. Energy generation becomes more and more decentralised, intermittency and fluctuations suddenly are becoming topics of interest within day-to-day life and energy system operators are facing many new obstacles never encountered before. In this context, the anticipation for hydrogen as a resource for energy conservation and -management is big. This research focuses on the optimisation of the hydrogen pathway for investment and operational models. The hydrogen pathway is divided into three sections: hydrogen generation with means of water electrolysis, also known as 'green hydrogen', storage in compression vessels and reconversion of hydrogen into electricity in the form of a fuel cell technology (also known as Power-to-Gas).

The research focuses on identifying technical parameters and operational policies of the hydrogen pathway with water electrolysis systems that can be translated into optimisation constraints, assessing the level of detail required to create an accurate optimisation model. A generic model is developed that can be scaled for further research, making different case studies and sizing possible. The research compares the performance of the models in terms of accuracy to the computational burden. The comparison is done for the level of detail and complexity added to the model.

After a literature review of technical parameters and operational policies regarding the technologies, two models were created in a mathematical framework. The models proposed were Linear Programming (LP) and a Mixed-Integer Programming (MIP) Model. Within the LP model six sensitivity analyses have been performed, to be precise on *Capital Expenditures (CAPEX), efficiency, lifetime, ramping rates, interest rates* and finally *different time horizons*. The outcome of these analyses is to invest within and operate technologies in a combined manner, whereby each component of technologies contributes towards minimising the objective value: the Total Annualised Cost. These are the effect of allotted constraints, such as the ramping constraint.

The LP and MIP combined framework led to the configuration of 16 different types of constraints. The constraints to be modelled were: minimum uptime and downtime, start-up costs, degradation due to cycling and the part-load operation. The most outstanding findings of the sensitivity analysis towards the MIP model and the 16 different configurations were:

- The impact of the start-up cost on the obtained results is limited. However, there is an extra computational complexity added to the optimisation model. Therefore, the start-up cost can be neglected when modelling larger data sets. Similarly, this advice does not uphold when the start-up trajectories have to be split in two, namely: warm and cold start-up trajectories, as this was not part of this research. The effects of such on the model and the obtained results are not assessed.
- Although the model becomes more precise and realistic with the implementation of the additional constraints, the TAC does not decrease, but on the contrary increases. Therefore, the constraints added, do add to the TAC as defined within the research.

As the time allotted to this research is limited and the optimisation formulation for hydrogen models can be extended relentlessly, there are elements left outside the scope of this research. Therefore, for future research, a smaller time horizon and sizing for components are proposed.

Nomenclature

Abbreviations & Acronyms

AEL	Alkaline Electrolyser Cell	[–]
AFC	Alkaline Fuel Cell	[–]
ATR	Autothermal Reforming	[–]
BoP	Balance of Plant	[–]
CAPEX	Capital Expenditures	[\$ kW^{-1}]
CAES	Compressed Air Energy Storage	[–]
CCS	Carbon Capture and Storage	[–]
DSO	Distribution System Operator	[–]
GHG	Green House Gas	[–]
HER	Hydrogen Evolution Reaction	[–]
HHV	Higher Heating Value	[$J\ mol^{-1}$]
H2tP	Hydrogen-to-Power	[–]
LHV	Lower Heating Value	[$J\ mol^{-1}$]
LP	Linear Programming	[–]
MIP	Mixed Integer Programming	[–]
OER	Oxygen Evolution Reaction	[–]
OPEX	Operation Expenditures	[\$ $kW^{-1}yr^{-1}$]
PEMEL	Proton Exchange Membrane Electrolyser Cell (also Polymer Electrolyte Membrane Electrolyser Cell)	[–]
PEMFC	Proton Exchange Membrane Fuel Cell	[–]
PtG	Power-to-Gas	[–]
PtL	Power-to-Liquid	[–]
PtH2	Power-to-Hydrogen	[–]
PtP	Power-to-Power	[–]
PV	Photovoltaic, converting light into energy	[–]
SMR	Steam Methane Reforming	[–]
SoC	State of Charge	[–]
SOEL	Solid Oxide Electrolyser Cell	[–]
SOFC	Solid Oxide Fuel Cell	[–]
SPE	Solid Polymer Electrolyser, different name for *PEMEL*	[–]
STP	Standard Temperature and Pressure, $T^0 = 298.15K = 20°C$ and $p^0 = 10^5 Pa = 1bar$ as defined by the International Union of Pure and Applied Chemistry	[–]
Syngas	Synthetic Gas, made from H_2 and CO	[–]
TAC	Total Annualised Costs (*the objective function of this research*)	[$M€\ y^{-1}$]

TNO	”Nederlandse Organisatie voor Toegepast Natuurwetenschappelijk Onderzoek” English: Netherlands Organisation for Applied Scientific Research	[–]
TRL	Technology Readiness Level	[–]
TSO	Transmission System Operator	[–]
UC	Unit Commitment	[–]
vRES	variable Renewable Energy Sources	[–]

Symbols

Chemical

CO	Carbon monoxide, a greenhouse gas	[–]
CO_2	Carbon dioxide, a greenhouse gas	[–]
e^-	Electrons	[–]
H	Hydrogen atom	[–]
H^+	Positively charged hydrogen atom, also proton or cations	[–]
H_2	Molecular hydrogen	[–]
$H_{2(g)}$	Molecular hydrogen in gaseous form	[–]
H_2O	Water	[–]
$H_2O_{(g)}$ / $H_2O_{(vap)}$	Water in gaseous form, thus vaporised or steam	[–]
$H_2O_{(l)}$	Water in liquid form	[–]
KOH	Potassium hydroxide	[–]
$NaOH$	Sodium hydroxide	[–]
Ni	Nickel	[–]
O_2	Dioxygen, referred to as oxygen	[–]
O^{-2}	Oxide	[–]
OH^-	Hydroxide ions	[–]
YSZ	Yttria-stabilised zirconia	[–]

Greek

α	Dimensionless charge transfer coefficient	[–]
Δ	Difference	[–]
ΔV	Overpotential	$[V]$
η	Efficiency	[%]
$\eta_{Academic}$	Electrolyser efficiency used within academic research	[%]
η_F	Faradaic cell efficiency	[%]
$\eta_{Industry}$	Electrolyser efficiency used within industry	$[kWh\ kg_{H_2}^{-1}$ or $kWh\ Nm_{H_2}^{-3}]$
$\eta_{Theoretical}$	Theoretical electrolyser efficiency	[%]
$\eta_{Thermal}$	Thermal efficiency electrolyser	[%]
$\eta_{Voltage}$	Voltage efficiency electrolyser	[%]

Latin

\$ or USD	United States Dollar	[–]
€	Euro	[–]
C_0	Reference concentration	$[mol\ m^{-3}]$
C_1	Concentration of flow through the electrolyser	$[mol\ m^{-3}]$
F	Faraday's constant, equal to $96,485$	$[C\ mol^{-1}]$
G	Gibbs free energy	$[J]$
G^0	Gibbs free energy at $20\ ^\circ C$ and $1\ bar$ and with pure reactants	$[J]$
H	Enthalpy	$[J]$
H^0	Reaction enthalpy for the formation of one mole of water, at $20\ ^\circ C$ and $1\ bar$	$[J]$
I	Current	$[A]$
j	Electrode current density	$[A\ m^{-2}]$
j_0	Exchange current density	$[A\ m^{-2}]$
n	Number of electrons exchanged during the electrochemical splitting of molecules	[#]
n_{cell}	Number of cells	[#]
p	Pressure	$[Pa]$
p_{H_2}	Partial pressure of hydrogen	$[Pa]$
p_{O_2}	Partial pressure of oxygen	$[Pa]$
p_{H_2O}	Partial pressure of water	$[Pa]$
P	Power, rate of doing work	$[W]$
Q	Thermal energy requirement	$[J]$
R	Ideal gas constant, equal to 8.314	$[J\ K^{-1}mol^{-1}]$
S	Entropy	$[J\ K^{-1}]$
S^0	Entropy, at $20\ ^\circ C$ and $1\ bar$	$[J\ K^{-1}]$
T	Temperature	$[K]$
U	Internal energy	$[J]$
U	Voltage	$[V]$
U_a	Anode cell potential	$[V]$
U_c	Cathode cell potential	$[V]$
U_{cell}	Operating cell potential voltage	$[V]$
U^0_{cell}	Operating cell potential voltage, at $20\ ^\circ C$ and $1\ bar$	$[V]$
U_{rev}	Reversible voltage	$[V]$
U^0_{rev}	Reversible voltage, at $20\ ^\circ C$ and $1\ bar$	$[V]$
U_{tn}	Thermoneutral voltage	$[V]$
V	Volume	$[m^3]$
$\dot{V}_{H_2}$	Hydrogen production rate or hydrogen volume flow	$[mol\ s^{-1}$ or $Nm^3\ h^{-1}]$
W_{rev}	Energy required to split one mole of water at open-circuit conditions $(I = 0)$	$[J\ mol^{-1}]$
W_{irrev}	Energy required to split one mole of water at close-circuit conditions $(I \neq 0)$	$[J\ mol^{-1}]$
–	Gravimetric energy density	$[MJ\ kg^{-1}]$
–	Normal Cubic Meter per hour, at $0\ ^\circ C$ and $1\ bar$	$[Nm^3\ h^{-1}]$

–	Standard Cubic Meter per hour, at $20\ ^{\circ}C$ and $1\ bar$	$[Nm^3\ h^{-1}]$
–	Reversible voltage, open-circuit voltage or equilibrium voltage	$[V]$
–	Weight fraction of a substance within the total mass	$[Wt\%]$

List of Figures

1.1 CO_2 concentration in the atmosphere, from the work of Friedlingstein et al. [5] 2
1.2 Global primary energy and electricity consumption by source in 2020, from the work of Ritchie et al. [7] 2
1.3 Levelised costs of energy for different variable Renewable Energy Sources, from the work of IRENA [9] 3
1.4 Total net electricity generation in July 2021 for The Netherlands, from Energy-Chart.info [11] 3
1.5 Hydrogen production pathways, from the work of IEA [14] 4
1.6 Levelised hydrogen production costs [$USD\ kg^{-1}$] for 2019 and predictions for 2060, from the work of IEA [15] 5
1.7 Schematic overview of the hydrogen reconversion pathway, from the work of Welder et al. [16] 6

2.1 Global hydrogen demand by sector in the Net Zero Scenario, 2020-2030, edited from IEA [39]. 11
2.2 Intermittent character of wind energy production shown over the year, from the work of Crotogino et al. [43] 12
2.3 Large scale storage utilisation timescale and size from the work of Crotogino et al. [43] 12
2.4 State-of-the-art production pathways of low-carbon hydrogen at scale, from the work of The Royal Society [48] 13
2.5 Temperature (a) and Pressure (b) effect on reversible cell voltage [47] 17
2.6 Polarization curve of the three main electrolyser technologies, from the work of Cavaliere et al. [47] 19
2.7 Cell behaviour as a function of the applied cell voltage, from the work of Cavaliere et al. [47] 21
2.8 Schematic system overview of Alkaline Electrolyser, from the work of Holst et al. [61] . 22
2.9 Schematic system overview of Proton Exchange Membrane Electrolyser, from the work of Holst et al. [61] 23
2.10 Schematic system overview of Solid Oxide Electrolyser Cell, from the work of Buttler et al. [56] 25
2.11 Comparative overview of the working principles of the AEL, PEMEL and SOEL, from the work of Sapountzi et al. [75] 27
2.12 Gravimetric energy density versus volumetric energy density for different types of fuel based on LHV, from the work of the U.S. Department of Energy [80] 28
2.13 Density of hydrogen gas ($kg\ m^{-3}$) compared to an ideal gas, at $T = 298K$, from the work of Mulder et al. [12] 29
2.14 Proposed hydrogen network by Gasunie [87] 31
2.15 Proton Exchange Membrane Fuel Cell versus Proton Exchange Membrane Electrolyser, from the work of Guenot et al. [25] 32
2.16 Comparison in between the system and auxiliary specific power consumptions for a $5\ Nm^3\ h^{-1}$ PEMEL, from the work of Godula-Jopek et al. [35] 33
2.17 PEMEL electrolyser load range for different membrane thicknesses, from the work of Babic et al. [96] 34
2.18 Start-up sequence for a $5\ Nm^3\ h^{-1}$ PEMEL, from the work of Godula-Jopek et al. [35] . 35

3.1 Plan of Approach for the research 39
3.2 Schematic overview of the hydrogen pathway considered within the system 42
3.3 System scope considered for the system 43
3.4 Day-ahead electricity prices on an annual basis for The Netherlands in 2020 [112] . . . 45

3.5 Day-ahead electricity prices on a daily basis for The Netherlands in April 2020 [112] . . 45
3.6 Electricity demand yearly profile 46
3.7 Hydrogen demand yearly profile 46

5.1 Total Energy Overview - LP Simulation 62
5.2 Sensitivity analysis on TAC to changing AEL CAPEX 64
5.3 Sensitivity analysis on TAC to changing PEMEL CAPEX 64
5.4 Sensitivity analysis on TAC to changing SOEL CAPEX 64
5.5 Sensitivity analysis on TAC to changing AEL Lifetime 65
5.6 Sensitivity analysis on TAC to changing PEMEL Lifetime 65
5.7 Sensitivity analysis on TAC to changing SOEL Lifetime 65
5.8 Sensitivity analysis on TAC to changing AEL Efficiency 66
5.9 Sensitivity analysis on TAC to changing PEMEL Efficiency 66
5.10 Sensitivity analysis on TAC to changing SOEL Efficiency 66
5.11 Total Energy Overview sensitivity to changing efficiency 67
5.12 Sensitivity analysis on TAC to changing AEL Ramping Rates 68
5.13 Sensitivity analysis on TAC to changing PEMEL Ramping Rates 68
5.14 Sensitivity analysis on TAC to changing SOEL Ramping Rates 68
5.15 Sensitivity analysis on TAC for different interest rates 68
5.16 Total Energy Overview - 2030 scenario 70
5.17 Total Energy Overview - 2050 scenario 70
5.18 Sensitivity analysis on TAC for different constraint configurations 73

6.1 Sensitivity analysis on Total Annualised Costs for changing SOEL CAPEX 76

List of Tables

2.1 Hydrogen and selected physical properties [35] . . . 9
2.2 Hydrogen compared to other fuels, rounded to one decimal values [35] . . . 10
2.3 Main characteristics of Alkaline Electrolysis **system**[1] [24, 35, 55, 56, 66, 67, 68, 69] . . . 23
2.4 Main characteristics of Proton Exchange Membrane Electrolysis **system**[2] [24, 35, 55, 56, 66, 67, 68, 70, 72, 73, 74] . . . 24
2.5 Main characteristics of Solid Oxide Electrolysis Cell **system**[3] [35, 56, 66, 67, 68, 72, 73, 77] 26
2.6 Comparison in between AEL, PEMEL and SOEL technologies [35, 50, 55, 56, 62, 63, 64, 65, 66, 67, 68, 70, 71, 72, 75] . . . 27

3.1 Model data input for the electrolyser technologies for 2020 based on literature review as found in Table 2.3*, Table 2.4⁻ and Table 2.5^{o} . . . 44
3.2 Model data input for the fuel cell technology [92, 108, 109, 110, 111] . . . 44
3.3 Model data input for the storage and charging/discharging technology [83, 109] . . . 45
3.4 All possible model configurations based on four components (including Model 16 - 'Base Case') . . . 48

5.1 Model data input for the electrolyser technologies for 2020 based on literature review as found in Table 2.3*, Table 2.4⁻ and Table 2.5^{o} . . . 61
5.2 Model data input for the fuel cell technology [92, 108, 109, 110, 111] . . . 62
5.3 Model data input for the storage and charging/discharging technology [83, 109] . . . 62
5.4 Sensitivity analysis, 'Base Case' and the reference ranges per type of electrolyser . . . 63
5.5 Model data input for the electrolyser technologies for 2030 [66, 68, 69, 74, 77] . . . 69
5.6 Model data input for the electrolyser technologies for 2050 [66, 68, 69, 74, 77] . . . 69
5.7 All possible model configurations based on four components (including Model 16 - 'Base Case') . . . 71
5.8 Optimisation results for all configurations, defining both the computational time and the Total Annualised Costs . . . 72

7.1 Electrolyser Footprint and Electrode Area [68, 119] . . . 77

Contents

Preface iii

Abstract v

Nomenclature x

List of Figures xi

List of Tables xiii

1 Introduction 1
- 1.1 The Energy Transition . . . 1
  - 1.1.1 The Need for Transition . . . 1
  - 1.1.2 Hydrogen within the Future Energy Outlook . . . 3
- 1.2 Research Scope and Research Questions . . . 5
- 1.3 Contribution to Research . . . 7
- 1.4 Report Structure . . . 7

2 Hydrogen Electrolysis in Literature 9
- 2.1 Hydrogen . . . 9
- 2.2 Future Energy Carrier . . . 10
- 2.3 Balance of Power . . . 11
- 2.4 Hydrogen Generation with Electrolysis . . . 13
  - 2.4.1 Water Electrolysis Fundamentals . . . 14
  - 2.4.2 Thermodynamic Essentials . . . 15
  - 2.4.3 Efficiency & Overpotentials . . . 17
  - 2.4.4 Alkaline Electrolysis (AEL) . . . 22
  - 2.4.5 Proton Exchange Membrane Electrolysis Cell (PEMEL) . . . 23
  - 2.4.6 Solid Oxide Electrolysis cell (SOEL) . . . 25
  - 2.4.7 Summary of Electrolysis Technologies . . . 27
- 2.5 Hydrogen Storage Technologies . . . 28
  - 2.5.1 Compressed Hydrogen Storage . . . 29
  - 2.5.2 Liquid Hydrogen Storage . . . 30
  - 2.5.3 Linepack . . . 31
- 2.6 Hydrogen Fuel Cell . . . 32
- 2.7 Technical Parameters and Operational Policies . . . 33
  - 2.7.1 Nominal Load and Part-Load Operation . . . 33
  - 2.7.2 Load Range . . . 34
  - 2.7.3 Cold and Warm Start-Up . . . 35
  - 2.7.4 Ramping Up and Ramping Down . . . 36
  - 2.7.5 Standby Losses . . . 36
  - 2.7.6 Lifetime and System Degradation . . . 36
- 2.8 Optimisation of Electrolysis Processes . . . 37

3 Methodology 39
- 3.1 Plan of Approach . . . 39
- 3.2 Modelling and Mathematical Framework . . . 40
  - 3.2.1 AIMMS . . . 41
  - 3.2.2 MATLAB . . . 41

3.3 System Description . . . 42
3.4 Data Input . . . 44
3.5 Sensitivity Analysis . . . 47
3.6 MIP Case Descriptions . . . 48

4 Mathematical Formulation of the Model 49
4.1 Linear Programming Model . . . 50
4.1.1 Objective Function LP Model . . . 52
4.1.2 Constraints . . . 52
4.2 Mixed Integer Programming Model . . . 56
4.2.1 Objective Function MIP model . . . 57
4.2.2 Constraints . . . 57

5 Optimisation Results 61
5.1 Linear Programming Optimisation . . . 61
5.1.1 Sensitivity Analysis of the LP Case . . . 63
5.2 Mixed Integer Programming Optimisation . . . 71

6 Conclusions 75

7 Discussion & Research Recommendations 77
7.1 Discussion . . . 77
7.2 Research Recommendations . . . 79

Bibliography 81

1 Introduction

The energy transition is one of the major challenges of the 21st century, impacting the way energy is generated, conserved and consumed. Energy generation becomes more and more decentralised, intermittency and fluctuations suddenly are becoming topics of interest within day-to-day life and energy system operators are facing many new obstacles never encountered before. In this context, the anticipation for hydrogen as a resource for energy conservation and management is big. This research focuses on hydrogen generation with means of water electrolysis, also known as 'green hydrogen', storage in compression vessels and Gas-to-Power (GtP) concepts in the form of fuel cell technologies.

Within this chapter, the context of the research is described. First off, the societal and economical relevance concerning the energy transition is sketched, after which the relevance of hydrogen within the energy transition is described. Both the energy transition and the relevance of hydrogen are presented within the Dutch Energy case. Thereafter, the problem definition is given. Finally, the structure of the report is presented.

1.1. The Energy Transition

In this section, the energy transition is discussed from two different perspectives, namely: the need for an energy transition and the role of hydrogen within this transition.

1.1.1. The Need for Transition

Since the industrial revolution took off in the 18th century, humankind has designed and introduced numerous types of industrial machinery. These machines have brought many prosperous achievements, with a majority of these applications using fossil fuels as feedstock. However, the late 20th century has brought an inflexion point into the perception of fossil fuel feedstock. Both the continuously increasing global Green House Gas (GHG) emissions [1, 2] and the near depletion of fossil fuels have to lead to global protocols and agreements to mitigate this dependency. The Paris Agreement, an international treaty with legally binding consequences was created in 2015 as a culmination [3].

According to United Nations Framework Convention on Climate Change [4] this treaty stipulates that the participating 195 countries adhere to: "...to limit global warming to well below 2, preferably to 1.5 degrees Celsius, compared to pre-industrial levels. To achieve this long-term temperature goal, countries aim to reach global peaking of greenhouse gas emissions as soon as possible to achieve a climate-neutral world by mid-century."

However, if taking a closer look at trends of GHG emissions, it can be observed that a contradictory trend is still ongoing. For example, the trend for the CO_2 concentration in the atmosphere is still on an upward trajectory, as seen in Figure 1.1 [5].

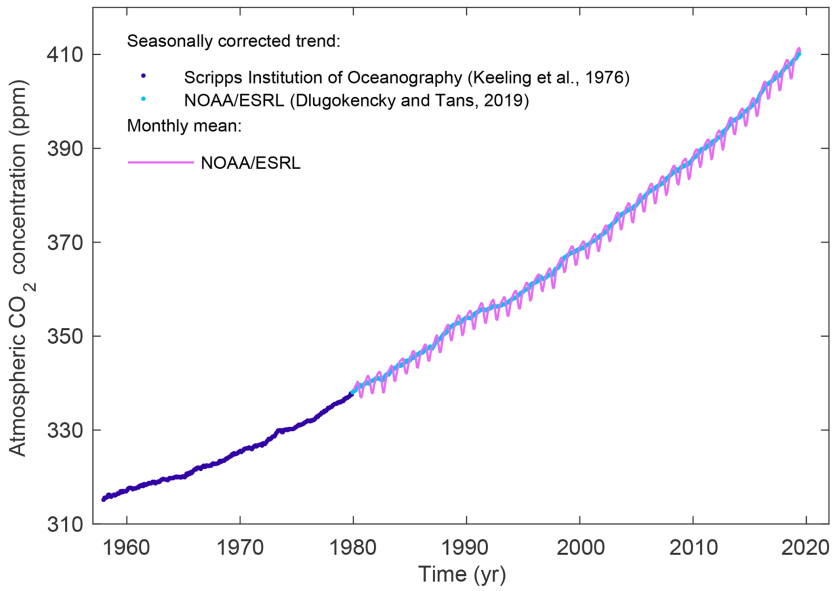

Figure 1.1: CO_2 concentration in the atmosphere, from the work of Friedlingstein et al. [5]

With global energy demand increasing annually and expected growth of energy demand of nearly 50% by the year 2050 [6], this agreement poses many challenges. Especially put in the previous context, the dependency on fossil fuels as feedstock in energy and electricity consumption can be depicted in Figure 1.2. This figure shows that the dependency on fossil fuels such as oil, coal and gas is still over 84% of total energy consumption worldwide as of 2020 [7].

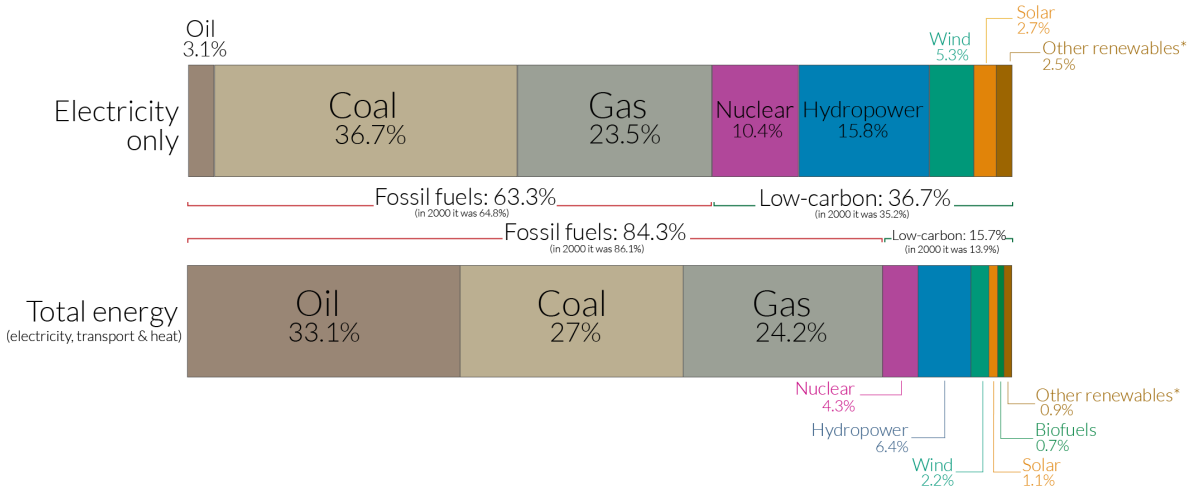

Figure 1.2: Global primary energy and electricity consumption by source in 2020, from the work of Ritchie et al. [7]

To adhere to The Paris Agreement, one of the key changes in the future energy outlook will be the implementation of renewable energy sources. The combination of variable renewable energy sources (vRES) with efficiency improvements to existing energy infrastructure, can lead to the fulfilment of 90% of carbon dioxide (CO_2) reduction targets set according to IRENA [8]. The implementation of vRES is therefore one of the main pillars of the energy transition. This development is depicted in numerous energy outlooks and research articles, as in the case of the yearly Energy Outlook of IEA.

The perspective of the depletion of fossil fuels and the societal outcry for GHG emission-free energy sources has led to investments, research and development of vRES. This is especially depicted when taking a closer look into the levelised costs of energy for vRES technologies, as shown in Figure 1.3 [9].

The decrease of the levelised costs of these technologies has also led to a cost-competitive situation with fossil fuels, making the implementation on a larger commercial scale possible. This trend can be observed in the increase in vRES investments and planned projects all around the globe, where IEA (2020) reported expected annual growth of $305\ GW$ between the years 2021-2026 [10].

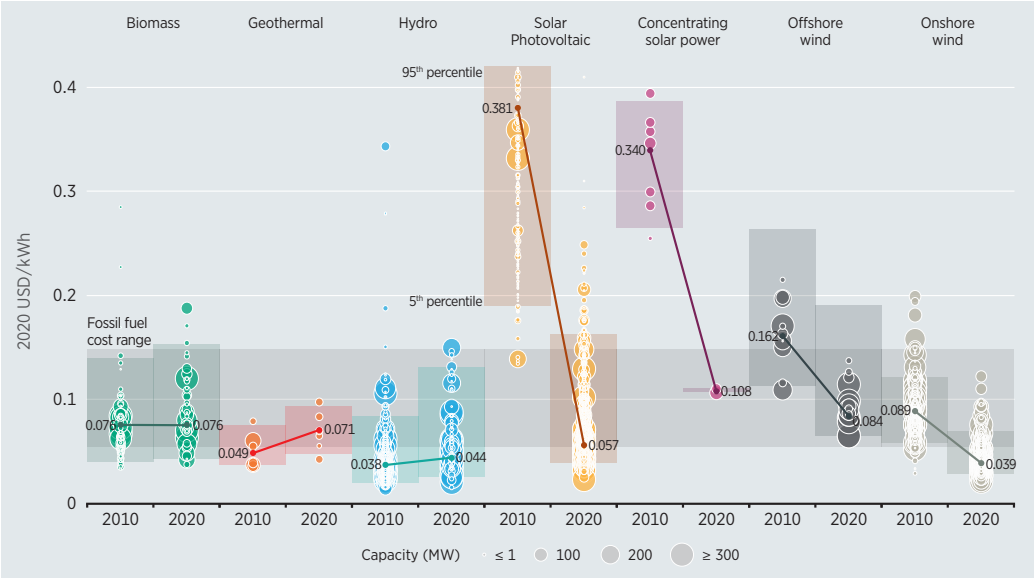

Figure 1.3: Levelised costs of energy for different variable Renewable Energy Sources, from the work of IRENA [9]

1.1.2. Hydrogen within the Future Energy Outlook

With the substitution of fossil fuels by vRES, the energy landscape undergoes a big change. Unlike fossil fuels, the vRES are intermittently generated, depending on weather conditions. This implies that the generated energy needs storage to supply demand in low generation periods (i.e., nights, winters, etc.). The intermittent character is depicted in Figure 1.4, where the electricity generation for The Netherlands is shown for the month of July 2021. Especially the intermittency of wind and solar energy can be clearly depicted. Furthermore, vRES are characterised by distributed generation, meaning that the grid power quality cannot be maintained by utilising power reserves from plants, such as gas or coal plants. Lastly, the load is not met during all times (especially the weekends), however, this representation of the Dutch Energy case does not include the import and export of electricity over national borders.

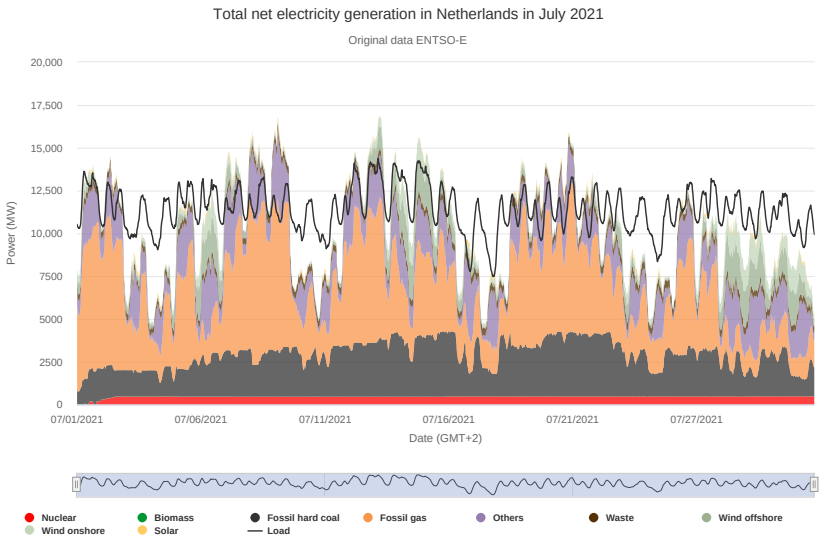

Figure 1.4: Total net electricity generation in July 2021 for The Netherlands, from Energy-Chart.info [11]

Hydrogen (H_2) can play a key role in the future energy outlook, as a fuel storing the excess energy from the high penetration of vRES. The concept of storing the power is known in the literature as PtX, meaning Power-to-X, where the X can be gas or liquid (PtG and PtL respectively). Hydrogen has benefits over other storage alternatives, amongst others: no GHG emissions (if produced with renewable energy sources), high enthalpy (energy-like state-function), distribution through natural gas pipelines and low self-discharge when stored. However, hydrogen also knows some common disadvantages, such as the energy loss when converting electricity to hydrogen and back to electricity (PtP, Power-to-Power) and the high costs for GHG emission-free hydrogen production routes.

As hydrogen (in di-atomic form) is not a substance that is present in the atmosphere, these hydrogen production routes are of particular interest to grasp. There are different pathways of hydrogen production and these are divided into clusters depending on the energy source used [12, 13]:

- Black (or brown) hydrogen - Hydrogen that is created by burning black coal or lignite (brown coal), this form of hydrogen production leads to GHG emissions and is not environmentally friendly.
- Magenta (or pink) hydrogen - disassociation of methane to produce both hydrogen and carbon, leads to the release of GHGs and thus is not environmentally friendly.
- Grey hydrogen - One of the most common hydrogen production technologies, even dubbed the workhorse of today's industry together with the blue hydrogen route, is the generation of hydrogen by the gasification of natural gas. Grey hydrogen is the umbrella term for different types of production routes whereby natural gas is consumed, such as Autothermal Reforming (ATR), Steam Methane Reforming (SMR) and Partial Oxidation (POX).
- Blue hydrogen - Hydrogen generation with natural gas, with the important difference that the generated CO_2 is sequestrated. If the carbon dioxide is also stored this is called Carbon Capture and Sequestration or CCS in short, a commonly used practice in nowadays hydrogen production. If the captured carbon is also utilised in the industry this is called Carbon Capture Utilisation and Sequestration (CCUS).
- Yellow hydrogen - A relatively new term, the production of hydrogen with only the usage of PV (photovoltaic cells, or solar) is dubbed yellow hydrogen. This production route is relatively new but is an environmentally friendly way of hydrogen production.
- Green hydrogen - Finally, the route whereby the energy input is in the form of renewably generated electricity is called the green hydrogen route. This route encompasses all technologies considering water electrolysis, technologies such as: Alkaline Electrolysers (AEL), Proton Exchange Membrane Electrolysers (PEMEL), Solid Oxide Electrolysers (SOEL) and Anion-Exchange Membrane Electrolysers (AEM). As seen in Figure 1.5 only 0.72% of global dedicated hydrogen production comes forth from green hydrogen [14], a discomforting figure when put in perspective of the earlier introduced Climate Goals and The Paris Agreement.

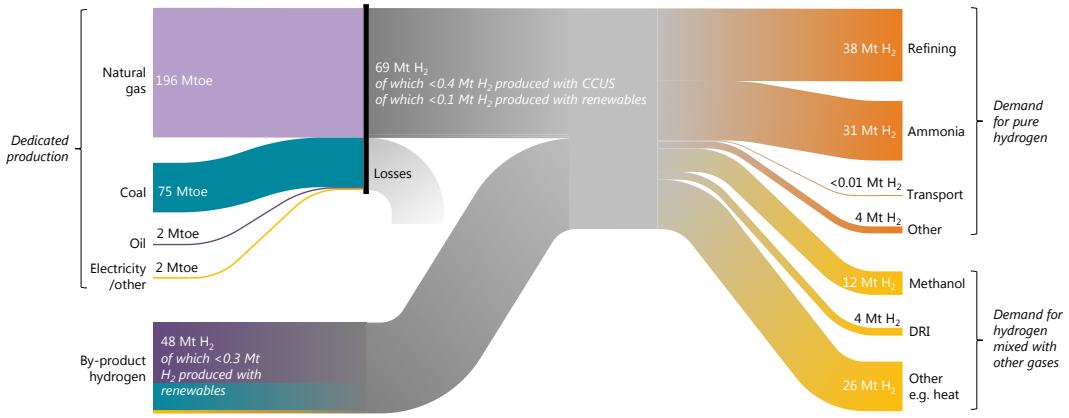

Figure 1.5: Hydrogen production pathways, from the work of IEA [14]

Considering the description given for hydrogen production technologies and the status quo in production technologies, it is good to understand the emphasis on the current production technologies in industrial processes. Therefore, the levelised cost of hydrogen production in US Dollars per kg of hydrogen production is depicted for 2019 along with a prediction for costs by 2050 Figure 1.6. In this figure, five different sources of hydrogen production are depicted, where: natural gas stands for the usage of SMR, natural gas with CCS stands for SMR with Carbon Capture Storage, and coal with and without CCS is the gasification of coal with or without CCS (only used in China) and finally low-carbon electricity stands for all technologies regarding water electrolysis [15]. It becomes evident why the green hydrogen route is not opted over alternatives such as grey, blue and black hydrogen production routes, as the costs for the production are almost 4 to 8 times as high.

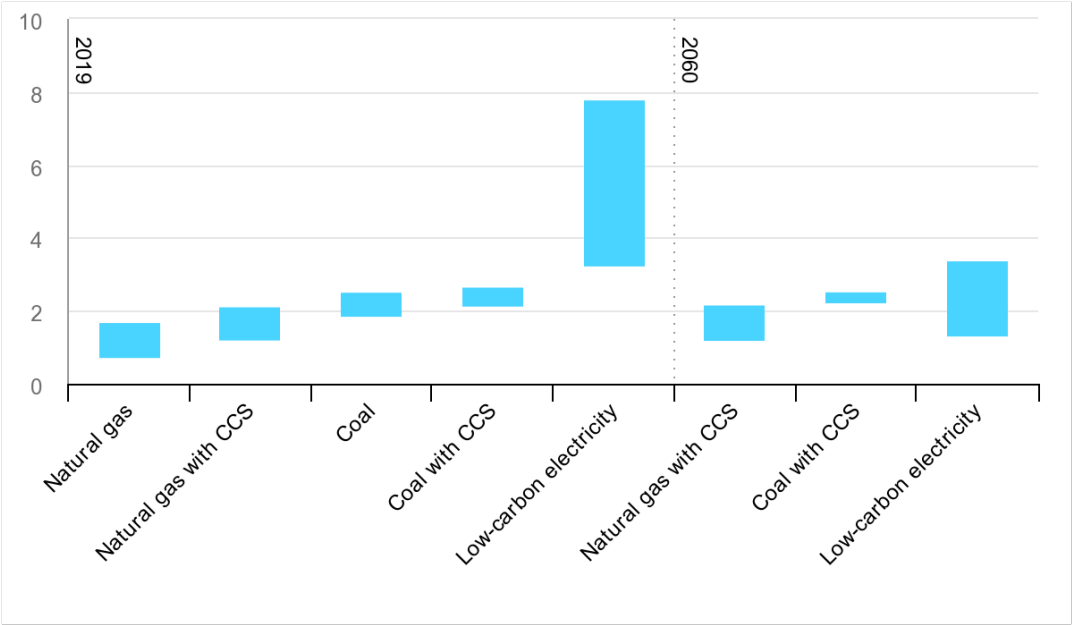

Figure 1.6: Levelised hydrogen production costs [$USD\ kg^{-1}$] for 2019 and predictions for 2060, from the work of IEA [15]

With these figures and facts in mind, investments in green hydrogen production are intensified. Aligning with these intensifications, the focus of this research is on the production route with water electrolysis and thus green hydrogen production.

1.2. Research Scope and Research Questions

The challenges described in the introduction are clear, the world is dealing with an energy transition towards variable Renewable Energy Sources and thereby a form of energy storage is compulsory. One of the storage options is hydrogen, a technology that contains energy and can release this energy back in any form required. One such route is depicted in the hydrogen reconversion pathway (PtP) as depicted in Figure 1.7 [16]. Hereby, the surplus of vRES on the electric grid is coupled to an electrolysis unit a consequent storage facility and a reconversion technology. This reconversion technology is called the fuel cell and converts hydrogen back into electrical energy, 'reconverting' the hydrogen into electricity.

The goal of this Master Graduation Project (hereafter: research) is to create an efficient and accurate Mixed Integer Programming (MIP) hydrogen model. The model will be optimised for both investment and operational models. The model at hand will be compared to a Linear Programming (LP) hydrogen model, to validate the model, but also to assess the level of detail required in modelling to obtain different outputs.

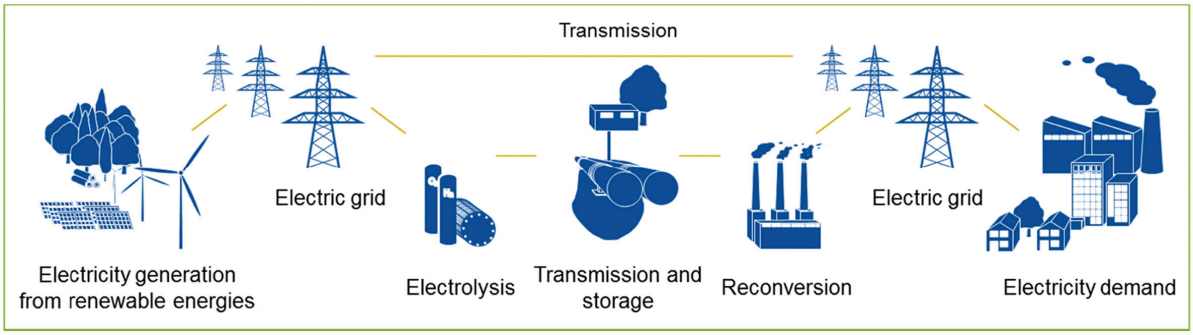

Figure 1.7: Schematic overview of the hydrogen reconversion pathway, from the work of Welder et al. [16]

To create both models, an in-depth analysis (from the literature) will be carried out based on the requirements and constraints for the hydrogen technologies. The hydrogen technologies considered are clustered as follows:

- Electrolysis technologies
  - Alkaline Electrolysers (AEL)
  - Proton Exchange Membrane Electrolysers (PEMEL)
  - Solid Oxide Electrolysers (SOEL)
- Storage technologies
  - Compressed hydrogen storage
  - Liquid hydrogen storage
  - Linepack
- Fuel cell technology, only Proton Exchange Membrane Fuel Cell (PEMFC)

Key (operational) technical parameters and operational policies for the electrolysis technologies will be assessed, both on technological as well as financial merits. Hereafter, a mathematical model that captures the technical parameters and operational policies of hydrogen technologies will be adopted. The model will be generic, such that it can be scaled for different types of case studies. Lastly, a trade-off will be made between the technology mixes, based on the identified constraints.

Both the theoretical/mathematical approach as well as a case simulation are of importance for the model. The created model will help to assess the energy outlook of hydrogen. The research goal is therefore to identify:

Asses the optimal level of detail for modelling the hydrogen reconversion pathway with electrolysis and the effects of different levels of detail on the computational time.

The following sub-questions will be of aid in assessing the research goal:

1. What is the current status quo on hydrogen technologies and their models?
2. What are the technical parameters and operational policies for H_2-technologies and how do these translate into constraints?
3. How can new H_2-models be built up and how can existing H_2-models be improved for different types of scenarios? Create new mathematical frameworks and validate technical parameters and operational policies by implementing a generic case study for optimal investment and operational models.

1.3. Contribution to Research

Hydrogen technologies are an emerging type of technology, with many investments and research initiatives as a result. Hydrogen technologies are diverse and it reflects in the research performed on the technologies. Topics such as the generation (with fossil fuel and renewable production routes both discussed extensively), transportation, storage and the usage of fuel cells are discussed. As hydrogen as an energy carrier can also be used in energy-intensive industries and refineries, research into usage for ammonia, steel production and fertilisers has also been conducted frequently.

When taking a closer look into the existing literature on hydrogen optimisation modelling, the research can be separated into two: research conducted either on a detail level or within multi-energy systems. On the detail level, the electrolysis technologies are handled separately such that literature exists on optimal operation for Alkaline Fuel Cells/Electrolysers [17, 18, 19], for Proton Exchange Membrane Fuel Cells/Electrolysers [20, 21, 22, 23, 24, 25] and for Solid Oxide Fuel Cells/Electrolysers [26, 27]. Research conducted focuses on thermodynamic and electrochemical properties and obtains simulation or experimental models as close to real operational models as possible.
On the multi-energy system-level, the emphasis is on the structure of the energy system as a whole [28, 29, 30, 31]. The level of detail is disregarded to an extent that the model covers simplification of reality, as the created models need to be able to run fast and simulate different types of constraints.

This research contributes in the following aspects to the optimisation modelling of the optimal energy mix of hydrogen technologies with water electrolysis as a production route:

1. The research focuses on identifying technical parameters and operational policies of the water electrolysis systems that can be translated into optimisation constraints, assessing the level of detail required to create an accurate optimisation model.

2. A generic model is developed that can be scaled for further research, making different case studies and sizing possible.

3. The research compares the performance of the models in terms of accuracy to the computational burden. The comparison is done for the level of detail and complexity added to the model.

1.4. Report Structure

The report is structured in the following way: in chapter 2 the literature regarding hydrogen electrolysis is introduced and discussed. The literature starts with a general description of hydrogen, and its use-cases and elaborates on the generation with electrolysis, storage of hydrogen and reconversion of hydrogen, before discussing relevant parameters to model the technologies. In chapter 3 the methodology for the modelling of the optimisation problem is described as well as a description of the case study that is being performed. In chapter 4 two mathematical frameworks are given for the optimisation of hydrogen modelling, one Linear Programming that serves as the base case and one Mixed Integer Programming that is a more realistic model. In chapter 5 the results of the case studies are given and analysed. The report finishes with a conclusion in chapter 6 and discussion with recommendations for future research in chapter 7.

2

Hydrogen Electrolysis in Literature

This chapter covers an overview of the most prominent hydrogen production and hydrogen storage technologies in literature. The relevance of these technologies is dealt with, as well as a discussion of possible implications on the power system stability, such as ramping up and down, and switching on and off behaviour. The production technologies are divided into a section regarding fossil fuels-related hydrogen production techniques and technologies that require water electrolysis for the oxidation process. The storage technologies are divided among others into compressed gas, cryogenic liquid, metal hydrides and pipelines.

2.1. Hydrogen

Hydrogen is the name of the chemical element which is first in the periodic table and is noted with the symbol *H*, having the atom number of 1. The element is the most lightweight of all elements with an atomic weight of 1.008 and the most abundant amongst elements, being present in more than 70% of all elements in the universe [32]. The name comes forth from the Greek 'hydro' and 'genes' meaning water forming [32] and as such it is a well known part of water (H_2O) and hydrocarbons. Hydrogen has many typical characteristics, among which it is odourless, tasteless, colourless and non-toxic [33]. Another characteristic of hydrogen is that is highly flammable and explosive above a concentration of 4% by volume [34], when in contact with air or with pure oxygen. This last characteristic does complicate the usage of hydrogen in many technologies and will be discussed later in this chapter.

Although hydrogen is the chemical element with the highest abundance in nature, it does not appear in stable single element form (also called atomic hydrogen) at Standard Temperature and Pressure (STP, as defined by the International Union of Pure and Applied Chemistry as $0\ ^\circ C$ and $1\ bar$) conditions. Under these conditions, hydrogen can be found in diatomic form, meaning two *H* atoms bind to form H_2 gas (also named molecular hydrogen). An overview of selected physical properties of molecular hydrogen can be found in Table 2.1 as found in [35].

Table 2.1: Hydrogen and selected physical properties [35]

Property	Value	$Unit$
Molecular weight	2.016	mol
Melting point	13.96	K
Boiling point (at $1\ atm$)	14.0	K
Gas density (at $0\ ^\circ C$ & $1\ atm$)	0.0899	$kg\ m^{-3}$
Net heat of combustion (at $25\ ^\circ C$ & $1\ atm$)	241.9292	$kJ\ g^{-1}mol^{-1}$
Flammability limit in oxygen	4-94	%
Flammability limit in air	4-74	%

2.2. Future Energy Carrier

Since its discovery by Henry Cavendish, hydrogen has been studied and assessed. Hydrogen is a good energy carrier, meaning it can be used to store energy and later be used in energy consumption. Therefore, many countries, regions and initiatives are now developing policies and investing in the research and development of hydrogen as a future keystone of the economy [36, 37, 14]. In literature and media, there is a name dubbed for this trend as the 'hydrogen economy', which means an economy that is based upon the use of hydrogen as feedstock, fuel and an energy carrier [38].

With an energy density per mass volume (gravimetric energy density) of $120\ MJ\ kg^{-1}$ hydrogen is the most energy-dense fuel available. However, one of the challenges with such a future scenario is that hydrogen has a comparable lower volumetric density at STP when compared to fossil fuels such as methanol, petrol, diesel and kerosene. Hydrogen in liquid form has four times higher volumetric density, but in comparison is once again outperformed by fossil fuels. An overview of the main characteristics of hydrogen against other fuels can be found in Table 2.2 as found in [35]. In section 2.5 the relevance of these parameters will become more apparent when discussing hydrogen storage.

In Table 2.2 the energy content for hydrogen is referred to with two different heating values. In literature and industry, the energy content for hydrogen is often mentioned with either a Lower Heating Value (LHV) or with a Higher Heating Value (HHV). The difference between both is the molar enthalpy of the vaporisation of water. The usage of LHV becomes apparent when using technologies with operational temperatures above the boiling temperature of water (>$100\ ^{\circ}C$), whereby the water is vaporised and not condensed back to liquid form. Within this research, the Higher Heating Value of hydrogen will be used. In subsection 2.4.3 the effect of using LHV and HHV for efficiency calculations will be discussed.

Table 2.2: Hydrogen compared to other fuels, rounded to one decimal values [35]

Fuel type	**Gravimetric energy density**		**Volumetric energy density**	
	$MJ\ kg^{-1}$	$kWh\ kg^{-1}$	$MJ\ l^{-1}$	$kWh\ l^{-1}$
Hydrogen gas (LHV)	120	33.3	2.1	0.6
Hydrogen liquid (LHV)	120	33.3	8.4	2.3
Hydrogen gas (HHV)	141.7	39.4	2.5	0.7
Hydrogen liquid (HHV)	141.7	39.4	10	2.8
Methanol	19.7	5.4	15.7	4.4
Petrol	42	11.4	31.5	8.8
Diesel	45.3	12.6	35.5	9.9
Kerosene	43.5	12.1	31.0	8.6

Hydrogen is also used as feedstock or energy carrier for industrial applications or refining processes. The most common uses of hydrogen are in the production of ammonia, methanol and the steel and iron-making industry. It is expected that hydrogen will play a major role in the decarbonisation of industry and its applications, as also seen in many types of research by the International Energy Agency and depicted in Figure 2.1 [39].

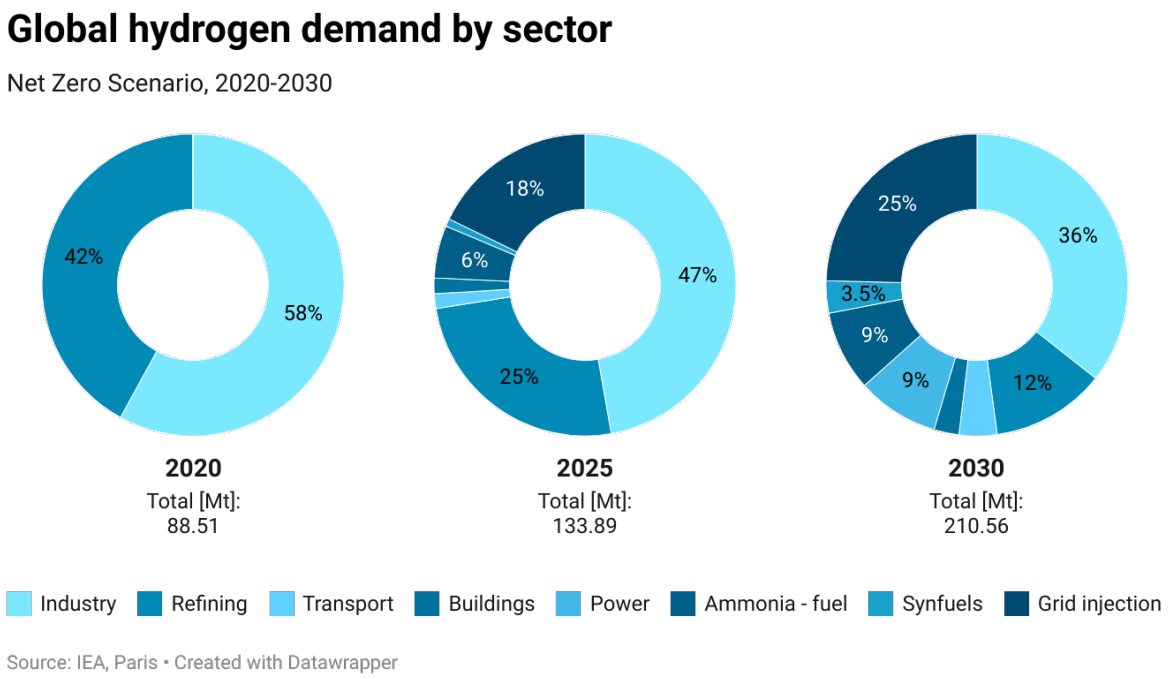

Figure 2.1: Global hydrogen demand by sector in the Net Zero Scenario, 2020-2030, edited from IEA [39].

2.3. Balance of Power

The conservation of energy is as important as the generation or efficient utilisation of the generated energy. The white paper of the International Electrotechnical Commission on Electrical Energy storage specifies the need for energy storage in terms of roles and needs for storage [40]. In the paper it is stated that energy storage can play a role in:

- ”Reduction of the energy costs at peak-demand periods
- Continuous and flexible supply of energy
- Overcoming grid failures and outages, especially in cases of the long distance between the location of generation and consumption
- Preventing congestion in power grids”.

In addition to previous mentioned general remarks on energy storage systems, the challenge with variable Renewable Energy Sources (vRES) is the intermittent character as indicated within the name. This means that power generation is not continuous and flexible but is especially dependent on weather conditions. This is trivial for solar energy and wind energy but also holds for hydropower, which is dependent on rainfall (which in its turn is influenced by solar irradiation and wind) [41].

The benefits of combining energy storage with vRES becomes also apparent from its characteristics. With energy storage the demand can be shifted in time, the power quality on the network can be maintained, the power grid can be used more efficiently, and isolated grids can be provided with electricity more easily as a smaller investment is needed in directly installed capacity and there is always an emergency power back-up [40]. As indicated in the ’Energy Storage Systems Cost Update’ report by Sandia National Laboratories energy storage can be divided into four clusters: either short-term or long-term storage both with possibilities for frequent discharge and non-frequent discharge [42]. Hereby, short-term is defined in the order of minutes, whereas long-term storage is defined in the order of hours. The cycling behaviour is categorised as, either daily load-levelling (frequency regulation, voltage regulation, etc.) for frequent discharge and a reserve capacity for non-frequent discharge.

Hydrogen as an energy carrier can especially be of use in the seasonal balance of power, meaning it is categorised in the section of long-term storage which is dispatched non-frequently. This intermittency comes forth from seasonal fluctuations in energy demand, but also the implementation of variable Renewable Energy Sources (vRES). These have an intermittent character, both on a daily and seasonally basis, with lower generation levels in the autumn and winter seasons. An example of the intermittency of wind energy production is given in Figure 2.2 [43].

The intermittent behaviour has implications on the electricity grid stability for both Transmission System Operators (TSOs) and Distribution Network Operators (DSOs) worldwide. By storing excess energy the demand side response is managed and also expensive grid expansions can be prevented. Hydrogen can play the role of power balancing factor, especially in the tertiary reserves (or replacement reserves) on the electricity markets [44].

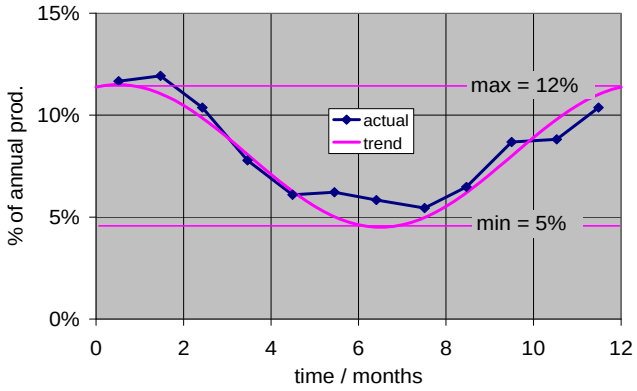

Figure 2.2: Intermittent character of wind energy production shown over the year, from the work of Crotogino et al. [43]

Hydrogen has three major benefits over alternative storage techniques such as redox flow batteries, Compressed Air Energy Storage (CAES) and hydroelectric power potential. Firstly, hydrogen storage can be performed on a large scale underground (e.g., in salt caverns), overcoming the area requirements as per hydroelectric power. Secondly, hydrogen storage has a low energy investment cost, especially when compared to battery storage [45]. Lastly, hydrogen storage has a very low self-discharge rate compared to the other alternatives, making it competitive for long-term storage options [45, 46].

The aforementioned benefits can be represented in a figure overview. The preferences for large scale storage options are displayed for the timescale versus the size of the system in Figure 2.3 [43]. The preferred timescale for hydrogen storage is depicted in the range of days to months, meaning hydrogen storage can provide the seasonal power balance.

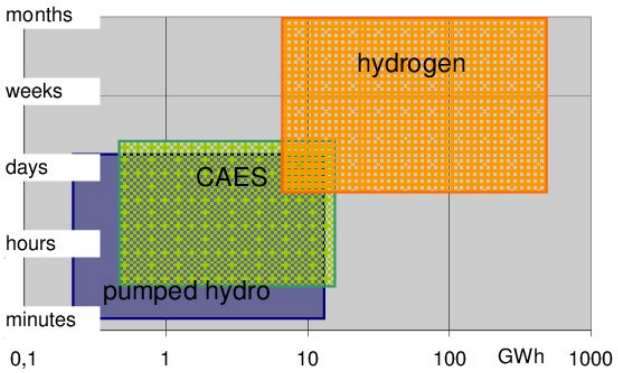

Figure 2.3: Large scale storage utilisation timescale and size from the work of Crotogino et al. [43]

2.4. Hydrogen Generation with Electrolysis

Hydrogen in the molecular structure form (H_2) does not solely exist in nature and therefore it requires production techniques to be made available as fuel. For this production process, many techniques are available and with the prospect of the hydrogen economy, many new technologies do emerge [47]. The major hydrogen pathways can be split into two categories, namely: variants that involve fossil fuels as a resource, having carbon as a byproduct and variants that do not have any carbon byproduct (amongst others water electrolysis). In Figure 2.4 all current pathways for the production of low-carbon hydrogen at scale are included [48].

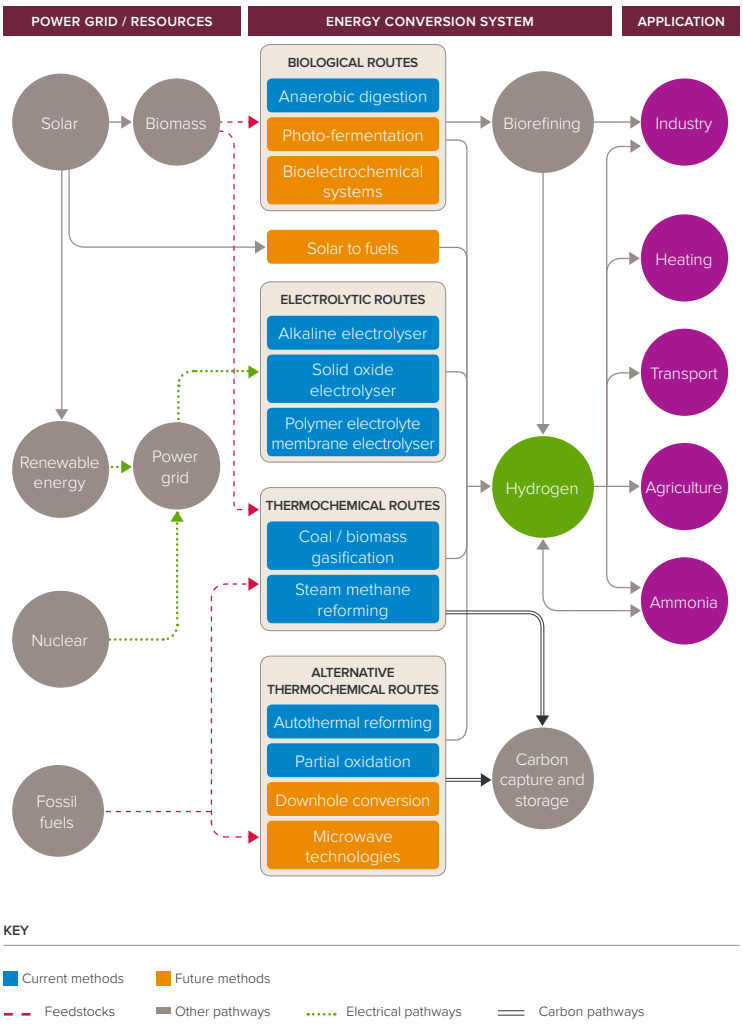

Figure 2.4: State-of-the-art production pathways of low-carbon hydrogen at scale, from the work of The Royal Society [48]

The first variant refers to technologies where fossil fuels (most often natural gas) are reformed, such as Steam Methane Reforming (SMR) and Autothermal Reforming (ATR). These technologies do produce by-products, among others CO_2, and can be combined with Carbon Capture and Storage (CCS) techniques to mitigate the effects of the CO_2 byproducts.

The latter refers to technologies where water molecules are split with the aid of electrical energy and hydrogen is obtained as output, through an electrochemical conversion known as water electrolysis. This form of hydrogen production does not have any byproducts and is therefore seen as the ‘green’ or renewable way of hydrogen production. This research focuses on the ’green’ hydrogen production techniques and defines the main aspects of various techniques, such that a comparison can be drawn in between key parameters for optimisation purposes.

2.4.1. Water Electrolysis Fundamentals

In this section, the three most prominently used water electrolysis cells are analysed in alphabetical order, namely the Alkaline Electrolysis, Proton Exchange Membrane Electrolysis Cell and Solid Oxide Electrolysis Cell. However, before elaborating on the technologies, first, an introduction to the fundamentals of water electrolysis will be given.

The technique of water electrolysis goes back to the Dutch duo of Adriaan Paets van Troostwijk and Jan Rudolph Deiman who did perform the first electrolysis with their Leyden jar in 1789 [49]. However, the principle of the Leyden jar was not based upon a constant voltage output. When Alessandro Volta invented the voltaic pile, which was amongst others able to produce a constant voltage output, William Nicholson and Anthony Carlisle showed the potential of water electrolysis in an undivided cell in the year 1800. Michael Faraday defined the physical laws for electrolysis in 1834 [50]. All of these discoveries and research have led to the development of electrolysers as we know them in the present.

To define the chemical principles taking place within electrochemistry, the reaction equations are defined. In the case of water electrolysis, this is defined by a single electrochemical reaction as given in (2.1) [51]. In this reaction at STP, the input for the reaction is liquid water ($H_2O_{(l)}$) and the output is gaseous hydrogen ($H_{2(g)}$) and oxygen ($O_{2(g)}$). However, this is a simplification of the overall reaction kinetics taking place.

$$2H_2O_{(l)} \xrightarrow[electrolysis]{} 2H_{2(g)} + O_{2(g)} \tag{2.1}$$

One of the simplifications is that the above reaction does not consider in which media the reaction is taking place. The use of an acidic or alkaline media will change the behaviour of the reaction. The reaction in alkaline media can be described in three steps:

1. At the cathode hydrogen gas (H_2) and hydroxide anions (OH^-) are formed. As in this reaction hydrogen is formed, this is called the Hydrogen Evolution Reaction (HER) and the subsequent reaction is defined in (2.2) [35, 50, 51];

2. The negatively charged hydroxide ions move from the negative cathode to the positive anode through the electrolyte, because of the electric field set-up across the cell;

3. Finally, the hydroxide anions react to form oxygen and water. Similar to the HER, this step is called the Oxygen Evolution Reaction (OER) as oxygen is formed at this step, as defined in (2.3) [35, 50, 51].

$$2H_2O_{(l)} + 2e^- \rightarrow H_{2(g)} + 2OH^- \tag{2.2}$$

$$4OH^- \rightarrow 2H_2O_{(l)} + O_{2(g)} + 4e^- \tag{2.3}$$

Similarly, for the reaction in acidic media the reaction subsequently at the anode and cathode is given by (2.4) and (2.5) respectively [51]. The reader is noted these are still simplifications of the overall kinetics taking place.

$$2H^+ + 2e^- \rightarrow H_{2(g)} \tag{2.4}$$

$$2H_2O_{(l)} \rightarrow 4H^+ + O_{2(g)} + 4e^- \tag{2.5}$$

The above reactions give an overview from a chemical point of view for the reactions taking place. However, from an energy point of view, the reaction of water splitting will not occur spontaneously as the reaction requires external energy to take place. Therefore, a brief introduction to the thermodynamics and energy requirements will be given in subsection 2.4.2.

2.4.2. Thermodynamic Essentials

Thermodynamics is the field of studies that relates energy, heat, temperature and work. Through thermodynamic principles, the required energy of the water-splitting reaction can be defined. As the reaction is non-spontaneous, energy is required to let the reaction take place. In other words, the reaction is endothermic ($\Delta H > 0$). Thermal energy and electrical energy are added as input for the electrochemical process to occur.

The electrical energy required at equilibrium to split 1 mole of water is given by the Gibbs free energy change (ΔG). The thermal energy requirement (Q) is denoted as $T\Delta S$. Adding both gives the relation as given in (2.6)

$$\Delta H^0 = \Delta G^0 + Q = \Delta G^0 + T\Delta S^0 \tag{2.6}$$

where H^0 is the reaction enthalpy for the formation of one mole of water at STP, G^0 is the minimum amount of electrical energy required for the reaction named Gibbs free energy at STP, Q is the required thermal heat, T is the temperature and S^0 is the entropy change of the reaction at STP. The Gibbs free energy (thus the required electrical work) at STP is equal to $237.2\ kJ\ mol^{-1}$. The thermal energy required at STP is equal to $48.6\ kJ\ mol^{-1}$. This results in the chemical reaction for the water electrolysis as in (2.7), whereby the emphasis is on the plus sign for the overall reaction indicating a non-spontaneous reaction.

$$\Delta H^0(H_2O_{(l)}) = \Delta G^0(237.2\ kJ_{el.}\ mol^{-1}) + Q(48.6\ kJ_{Heat}\ mol^{-1}) = +285.8\ kJ\ mol^{-1} \tag{2.7}$$

The equation in (2.7) gives the overall energy requirement for the splitting of water liquid at STP. The reaction can also take place with water vapour, lowering the amount of energy required for the splitting of water, as the thermal heat requirement is lowered. The resulting equation for the splitting of water vapour is given in (2.8).

$$\Delta H^0(H_2O_{(vap)}) = +241.8\ kJ\ mol^{-1} \tag{2.8}$$

The difference between the energy requirement of exactly $44.04\ kJ\ mol^{-1}$ for water in liquid and vapour form, is the difference explained in section 2.2, between the HHV and LHV of water (liquid) and water vapour (steam) respectively. Since electrolyser units and fuel cells commonly operate under the range of <$100\ ^\circ C$, within this research the HHV will be used for calculations unless specified otherwise. The reader is noted that some experts do recommend the usage of LHV when considering electrolysis systems and that it is a more common way of noting the efficiencies in European countries. However, the choice is not undisputed.

The reversible voltage (also called the open circuit potential or the equilibrium voltage) required to split the water molecules is defined as U_{rev}, the free energy required to proceed with the electrolysis in $Volts$. There is a relationship between the Gibbs free energy and the reversible voltage, as defined in (2.9)

$$U_{rev}(T,P) = \frac{\Delta G(T,P)}{nF} \tag{2.9}$$

where n is the number of electrons exchanged during the electrochemical splitting of water ($n = 2$) and F ($C\ mol^{-1}$) is Faraday's constant; the electric charge of 1 mole electrons^{-1} equal to $96,485$.

Combining this expression for the Gibbs free energy under standard conditions results in (2.10).

$$U^0_{rev} = \frac{\Delta G^0}{2F} = 1.2293\ V \approx 1.23\ V \tag{2.10}$$

In the case that the required heat for the electrochemical reaction to take place is also delivered in the form of electrical energy input, the reaction would be defined as thermoneutral, increasing the required voltage. This voltage is referred to as the thermoneutral voltage (U_{tn}) and is defined as given in (2.11).

$$U_{tn}^{0} = \frac{\Delta H^{0}}{2F} = 1.4813\ V \approx 1.48\ V \tag{2.11}$$

To summarise, the electrochemical reaction for splitting water can be divided into three ranges, based on the applied voltage (U in V) to the system [35]:

1. $U < U_{rev}$, the applied voltage is less than the minimum required reversible voltage. Electrolysis will not take place as the reaction does not start.

2. $U_{rev} < U < U_{tn}$, the energy required to initiate the electrical reaction is supplied, however, as the thermoneutral voltage is not met, the reaction will subtract heat from the surroundings. The electrolyser will not perform in this range, as the current density will be so low that the system will need overdimensioning, leading to a high initial investment.

3. $U > U_{tn}$, the required energy is supplied to the reaction, overcoming also the thermal energy requirement. The electrochemical reaction will take place, with an increasing current density and heat generation as a consequence.

Temperature and Pressure Influence

In the definition of the reversible voltage Equation 2.9, the voltage and the Gibbs free energy have a dependence noted for temperature and pressure. This dependency is elaborately discussed in the literature. A brief overview is given in this subsection.

The entropy and Gibbs free energy are both thermodynamic state functions, meaning that they change as a function of temperature and pressure. Since the entropy and Gibbs free energy influences the cell voltage and the enthalpy of the electrochemical reaction, both Gibbs free energy and entropy show thermodynamic behaviour. This behaviour is captured in the Nernst equation, which describes the potential of the electrochemical reaction occurring, based on half-cell reactions and total reaction [52]. Therefore, the simplified Nernst equation as given in (2.12) can be used to calculate the reversible cell voltage at different temperature and pressure levels,

$$U_{rev}(T,P) = U_{rev}^{0} + \frac{RT}{2F}\ln\left(\frac{(p_{H_2})(p_{O_2})^{\frac{1}{2}}}{(p_{H_2O})}\right) \tag{2.12}$$

where R denotes the ideal gas constant (with $R = 8.314\,J\,K^{-1}mol^{-1}$) and p_{H_2}, p_{O_2} and p_{H_2O} denote the partial pressures of hydrogen, oxygen and water respectively, all in Pa.

The effects of pressure and temperature are captured well in Figure 2.5. It can be noted that higher operating temperatures reduce the requirement for electrical energy (represented by the reversible cell voltage) more than increases the need for more thermal energy (represented by the thermoneutral voltage line). Referring back to Equation 2.6, G^0 is decreased more than the increase of Q. This means that at higher temperatures, the electrolysis process requires less energy overall and the efficiency of the cell increases. Therefore, over the years, several water electrolysis technologies for high-temperature electrolysis have been developed, as will be seen further in this section.

Similarly, it can be noted that a pressure increase leads to an increase in reversible cell voltage and thus a decreasing efficiency. However, it can be relevant to operate at elevated pressure levels, as the storage is most often done at elevated pressures. Therefore, optimisation has to be made between the efficiency loss of the electrochemical reaction and the efficiency gain of the overall system (which follows from the benefit of not needing auxiliary equipment such as compressors).

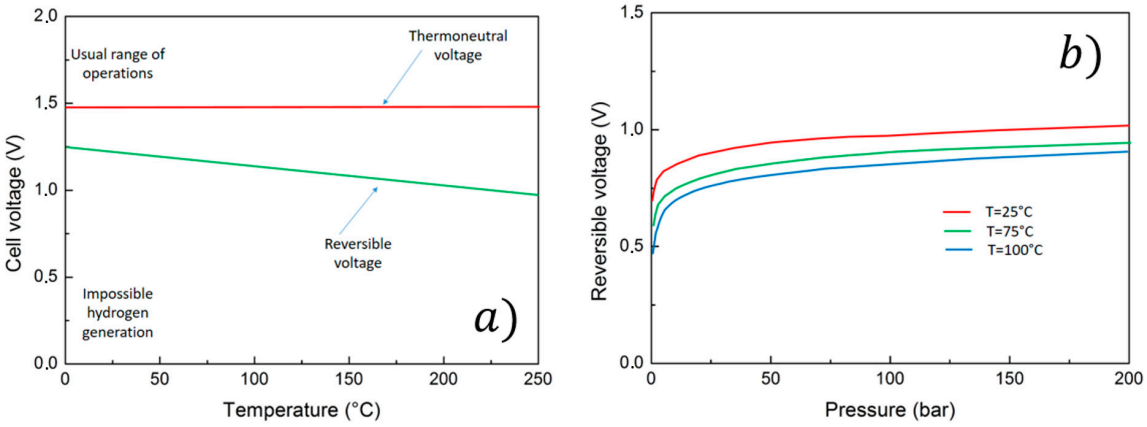

Figure 2.5: Temperature (a) and Pressure (b) effect on reversible cell voltage [47]

2.4.3. Efficiency & Overpotentials

Efficiency in general describes the performance of a system in terms of input versus output. The input in terms of electrolysers is electrical or thermal energy, whereby the output is chemical energy in the form of hydrogen molecules. The difference between the input and output are losses that can have different causes. An introduction to the main energy dissipating factors and thus the factors influencing efficiency are given within this section.

Efficiency

The efficiency of the electrolyser is key in determining the performance and thus the cost of the cell and the entire system. Therefore, it is important to have a clear understanding of the definition of efficiency. However, there are many different formulations in literature given for the efficiency of an electrolyser cell. The contribution to the diversity of efficiency definitions are amongst others, loose usage of the operating temperature and operating pressure, the usage of HHV vs. LHV and the input form of energy (e.g., thermal, electrical, etc.), which all dictate the efficiency calculations. Furthermore, energy efficiencies for electrolysis describe different parameters, being energy efficiency (theoretical or industry efficiency), voltage efficiency and Faradaic cell efficiency (also current efficiency) or are considered on different levels, being cell-level, stack-level or system-level [35, 50, 19].

To avoid ambiguous definitions, the efficiency statement as stated within the research always considers energy efficiency and is regarding the electrolyser system as a whole (system-level). Energy efficiency for the system means that the input of all energy (electrical and thermal) is compared to the hydrogen energy output of the system.
Similarly, for the efficiency used for Alkaline Electrolysers and Proton Exchange Membrane Electrolysers the HHV value will be used, as the input for these technologies is water. In the case of Solid Oxide Electrolysers, which operate at temperature ranges of $700 - 900\ ^{\circ}C$, the input is water vapour and therefore LHV will be used for efficiency calculations (as discussed in subsection 2.4.3).

As introduced in the first paragraph, many definitions exist for electrolyser efficiencies. To start, the voltage efficiency ($\eta_{Voltage}$) defines the voltage effectively used at both the anode and cathode over the required potential voltage to split 1 mol of water at STP, as in Equation 2.13 [19]. Hereby, U_a and U_c are the effective voltages of the anode and cathode respectively both in V, and U_{cell} (V) is the potential voltage applied to the cell.

$$\eta_{Voltage} = \frac{U_a - U_c}{U_{cell}} \tag{2.13}$$

Note, that the denominator does not cover the electrolyser as a system, but only the cell that produces the hydrogen. The voltage efficiency particularly proves itself useful to compare the performance of the electrolyser without components such as storage, power controllers, compressor tanks, humidifiers, etc. [53].

In the case of the Faradaic efficiency (η_F), the numerator equals the reversible cell voltage ($1.23\ V$ as defined in Equation 2.10), whilst the denominator covers the Gibbs free energy plus any losses, once again equal to the applied cell voltage (U_{cell}), as given in Equation 2.14 [54]. Finally, the thermal efficiency definition is similar to the Faradaic efficiency definition, with the mutation to the thermal energy in the numerator ($1.48\ V$ as defined in Equation 2.11).

$$\eta_F = \frac{U^0{}_{rev}}{U^0_{rev} + Losses} = \frac{1.23V}{U_{cell}} \tag{2.14}$$

In academic and scientific research the efficiency definition ($\eta_{Academic}$) as stated in Equation 2.15 is commonly used [54]. Hereby, the nominator is the reversible energy requirement (W_{rev}) to split 1 mol of water at STP in open-circuit conditions (no current flowing through the system) and the denominator equals the real amount of energy (W_{irrev}) required to split the 1 mol of water at STP (current flowing through the circuit), both in $J\ mol^{-1}$.

$$\eta_{Academic} = \frac{W_{rev}}{W_{irrev}} \tag{2.15}$$

A theoretical efficiency calculation ($\eta_{Theoretical}$) for hydrogen electrolysis is given in Equation 2.16 [55], similar to the voltage efficiency described above. However, the theoretical efficiency stated does not consider the supply of thermal energy, meaning that the efficiency value exceeds unity in specific cases. Therefore, this theoretical efficiency is not used within this research.

$$\eta_{Theoretical} = \frac{\Delta H^0}{\Delta G^0} = -\frac{\Delta H^0}{nFU_{cell}} \tag{2.16}$$

In industry, a commonly used way of defining the electrolyser efficiency ($\eta_{Industry}$) is stated in Equation 2.17 [35, 56, 54], whereby the hydrogen production rate is used. This approach leads to an efficiency not defined in percentages, but rather in an efficiency expressed in specific energy consumption of the system ($kWh\ kg^{-1}_{H_2}$ or $kWh\ Nm^{-3}_{H_2}$).

$$\eta_{Industry} = \frac{\dot{V}_{H_2} HHV_{H_2}}{P_{thermal} + P_{electrical} + P_{auxiliary}} \tag{2.17}$$

Hereby, $\dot{V}_{H_2}$ is the hydrogen production rate of hydrogen volume flow ($mol\ s^{-1}$ or $Nm^3\ h^{-1}$) as given in Equation 2.18, HHV_{H_2} the higher heating value of hydrogen ($J\ mol^{-1}$) and the power terms in the denominator are respectively the thermal, electrical and auxiliary power provided to the system (in W). When referred to as 'efficiency' within this research, the expression in Equation 2.17 is considered, being the energy efficiency on the system-level.

Aside from the energy efficiency, the hydrogen production rate also relates to the efficiency of the system. However, the relation is not concerning the energy efficiency, but the Faradaic cell efficiency, also known as the current density. The expression that follows is expressed in Equation 2.18, whereby the Faradaic cell efficiency η_F, the current I (A) fed to the electrolyser, the number of cells n_{cell}, the electron charge n $(n = 2)$ and Faraday's constant F $(C\ mol^{-1})$, express how much hydrogen is produced, the hydrogen production rate $\dot{V}_{H_2}$.

$$\dot{V}_{H_2} = \eta_F \frac{In_{cell}}{nF} \tag{2.18}$$

Note that with a Faradaic efficiency of 100%, the hydrogen production rate would be proportional to the current density. Thus, the ratio between the actual and theoretical hydrogen production rate is defined by the Faradaic efficiency. Ideally, this number is as close as possible to unity. The offset from unity is caused by gas cross permeation and parasitic reactions [35, 56]. The gas cross-over permeation is a relevant parameter for the electrolyser system, as it increases with increasing temperature and pressure levels within the electrolyser. Gas cross-over also increases with lower current densities (thus when there is a lower hydrogen production rate). This aspect will be discussed later within section 2.7, where the performance of different electrolysis technologies will be discussed at part-load operation.

The efficiency of an electrolyser can be obtained from a polarization curve. The polarization curve is a plot of the cell voltage versus the current density, as can be seen in Figure 2.6 [47], whereby a decrease in cell voltage indicates an increase in efficiency. As can be observed from the figure, the cell voltage increases with higher current density and thus higher hydrogen production rate.
The figure shows ranges of operating points since the performance of an electrolyser depends on multiple factors. Hence, per manufacturer, technology and operation conditions the shift within the range can be observed.

Lastly, it is important to note that the efficiency shown in a polarization curve is based on the cell voltage only, hence the term voltage efficiency being used within the electrochemical industry. This efficiency does not cover yet the whole system, meaning the losses within components such as the Balance of Plant (BoP), hydrogen storage, compressor, transformer, thyristor, et cetera.

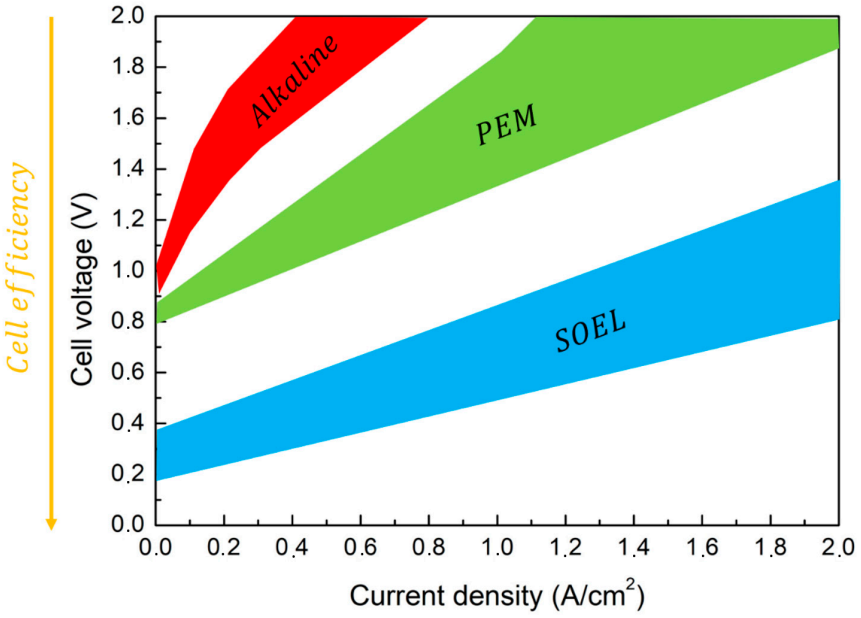

Figure 2.6: Polarization curve of the three main electrolyser technologies, from the work of Cavaliere et al. [47]

Overpotentials

The losses occurring within the system do not have one cause. Overall the electrochemical reaction will have resistance from within the system to the reaction taking place. This resistance leads to losses or energy not being used for electrolysis. To overcome these losses, the system will require extra applied voltage above the thermoneutral voltage for the reaction to take place, hence the name 'overpotential' (or overvoltage, denoted as ΔV). The three main causes for overpotential are introduced within this subsection, being activation overpotential, ohmic overpotential and concentration overpotential.

Each of the overpotentials is dominant in a different domain of the reaction or different segments of the electrolyser. The activation overpotential finds its origin in the anodic and cathodic electrodes, the ohmic overpotential is an effect of resistance within the electrode, electrolyte and (if applicable) the membrane, whereby the diffusion overpotential is predominant at higher current densities due to mass transport phenomena occurring especially at the porous electrode material.

Activation Overpotential

As the name indicates, the activation overpotential is most predominant when the activation energy of the electrochemical reaction needs to be overcome. The activation overpotential is caused by charge transfer and mass-transport phenomena, an effect of the current flowing through the electrolytic cell [20]. The activation overpotential can be distinguished by the logarithmic behaviour at lower current densities within the polarization curve.

The activation overpotential is described by the Butler-Volmer equation for charge transfer kinetics. Most commonly, the activation overpotential is split in two, one part reflecting the activation energy required at the anode to oxidise the water and the second part being the activation energy for proton transport through the membrane. Most often, the cathodic reaction is neglected, as the activation overpotential due to the anodic reaction is dominant at low current densities [20, 21]. The cathodic reaction has fast kinetics at the electrode surface, playing a minor part in the overall activation overpotential [22].

Hence, the equation for the anodic activation overpotential is given in (2.19) and follows from the Butler-Volmer equation [57, 58]

$$\eta_{act} = \frac{RT}{nF\alpha} arcsinh(\frac{j}{j_0 n}) \tag{2.19}$$

where R ($J\ K^{-1}mol^{-1}$) is the ideal gas constant, T the temperature (K) on the anode, n the number of electrons exchanged, F ($C\ mol^{-1}$) Faraday's constant, α the dimensionless charge transfer coefficient for the anode, j the electrode current density and j_0 the exchange current density, both in ($A\ m^{-2}$). Note that this is a simplification in terms of the anodic reaction only, as expressed earlier.

Ohmic Overpotential

Ohmic overpotential is the result of internal resistance to the ions and electrons moving through the electrodes, membrane, electrolyte or stack. It is the result of the slow transport of electrons and ions from the electrode to the electrolyte and vice versa [59]. The resistance is also called ohmic resistance, directly affiliated with Ohm's law. Ohmic resistance is apparent in any type of conductor material, regardless of its structure. The resistance within the electrolytic cell causes losses in the form of heat dissipation, which requires overpotential to be overcome.

The relationship for ohmic overpotential, as stated, adheres to the same linear relationship as Ohm's law (2.20) [59]

$$\eta_{ohm} = RI \tag{2.20}$$

where R (Ω) is the internal resistance and I (A) is the current flowing through the electrolytic cell. The ohmic overpotential is dominant at higher current densities and can be distinguished in the polarization curve from the linear fit.

Diffusion Overpotential

The diffusion overpotential (also concentration overpotential) is caused by mass transportation boundaries [21]. Mass transportation phenomena are induced by the flow or movement of reactants through the electrolytic cell, in this case, the electrolyser. The electrolyser unit has a purified water inlet, whilst it provides hydrogen and oxygen on the outlet. The movement of reactants needs to maintain a balance for the electrochemical reaction to take place at the membrane-electrode junction. However, this movement faces resistance through the electrode and the membrane. Therefore, this resistance needs to be overcome by an overpotential applied to the electrolyser. At higher current densities the diffusion overpotential increases, hence it is more dominant at high current densities. This follows from the logic that a faster-moving flow of reactants faces a higher resistance.

Furthermore, the diffusion overpotential also covers another phenomenon in the electrolysis cell, namely the bubble effect. The hydrogen and oxygen gasses produced within the aqueous electrolyte environment are present in the form of bubbles. This effect is known as the bubble effect [47]. The greater the volume these bubbles cover, the less effective cell area is left for the reactions to take place, both within the electrolyte and on the electrode surface. An increase in current density leads to an increase in both the number and the size of the bubbles, and thus in the volume occupied by the bubbles [47], whilst an increase in pressure leads to a decrease of gas bubbles due to faster transport [35]. To mitigate the effects of bubbles, zero-gap electrolyser configurations are being developed [50].

With the use of the Nernst equation, the diffusion overpotential can be estimated (2.21) [21]

$$\eta_{diff} = \frac{RT}{nF} \ln \frac{C_1}{C_0} \tag{2.21}$$

where R ($J\ K^{-1}mol^{-1}$) is the ideal gas constant, T the temperature (K), n the number of electrons exchanged, F ($C\ mol^{-1}$) Faraday's constant, C_1 is the concentration of the flow through the electrolyser and C_0 is the reference concentration, both in $mol\ m^{-3}$. Lastly, it is noted that the reference equation in (2.21) is most often split between an anodic and cathodic diffusion overvoltage equation, yielding two similar equations.

Mass Flow Rates

As described in the subsection regarding the Diffusion Overpotentials (Equation 2.4.3), mass transport phenomena play an important role within the cell and the continuation of the electrochemical reaction. The flow of water and gas (both oxygen and hydrogen gas) are caused by pressure differences, water concentration gradients and electro-osmotic drag [21]. The flow of mass through the electrodes and membrane depends then again on the porosity of the materials, the size of the mass and the intermolecular bonds. Although mass flow is relevant for the operation of the electrolyser, it is not discussed in any detail, as there is only an indirect contribution of mass transport phenomena to the cause of losses.

Total Overpotential and Cell Voltage

With the efficiency and the overpotentials of the electrolysers defined, it is now time to discuss the overall applied cell voltage. This is a sum of all previously introduced definitions as seen in (2.22).

$$U_{cell} = U_{rev} + \eta_{act} + \eta_{ohm} + \eta_{diff} \tag{2.22}$$

A graphical summary of all the above theoretical frameworks is neatly given in Figure 2.7 for the ideal cell behaviour as a function of the applied cell voltage (called 'potential' in the figure) [47].

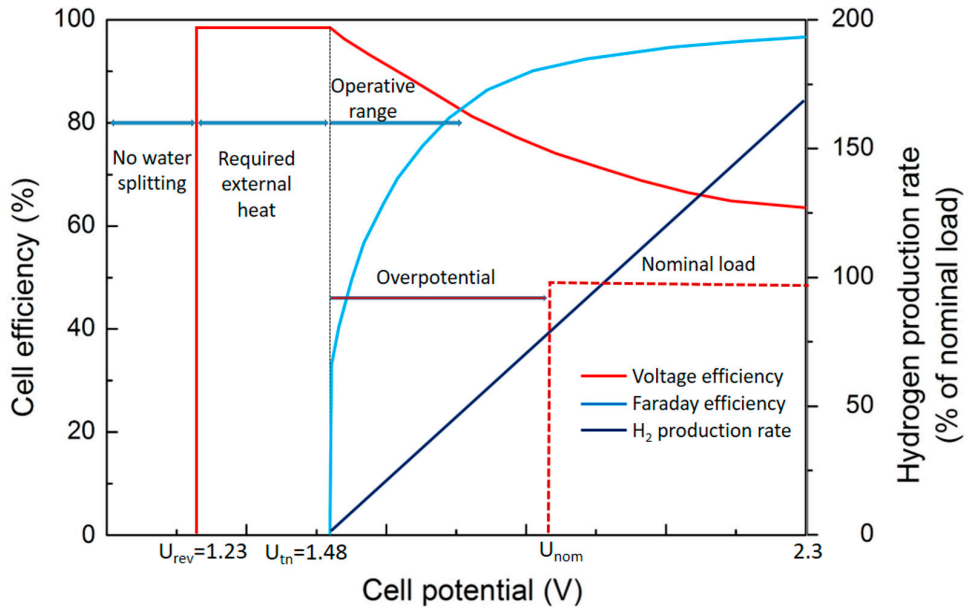

Figure 2.7: Cell behaviour as a function of the applied cell voltage, from the work of Cavaliere et al. [47]

2.4.4. Alkaline Electrolysis (AEL)

Alkaline Electrolysis (AEL or sometimes Alkaline Electrolysis Cell - AEC) is the most mature water electrolysis technique. It has been in use for hydrogen production in industrial processes since the beginning of the 20th century [60]. The AEL is characterised by the usage of a highly concentrated alkaline aqueous solution, most often consisting of potassium hydroxide (KOH) or sodium hydroxide (NaOH). The system furthermore consists of two electrodes functioning as cathode and anode, and immersed in the aqueous solution, separated with a diaphragm. A schematic system overview is given in Figure 2.8 from [61].

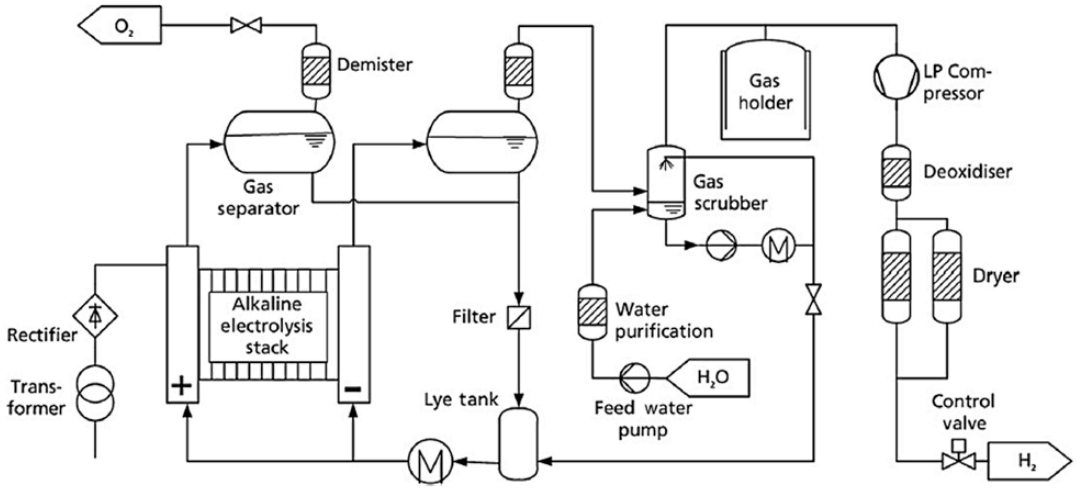

Figure 2.8: Schematic system overview of Alkaline Electrolyser, from the work of Holst et al. [61]

In AEL the hydroxide anions (OH-) are the charge-carrying ions and are carried through the diaphragm by the movement of water. The evolution of hydrogen (HER) occurs at the cathode, after the application of an external electrical current, decomposing water into hydrogen and hydroxide anions. At the anode the Oxygen Evolution Reaction (OER) takes place, yielding to the generation of oxygen and water by the oxidation of hydroxide-anions [24]. The half-cell reactions and total reaction for AEL are given in (2.23 - 2.25). To prevent critical contamination levels within the electrolytic cell, the hydrogen and oxygen have to be timely removed, but can also be achieved with the controlled circulation of the alkaline liquid solution [56].

$$\text{Anode: } 2OH^- \rightarrow \frac{1}{2}O_2 + H_2O + 2e^- \tag{2.23}$$

$$\text{Cathode: } 2H_2O + 2e^- \rightarrow H_2 + 2OH^- \tag{2.24}$$

$$\text{Total reaction: } H_2O \rightarrow H_2 + \frac{1}{2}O_2 \tag{2.25}$$

AEL systems are cost-competitive over other electrolysis technologies, as the system is composed of abundant electrode and electrolyte materials. Electrodes are most often made of iron or nickel steel [35]. It is furthermore a mature technology (Technology Readiness Level of 9) [62], long lifetimes and overall good efficiencies [55].

Challenges for the AEL are its limited current density and a limited load range. Note that with a low current density the hydrogen production rate is also low as introduced in subsection 2.4.3. The limited load range means that the AEL will operate within a window of 20-100% of nominal operation. At load levels below the threshold of 20%, the gas purity cannot be maintained, creating an explosion hazard [63]. Either the system needs to be turned off or a stand-by voltage needs to be applied. An extra reason to run at standby voltage is the degradation of the electrode coatings in the catalyst due to the reverse voltages when the system is switched on/off (cycling) [63, 64, 65].

To sum up the main characteristics of the AEL, the reader is referred to Table 2.3. All parameters are noted for the most extreme values found within the literature (both lower as well as an upper boundary), as the values differ highly per manufacturer of AEL and developments are followed-up rapidly.

Table 2.3: Main characteristics of Alkaline Electrolysis **system**[1] [24, 35, 55, 56, 66, 67, 68, 69]

Property	Value	$Unit$
Capacity (stack)	24	MW
Capacity	162	MW
Lifetime (stack)	90,000-120,000	hr
Lifetime	20-30	y
Operating Pressure range	1-3	MPa
Operating Temperature range	40-90	$^{\circ}C$
Operating Voltage range	1.8-2.4	V
Operating Current Density range	0.2-0.4	$A\ cm^{-2}$
Load range (% of nominal load)	20-100	%
Specific energy consumption	5.0-5.9	$kWh\ Nm^{-3}$
Efficiency (HHV)	60-71	%
CAPEX	800-1,500	$€\ kW^{-1}$
OPEX (excl. electricity)	17-51	$€\ kW^{-1}y^{-1}$
Warm start-up time range	60-300	sec
Cold start-up time range	3,600-7,200	sec
Degradation	0.25-1.5	$\%_{\eta_{LHV\ Stack}}\ y^{-1}$
H_2 **Gas purity**	99.5-99.9	%

2.4.5. Proton Exchange Membrane Electrolysis Cell (PEMEL)

With the introduction of Proton Exchange Membrane Electrolysis (PEMEL), also referred to as Polymer Electrolyte Membrane Electrolysis or sometimes Solid Polymer Electrolyte (SPE) [56], the need for caustic and strong bases changed. This electrolysis technology, first introduced by General Electric in the sixties, makes use of a 'Nafion'™ or similar membrane, which is a highly conductive fluorinated membrane. The cations (H^+, also protons) created within the electrochemical cell can easily permeate through this membrane. In Figure 2.9 a schematic system process flow diagram is depicted for the PEMEL [61].

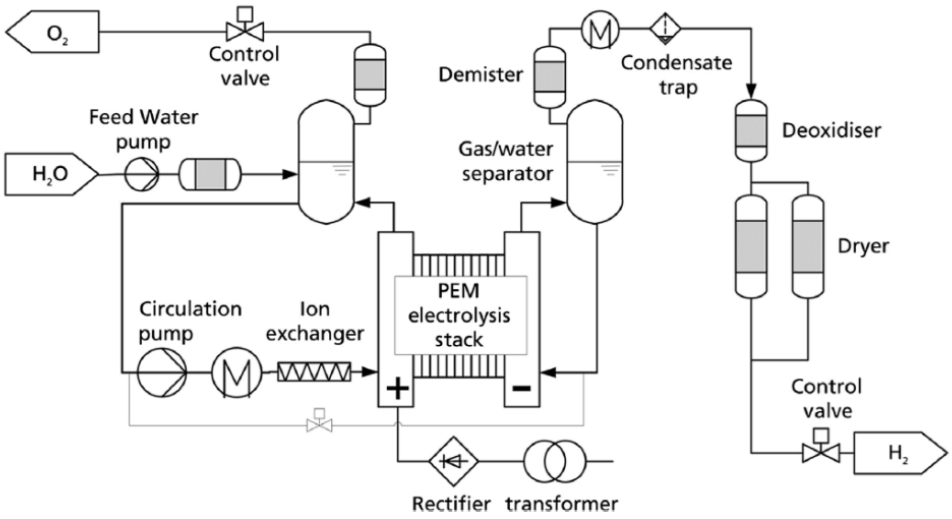

Figure 2.9: Schematic system overview of Proton Exchange Membrane Electrolyser, from the work of Holst et al. [61]

[1] Unless specified otherwise.

For the PEMEL water (H_2O) is fed into the system on the anode and the OER takes place, meaning the water is split into oxygen (O_2), cations (H^+) and electrons (e^-). The cations are carried through the fluorinated membrane, to recombine with the electrons driven through the external circuit to form hydrogen (H_2). The half-cell reactions and total reaction for PEMEL are given in (2.26 - 2.28).

$$\text{Anode: } H_2O \rightarrow \frac{1}{2}O_2 + 2H^+ + 2e^- \tag{2.26}$$

$$\text{Cathode: } 2H^+ + 2e^- \rightarrow H_2 \tag{2.27}$$

$$\text{Total reaction: } H_2O \rightarrow H_2 + \frac{1}{2}O_2 \tag{2.28}$$

The benefits of the PEMEL are numerous, amongst others: high gas purity and current density, wider operating range, faster ramping and capability for cycling. The last four parameters are all indicators that the PEMEL can operate more dynamically, for which it is well known within the industry. Furthermore, higher current densities (>2 $A\ cm^{-2}$), mean a higher hydrogen production rate, lower Operation Expenditures (OPEX), but also a more compact system size, especially relevant in applications such as the automotive or aerospace industry. With these technical parameters known, PEMEL is often cited as one of the future electrolyser technologies.

However, also the PEMEL knows its limitations and disadvantages. First and foremost, relevant components of the PEMEL are more expensive when compared to AEL [56, 70]. A good comparison can be drawn for the Nafion membrane, one of the key components of the PEMEL. This membrane is stated to be $800 - 1100\ \$\ m^{-2}$, whereas the membrane for AEL has a negligible cost [71]. But also the usage of noble (and rare) metals such as platinum, iridium and rhodium as catalysts, both at the anode and cathode, drive up the costs for PEMEL [72]. Another point of concern for the PEMEL is that the stack sizes are comparatively smaller, therefore making it necessary to use more stacks to reach bigger system sizes, resulting in a higher system cost. Lastly, the lifetime of the PEMEL is limited, with a less commercialised is not as developed as AEL, with a reported TRL of 7 to 8 [62].

The main characteristics of PEMEL technology are summarised in Table 2.4. All parameters are noted for the most extreme values stated within the literature (both lower as well as an upper boundary), as the values differ highly per manufacturer of PEMEL and developments are followed-up rapidly.

Table 2.4: Main characteristics of Proton Exchange Membrane Electrolysis **system**[2] [24, 35, 55, 56, 66, 67, 68, 70, 72, 73, 74]

Property	Value	$Unit$
Capacity (stack)	3	MW
Capacity	20	MW
Lifetime (stack)	20,000-62,000	hr
Lifetime	3-30	y
Operating Pressure range	10-20	MPa
Operating Temperature range	50-80	$^{\circ}C$
Operating Voltage range	1.8-2.2	V
Operating Current Density range	0.6-3.0	$A\ cm^{-2}$
Load range (% of nominal load)	0-100	%
Specific energy consumption	5.0–6.5	$kWh\ Nm^{-3}$
Efficiency (HHV)	54–71	%
CAPEX	1,860-2,320	$€\ kW^{-1}$
OPEX (excl. electricity)	32-66	$€\ kW^{-1}y^{-1}$
Warm start-up time range	<30	sec
Cold start-up time range	300-600	sec
Degradation	0.5-2.5	$\%_{\eta_{LHV\ Stack}}\ y^{-1}$
H_2 **Gas purity**	99.9-99.9999	%

[2] Unless specified otherwise.

2.4.6. Solid Oxide Electrolysis cell (SOEL)

With electrolyser technologies developing, research has focused on increasing the efficiency of electrolysers. Despite the overall energy demand (electrical energy + thermal energy) being constant, an increase in operating temperature decreases the need for electrical energy required for splitting the water molecules [35]. This implies an increase in electrolysis efficiency, especially with the application of waste heat resources. Therefore, lots of research has been put into high-temperature electrolysis technologies, with Solid Oxide Electrolysis cell (SOEL, also High Temperature Electrolysis - HTEL) as one of the most prominent alternatives.

The working principle for SOEL differs from the previously introduced types of electrolyser, such that the operating temperature starts from $500\ ^{\circ}C$ and upwards. Therefore, the system does not use liquid water, but rather steam, meaning the efficiency of the system is calculated with the LHV of water and thus increasing the overall efficiency.

The SOEL makes use of either oxide (O^{2-}) conductors, such as Yttria-stabilised zirconia (YSZ) or ceramic proton conductors. The electrode most often used is Nickel (Ni) [75]. A schematic system overview for SOEL is depicted in Figure 2.10 [56].

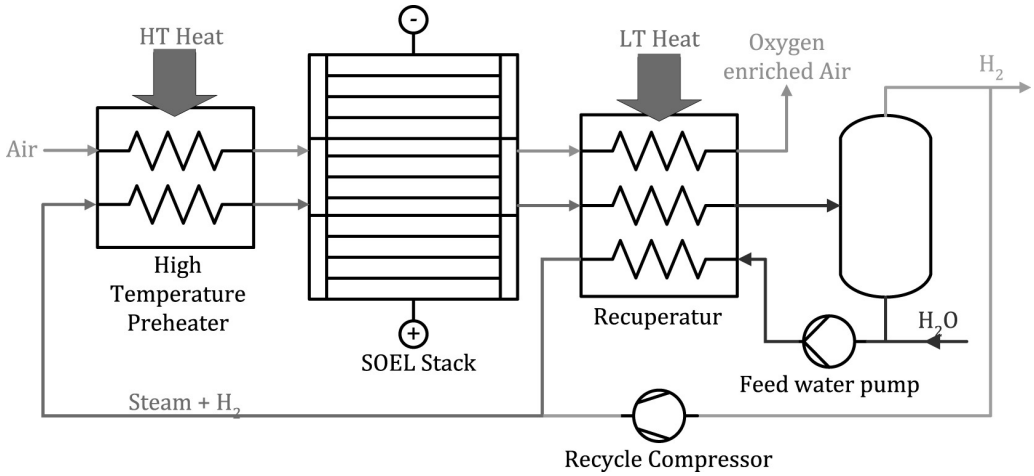

Figure 2.10: Schematic system overview of Solid Oxide Electrolyser Cell, from the work of Buttler et al. [56]

Although different half-cell reactions with SOEL are possible (as co-electrolysis of carbon dioxide (CO_2) is possible at higher temperatures), the half-cell reactions and total reaction stated in (2.29 - 2.31) are common half-cell reactions for the production of hydrogen [75]. A benefit of co-electrolysis is the fact that it reduces CO_2, a GHG, whilst producing hydrogen.

$$\text{Anode: } O^{2-} \rightarrow \frac{1}{2}O_2 + 2e^- \tag{2.29}$$

$$\text{Cathode: } H_2O + 2e^- \rightarrow H_2 + O^{2-} \tag{2.30}$$

$$\text{Total reaction: } H_2O \rightarrow H_2 + \frac{1}{2}O_2 \tag{2.31}$$

The advantages of SOEL are its high efficiency, the ability to produce hydrogen with co-electrolysis, which results in a reduction of both carbon dioxide, but also the production of syngas (synthetic gas), by the combination of steam and CO_2 and its compact form [35, 75]. From syngas hydrocarbons such as liquid fuels can be produced, posing an alternative fuel to mitigate GHG emissions [66]. The high efficiency is an effect of better reaction kinetics, more favourable thermodynamic heat utilisation and the possibility to use both steam and heat as input [56]. More precisely, the capability of using heat increases from 15% at room temperature, to approximately one-third at $1000\ ^{\circ}C$ [35]. Heat is both cheaper than electricity and leads to the possibility to reuse byproducts such as latent or waste heat.

Furthermore, an interesting benefit of the SOEL is that experiments from several manufacturers show that it can operate both as an electrolyser, producing hydrogen, and as a fuel cell, generating electricity from hydrogen [56]. However, this feature is still in an experimental phase and requires further development.

Disadvantages arise with a low TRL for SOEL of 6-7 [62]. This directly relates to a very high CAPEX (almost triple the price for AEL) [56, 66, 67], but also to a short lifetime. The poor durability performance, due to the high degradation of ceramic materials used within the high-temperature environment, is the focal point in many types of research [70, 62]. Furthermore, stability uses arise with the usage of SOEL due to its higher operating temperatures, making further research and development a necessity for commercialisation [76].

To conclude the introduction for SOEL, the main characteristics of this electrolysis technology are included in Table 2.5. All parameters are noted for the most extreme values stated within the literature (both lower as well as an upper boundary), as the values differ highly per manufacturer of SOEL and developments are followed-up rapidly.

Table 2.5: Main characteristics of Solid Oxide Electrolysis Cell **system**[3] [35, 56, 66, 67, 68, 72, 73, 77]

Property	Value	$Unit$
Capacity (stack)	0.05	MW
Capacity	n.a.[4]	MW
Lifetime (stack)	8,000-20,000	hr
Lifetime	n.a.	y
Operating Pressure range	1-15	MPa
Operating Temperature range	500-1,000	$^{\circ}C$
Operating Voltage range	0.7-1.5	V
Operating Current Density range	0.3-2.0	$A\ cm^{-2}$
Load range (% of nominal load)[5]	-100/+100	%
Specific energy consumption	3.7-3.9	$kWh\ Nm^{-3}$
Efficiency (LHV)	76-81	%
CAPEX	>2,000	$€\ kW^{-1}$
OPEX (excl. electricity)	n.a.	$€\ kW^{-1}y^{-1}$
Warm start-up time range	300-900	sec
Cold start-up time range	>10,800	sec
Degradation	3-50	$\%_{\eta_{LHV\ Stack}}\ y^{-1}$
H_2 **Gas purity**	n.a.	%

[3] Unless specified otherwise.
[4] For all 'n.a.', data not available during conduction of this research.
[5] Due to the ability to work both in electrolyser and fuel cell modes.

2.4.7. Summary of Electrolysis Technologies

With three distinct water electrolysis technologies introduced, a short recap of the technologies and comparisons between the three are given within this section. First off, the technologies are captured in a single image, to show the different working principles, as depicted in Figure 2.11 [75].

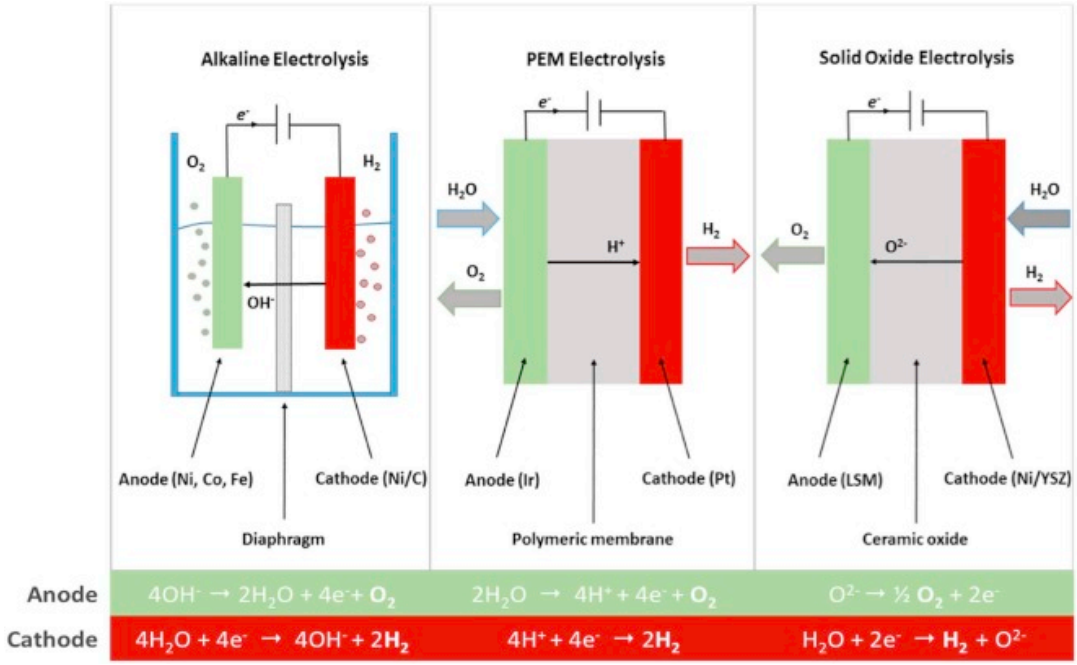

Figure 2.11: Comparative overview of the working principles of the AEL, PEMEL and SOEL, from the work of Sapountzi et al. [75]

Lastly, a final comparison of advantages and disadvantages between the technologies is drawn in Table 2.6. Hereby, the three technologies are compared amongst themselves, meaning that terms such as 'low', 'high' or likewise are in direct relationship to one other.

Table 2.6: Comparison in between AEL, PEMEL and SOEL technologies [35, 50, 55, 56, 62, 63, 64, 65, 66, 67, 68, 70, 71, 72, 75]

AEL	PEMEL	SOEL
Advantages		
Capacities on MW-scale	High current densities	High system efficiencies
TRL of 9, well established	Big partial-load range	Abundant materials
Cost-competitive (low CAPEX)	High hydrogen purity	Co-electrolysis, production of syngas
Reliable system	High voltage efficiency	Operation in electrolyser and fuel cell mode
Durability	Compact system	Use of heat waste
Abundant materials	Fast ramping	
Long lifetime	Capability for cycling	
Disadvantages		
Low current density	High CAPEX	TRL of 6-7
Partial-load range limited	Smaller stack size	Very high CAPEX
Low hydrogen production rate	Shorter lifetime	Very short lifetime
Low operational pressure	Difficulties for scaling up	Poor durability
Low hydrogen purity		High degradation of materials
Spacious system		Non-stable performance
		Non-commercialised technology
		Very small stack size

2.5. Hydrogen Storage Technologies

As introduced in section 2.3, the benefits of hydrogen manifest themselves most when used as a storage option for longer terms. Therefore, this section is devoted to the widely accepted storage options for hydrogen, with an assessment of its benefits and disadvantages. Amongst these technologies are considered compressed hydrogen storage, liquid hydrogen storage and linepack (storing hydrogen in the steel pipe infrastructure). Other storage options such as chemical storage (in metal hydrides or chemical hydrides) and underground storage options are not discussed. The chemical storage options are not considered as these technologies require $33 - 82$ times more energy to release the stored hydrogen (e.g., $0.45\ MJ\ kg^{-1}$ for liquid hydrogen and $37\ MJ\ kg^{-1}$ for salt-like metal hydrides) [78, 79]. Underground storage is outside the scope of this research as it is a technology used for storing hydrogen on a very large scale and is bound to specific locations, which is not considered within the case study.

First and foremost, it is worth mentioning the gravimetric energy density of hydrogen is the highest among the fuels. The gravimetric energy density ($MJ\ kg^{-1}$) is a ratio that defines the amount of energy stored per kilogram of fuel, which is triple for liquid hydrogen and or compressed hydrogen when compared to gasoline or methane. However, the downfall for hydrogen technologies is their relatively low volumetric energy density ($MJ\ L^{-1}$), which means the amount of energy stored per litre of fuel. This behaviour is well visualised in Figure 2.12, which shows a comparison for both the gravimetric as well as the volumetric energy densities for different types of fuels [80].

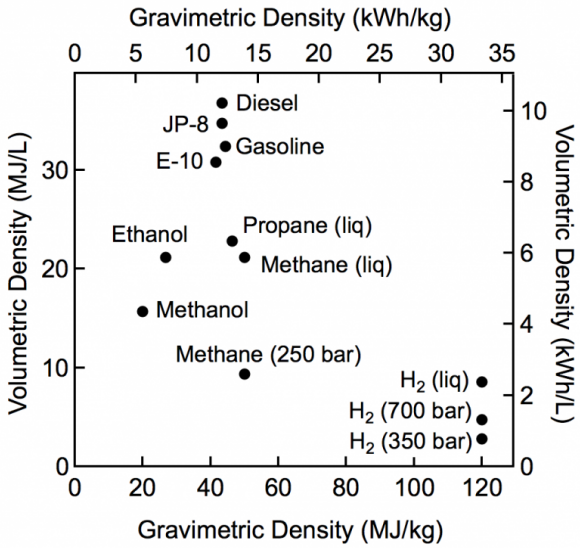

Figure 2.12: Gravimetric energy density versus volumetric energy density for different types of fuel based on LHV, from the work of the U.S. Department of Energy [80]

One might have already noticed the fact that hydrogen is stated to be either in liquid form or at pressures up to $350\ bar$ ($35\ MPa$) and $700\ bar$ ($70\ MPa$). However, hydrogen at standard atmospheric conditions is neither liquid nor dense, with a density of $0.09\ kg\ m^{-3}$. Therefore, hydrogen either needs to be cooled, below its boiling point at $-252.9\ ^{\circ}C$ or $20.25\ K$ or needs compression to create a more dense substance [81].

Except for previously mentioned challenges for hydrogen storage at dense volumes, hydrogen also exhibits several characteristics, such as permeability through solids, that need to be dealt with when storing it. This permeability can cause damage to materials, such as hydrogen blistering, which is a crack in the soft zone of the materials (such as steels) used for containing the hydrogen. Furthermore, as hydrogen is a light substance, it disperses fast, with proper ventilation systems, this characteristic is used as an advantage. To prevent damage by hydrogen, the usage of the materials in contact with hydrogen will be important, a combination of an impermeable protective coating and anti-corrosive materials can be of great help [82].

2.5.1. Compressed Hydrogen Storage

Compressed or pressurised hydrogen storage, as introduced is one of the ways to increase the volumetric energy density of hydrogen. The hydrogen gas is contained in steel or aluminium cylindrical vessels (Type-I), most often operated at an elevated pressure of $200\ bar$ ($20\ MPa$). The technology is widely developed (TRL9), as the gas vessels are used not only for the storage of hydrogen but for any type of gas. Alongside the vessel(s), the storage system consists of equipment such as the compressor and an expander, of which the vessel and the compressor are the main cost drivers [83].

Increasing the pressure of the hydrogen gas, has unsolicited side effects, such as:

1. Energy is consumed to compress the hydrogen, especially at atmospheric pressures that are higher than $30\ MPa$;
2. The compressed gas vessels that contain the hydrogen require a lot of material, which makes this type of storage technology less feasible for the transport sector;
3. Hydrogen at elevated pressures is not behaving as an ideal gas but is more voluminous than one would expect from an ideal gas. Therefore, the hydrogen gas is cooled down (isothermal) during the compression, to reduce volumetric expansion. This non-ideal gas behaviour is also depicted in Figure 2.13, where it is evident that the relationship is non-linear.

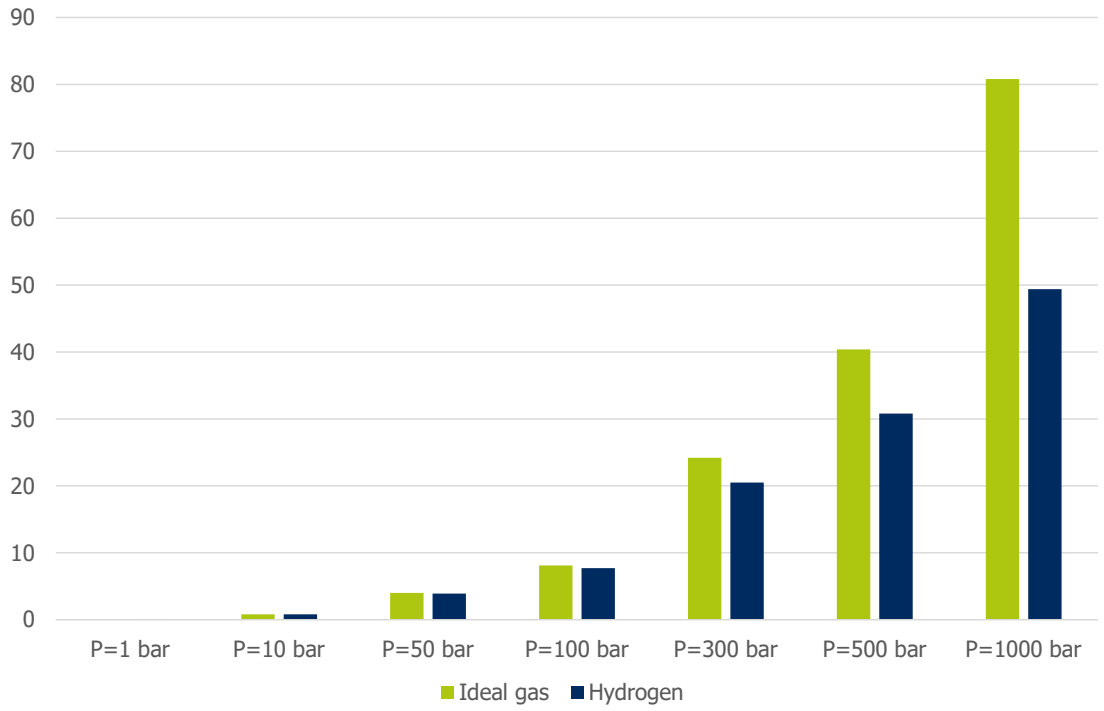

Figure 2.13: Density of hydrogen gas ($kg\ m^{-3}$) compared to an ideal gas, at $T = 298K$, from the work of Mulder et al. [12]

Compressed storage is a technology that is widely commercialised and scalable. It is a technology which is simple to implement, highly reliable, and cost-competitive, but also performs on high energy efficiencies [84]. Since it is also a technology that is capable of dynamic operation, it is chosen as the storage option for this research.

It is worth mentioning that the dynamic operation capabilities for the compressed storage vessel are limited by the charge and discharge rates, as high rates of hydrogen flow will cause big temperatures and pressure fluctuation. The temperature fluctuations will cause thermal stress, leading to the failure of the vessels. However, this limitation is outside of the scope of this research.

2.5.2. Liquid Hydrogen Storage

Liquid hydrogen storage (also often cited as cryogenic hydrogen storage) is a form of storage whereby once again storage vessels are used. However, hydrogen (as a gas) is not made denser by compression but made denser by cooling it down below its boiling point ($-252.9\ ^{\circ}C$ or $20.25\ K$), creating liquid hydrogen. Liquid hydrogen is denser than gaseous hydrogen in any case, as hydrogen needs to be compressed up to $800\ bar$ or $80\ MPa$ to be on the same density. A value that is not being reached in reality [81].

The hydrogen liquefaction cycle is diverse, however, most often the Hampson-Linde cycle is used. This cycle is based on the phenomena known as the Joule-Thomson expansion. The Joule-Thomson expansion dictates that an ideal gas stays at a constant temperature during expansion as the enthalpy change is equal to zero. However, as stated, hydrogen does not behave as an ideal gas. Therefore, the Joule-Thomson expansion with hydrogen leads to an increase or decrease in the gas's temperature, depending on the conditions. This behaviour is captured in (2.32), whereby a positive Joule-Thomson coefficient (μ_{JT}) means the gas cools down in the expansion and a negative Joule-Thomson coefficient means that the gas warms up in expansion:

$$\mu_{JT} = \left(\frac{\delta T}{\delta P}\right)_H = \frac{V}{C_p}(\alpha T - 1) \tag{2.32}$$

with μ_{JT} the Joule-Thomson coefficient at constant enthalpy (H), δT the change in temperature (K), δP the change in pressure (MPa), V the volume of the gas (m^3), C_p the heat capacity of the gas at constant pressure ($J\ K^{-1}\ kg^{-1}$) and α the thermal expansion coefficient for the gas ($^{\circ}C$) [12].

Hydrogen between $300\ K - 190\ K$ ($26.85^{\circ}C - -83.15^{\circ}C$) and below $50\ bar$ ($5\ MPa$) shows an inversion of the Joule-Thomson coefficient (between a positive and a negative value). Therefore, the Joule-Thomson expansion process is not used within this temperature range, but rather the throttling method is used. Hereby, the hydrogen is compressed and cooled down in a heat exchanger, whereby the temperature is kept constant (isenthalpic) and the pressure is decreased. This way part of the hydrogen liquefies, and the rest (which remains as a gas) is put through the same process once again, over and over again [81].

The aforementioned throttling process is very energy intensive [81]. The storage of hydrogen at low temperatures also requires a serious amount of insulation or 40% of energy loss for cooling [85]. Furthermore, liquid hydrogen (as with every gas) has boil-off, meaning that leakage and intruding heat leads to the formation of hydrogen gas. As the gaseous hydrogen is less dense, the pressure in the tank increase, leading to failure and safety concerns [86]. All in all, liquid hydrogen storage is not a method used commonly, despite the potential for highly dense storage.

2.5.3. Linepack

Another option for hydrogen storage is in the pipelines used for transport and distribution. This type of storage is also considered with natural gas and is built upon the principle that a gas or liquid can be compressed and expanded. If the hydrogen flow at the inlet is bigger than the hydrogen flow at the outlet, the volume of gas (or liquid) in the pipeline system will increase, leading to higher internal pressure in the pipeline. The hydrogen can also be compressed before inserting into the pipeline, exerting a similar result. An example of hydrogen infrastructure as depicted by Gasunie is given in Figure 2.14 for The Netherlands [87].

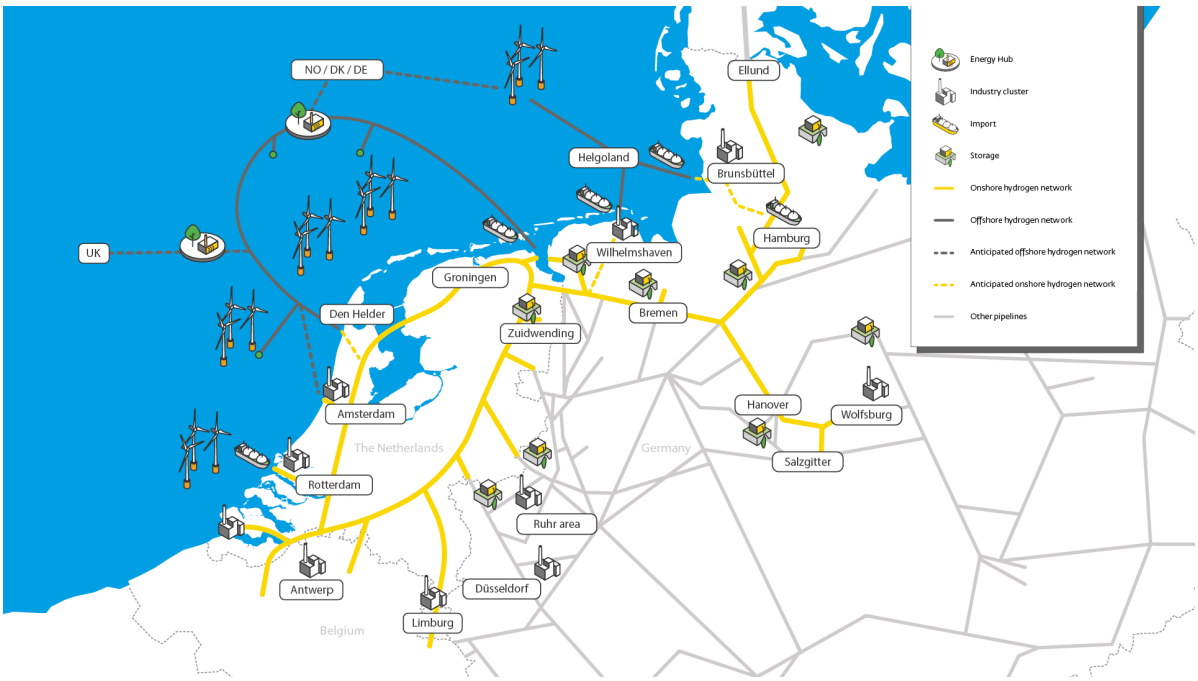

Figure 2.14: Proposed hydrogen network by Gasunie [87]

Within the introduction of linepack, it is assumed as if hydrogen can be stored similarly in the pipelines as natural gas. However, storing hydrogen in steel pipelines is not as straightforward as posed. Firstly, hydrogen insertion into a steel pipeline may cause embrittlement of the pipeline, as a consequence of hydrogen absorption into the steel, leading to material defects and possibly leading to failure [88]. To prevent embrittlement of the steel infrastructure, different solutions have been posed, such as to thicken the material (meaning current pipeline infrastructure cannot be used), but also the usage of drier hydrogen with a relative humidity level below 60% [89].

Secondly, considering the hydrogen energy content, to store the same amount of energy with hydrogen, more than three times the volume of natural gas should be stored ($40\ MJ\ Nm^{-3}$ for natural gas to $12\ MJ\ ^{-3}$ for hydrogen). To compensate for the difference in energy content the hydrogen flow needs to maintain a higher speed, inducing more vibrations, but also requires a change of compressor units as the hydrogen molecules are very small and require different and more expensive types of compressors [89, 90].

Lastly, it is worth mentioning that the pipeline equipment, such as the valves, seals, fittings and other materials will have to be retrofitted to be used with hydrogen [88, 89]. If not engineered properly hydrogen leakage and permeation might lead to hazardous situations.

2.6. Hydrogen Fuel Cell

Creating and storing chemical energy in hydrogen atoms is one part of the equation when considering the electrical power systems of the future. Using chemical energy in electrical form, means the hydrogen atoms need to be re-converted to generate electricity. This is done with a device found in 1839 by William Grove [91]: the fuel cell, a device that has hydrogen (and oxygen) as input and electricity as output. As hydrogen atoms are its input, one can imagine this is a very clean way of producing electricity, as the resulting products of the reconversion are: water, heat and electricity [92]. Therefore, fuel cells have been of interest in recent 7developments for fuel alternatives, considering applications in transport (cars, boats, aeroplanes), but also in industrial applications.

In principle the fuel cell is the same device as the electrolyser, only operating in the opposite direction caused by the current flow in the opposite direction [93]. As is the case with electrolyser units, the fuel cells are present in the same configurations, meaning Alkaline Fuel Cell (AFC), Proton Exchange Membrane Fuel Cell (PEMFC), Solid Oxide Fuel Cell (SOFC), et cetera. A comparison in between the technologies is drawn in Figure 2.15 for Proton Exchange Membrane devices [25].

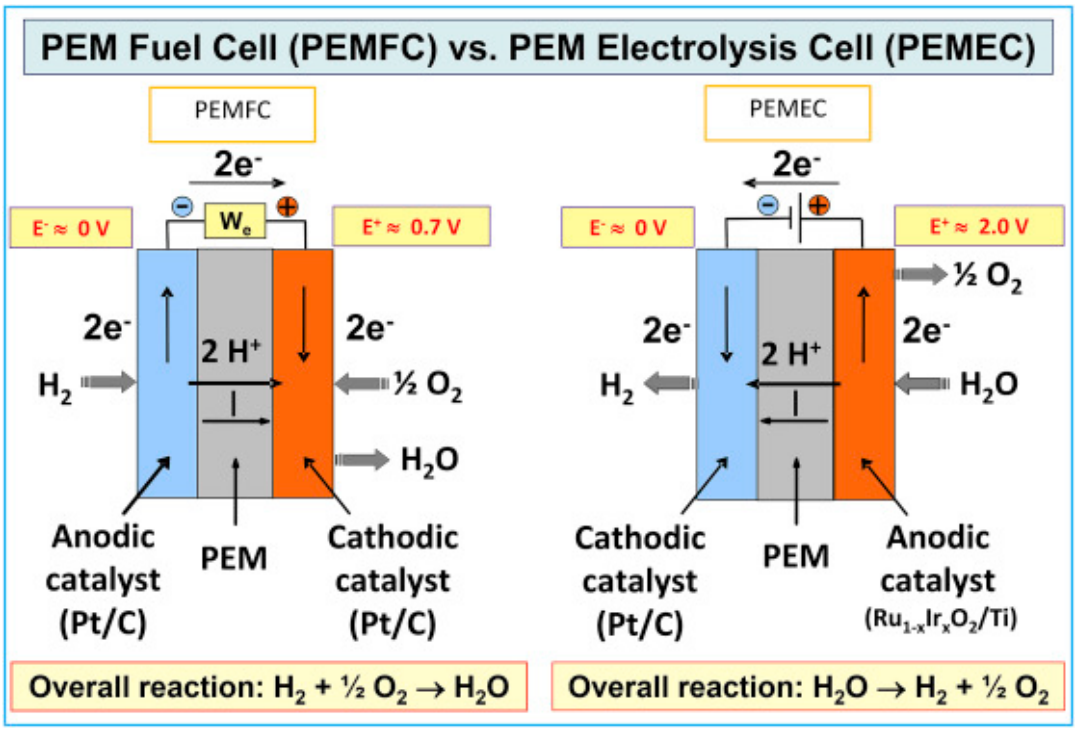

Figure 2.15: Proton Exchange Membrane Fuel Cell versus Proton Exchange Membrane Electrolyser, from the work of Guenot et al. [25]

Aside from the fuel cell being a green way of producing electricity, the combustion of hydrogen is also done at a higher efficiency when compared to fossil fuel combustion engines. The fuel cell technology also operates at low noise levels and neither does emit Green House Gases or pollutants that could lead to smog [92, 91].
However, disadvantages of the usage of fuel cells are: high system costs, low lifetime and durability (especially under dynamic operation), low current and power densities (due to slow reaction rates) and finally and funnily the fact that fuel cells can only operate with hydrogen as a fuel.

With electrolysis and reconversion being similar technologies, the section on fuel cells is kept dense. However, it is good to note that within this research the PEMFC is chosen as the fuel cell technology for the reconversion of electricity. Mainly, because the PEMFC shows the most potential for dynamic operation, meaning cycling, has a low turndown ratio and high efficiency.

2.7. Technical Parameters and Operational Policies

With the technologies of the system to be modelled introduced, the technical parameters and operational policies of the electrolysis technologies will be discussed within this section. Here, with technical parameters and operational policies is meant the limitations coming forth from the technological aspect and operational requirements for electrolysis units. These units will be prone to optimisation in the mathematical model and case study, as they can be represented with constraints, and therefore are discussed more elaborately.

2.7.1. Nominal Load and Part-Load Operation

Electrolysers units are, similar to gas plants, designed to operate at full capacity (also full-load, rated power or rating). The full capacity is often referred to as 'nominal', meaning that at nominal operation the electrolyser is running at 100% capacity. However, with the increase in vRES with an intermittent character, the demand for flexible operation of storage technologies has risen, emphasising the research and development of part-load operation for electrolyser units.

Interestingly, the performance of the electrolyser (on a cell or stack level) increases with the part-load operation. This effect is caused by a reduction of the current density and a limited Joule effect (heating of the unit due to Ohmic resistance) [35]. However, the efficiency of the system as a whole (including the Balance of Plant, rectifiers, etc.) decreases as the equipment is oversized, leading to an increase in energy consumption [56]. This behaviour is well captured in Figure 2.16, where the power consumption for the PEMEL electrolyser depicted increases at part-load operation almost equivalent to the increase in power consumption of all the auxiliary equipment.

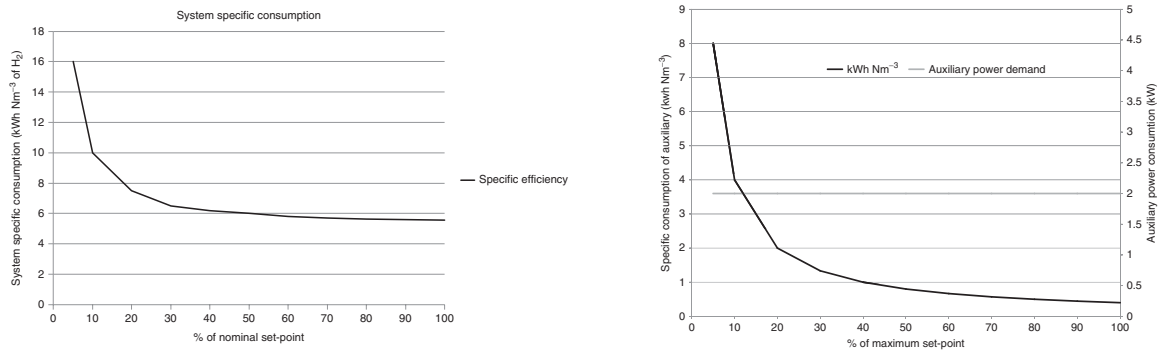

Figure 2.16: Comparison in between the system and auxiliary specific power consumptions for a 5 $Nm^3\ h^{-1}$ PEMEL, from the work of Godula-Jopek et al. [35]

Aside from the auxiliary equipment sizing, another loss at part-load is caused by a decrease of the Faradaic efficiency at part-load operation (η_F as introduced, relating the hydrogen production rate to the applied current density). The η_F decreases both due to an increase in parasitic current losses and due to an increase in cross permeation of hydrogen and oxygen gases, both at lower current densities [94]. The value for the Faradaic efficiency at nominal operation is reported to be in the range of 97.5-99.9%, whilst a strong decrease is reported at lower current densities [94, 95]. The parasitic current shows a linear relationship with the cell's potential, thus at higher current densities, the fraction becomes negligible. Furthermore, in the case of AEL, the parasitic current losses play a vital role [56].

2.7.2. Load Range

The load range is a term used for electrolysers often and indicates the operating window for the electrolyser. More precise, it is the percentage of the nominal load the system needs to maintain to stay operational. This term is relevant because not all electrolyser technologies can operate in the entire window from $0 - 100\%$. In literature the load range is also frequently translated into a turndown ratio, meaning the ratio of the nominal load for which the system is turned down, effectively indicating the same operating window for the electrolyser.

In terms of dynamic operation, the conventional AEL can be typically operated at $\sim 20\text{–}100\%$ of rated power, while operating in the lower half of that range usually results in significantly reduced gas quality and increasingly reduced system efficiencies. The lower boundary is approximate, as the operating conditions such as temperature, pressure and type of diaphragm material influence this parameter.

The gas quality reduces as the movement of hydrogen molecules through the diaphragm is blocked by the pressure difference, however, pressure decreases at partial-load. Similarly, the relevant gas cross-over of oxygen from the anode to the cathode is dependent on the current density (higher at higher current density), which also decreases at partial-load. A mixture of hydrogen and oxygen can be explosive, therefore maintaining gas purity is of utmost importance within the electrolyser unit [65].

For the PEMEL the literature indicates a load range of $0 - 100\%$. However, there is a relationship between the membrane thickness and the load range of the PEMEL, as with thinner membranes gas permeability will be an issue for PEMEL as well [56, 96]. This behaviour is captured in Figure 2.17, whereby the turndown ratio is expressed as i_{crit}, the 2% hydrogen limit in oxygen and the upper boundary is the maximum cell voltage of $2.0\ V$ based upon the overpotentials in the cell and corresponding to an electrical input of $4.78\ kWh\ Nm^{-3}$ of hydrogen [96]. As can be seen in the figure, the range from the upper to the lower boundary becomes smaller for a thin membrane.

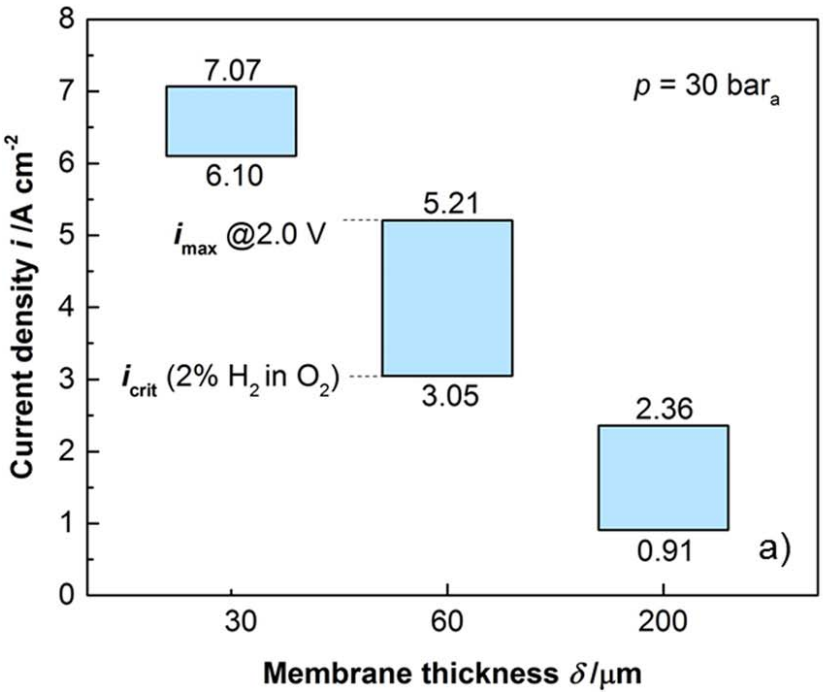

Figure 2.17: PEMEL electrolyser load range for different membrane thicknesses, from the work of Babic et al. [96]

The SOEL is a species on its own, whereby the range is defined to be $-100 - 100\%$, meaning that the electrolyser can also operate as a fuel cell. However, below thermoneutral voltage, the cell will cool down if no heat is fed into the system [56].

2.7.3. Cold and Warm Start-Up

As stated if electrolysers are outside of their load ranges the electrolysers need to be turned off. With the dynamic operation of electrolysers, the electrolysers are expected to be turned off more frequently. Every time the electrolyser is turned off, it requires several steps to start-up once again (pressurising, heating up, start-up verification, nitrogen purge, hydrogen leakage testing, etc.) [35]. Which steps are required are dependent on the type of start-up: cold or warm.

Warm start-up is meant when the system is not turned off entirely, but the production of hydrogen in the electrolyser units is being stopped and the system runs in a hot standby mode. The pressure and temperature window are maintained on both the hydrogen and oxygen flow within the system. For a warm start-up it is reported that AEL can reach full-load in a time window of $1-5\ min$ while the PEMEL can reach full-load within seconds [56]. For the SOEL it is stated that the system needs to maintain a temperature of $600°C$ in hot stand-by mode [97].

Contradictory literature is available regarding the amount of time the hot standby mode can be maintained for the AEL. The Alkaliflex project team reports that the hot standby mode for AEL is limited (a quantification is not given) [65], whereas Jensen et al. report that the electrolysers of Lurgi can stay in hot standby mode for $4-6\ h$ [98].

The cold start-up means that the system is shut off entirely and therefore system pressure and the temperature has to be built up again. For large-scale industrial AEL, the time to heat the system to operating temperatures is stated to be $1-2\ h$ [56]. Particularly the AEL also needs to undergo a nitrogen purge, to make sure that no remainder of crossover gasses is within the electrolyte [65]. For PEMEL cold start-up times of $5-10\ min$ are stated [56], whilst also $20\ min$ is indicated in literature [68]. A cold start-up sequence for the PEMEL is depicted in Figure 2.18 [35], where it can be seen that hydrogen production starts at $425\ s\ /\ \sim 7\ min$ after the system is started up. Lastly, for SOEL heating up the system takes up to several hours, to prevent thermal stress in the system [97].

Lastly, it is often stated that AEL cannot be cycled too often, as turning off the electrolyser will lead to reverse currents within the electrolysis unit. The reverse current can lead to damage to the electrodes and thus a faster degradation of the system [65, 99]. However, a clear quantification of 'too often' is not to be found in the literature.

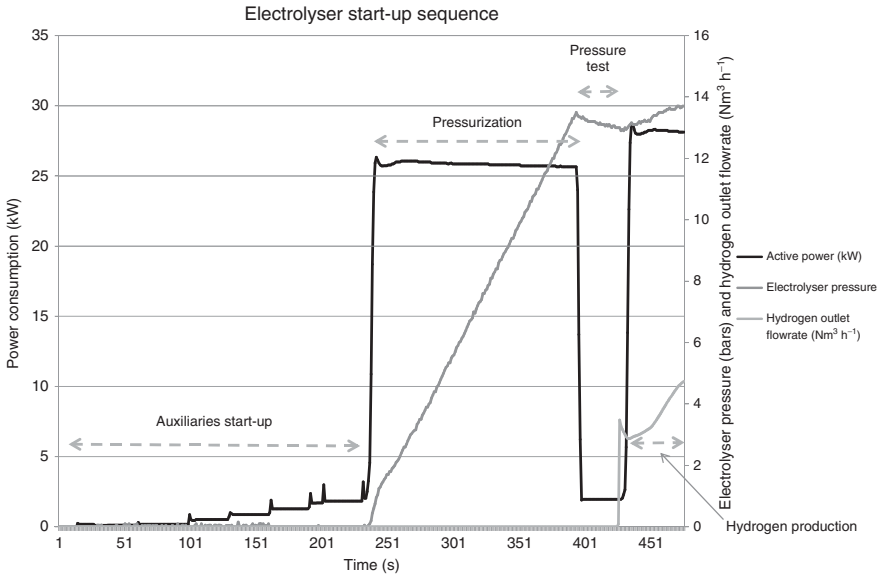

Figure 2.18: Start-up sequence for a $5\ Nm^3\ h^{-1}$ PEMEL, from the work of Godula-Jopek et al. [35]

2.7.4. Ramping Up and Ramping Down

Within the operating window defined above as the load range, both the AEL and PEMEL technologies show ramping capabilities of minimum nominal load to full load in the range of seconds [66, 56]. This ability also applies when the load needs to be ramped down. However, it is worth noting that an AEL that is not pressurised nor warm, cannot maintain the same capabilities [65]. For SOEL no data is to be found, as this technology is not commercialised yet.

With fast ramping capabilities, the electrolysers could also respond to transients and other power systems disruptions such as frequency regulation and voltage regulation [99]. However, as this research is not focused on power system dynamics and stability, this is outside of the scope of this work.

2.7.5. Standby Losses

The electrolyser can be operated in standby mode, whereby the system is not turned off entirely but kept at a mode which makes it possible to be up and running in a fast manner. As a combination of the above-introduced electrolyser operational characteristics, the standby mode will lead to losses. These losses are among others:

- Losses due to the purging of the system, required after a long standby period to prevent gas crossover in between the anodic and cathodic compartments [56];
- A protective current to be applied to the AEL when the system is in standby mode, to prevent reverse currents damaging the electrodes [65];
- Heating of the electrolyser to make the fast operation possible, especially relevant in the case of SOEL which requires a high standby temperature $(600°C)$ [56].

These losses can induce a major loss of energy, if not handled adequately. Therefore, the system operation needs to be carefully optimised.

2.7.6. Lifetime and System Degradation

The lifetime of the electrolysers is of utmost importance, both for the economical assessment of the electrolyser system and for the maintenance of the system. The reader is noted that electrolysers' lifetime is often split as:

- Electrolysis stack lifetime in hours, this is the parameter that dictates the lifetime of the hydrogen production unit. There is a dependency on the number of hours the system is operational, as the lifetime is expressed in hours. Full-load for AEL and PEMEL is defined as $8,497\ h$, considering regular maintenance [69, 74], whereas stack lifetimes are reported to be in the range of $90,000 - 120,000\ h$ for AEL, $20,000 - 62,000\ h$ for PEMEL and $8,000 - 20,000\ h$ for SOEL [56, 68, 67, 69, 74, 77].
- System lifetime in years, which considers the lifetime of the electrolyser as a whole (including BoP). The system lifetime is reported to be $20 - 40\ y$ for AEL, $20 - 30\ y$ for PEMEL and $20\ y$ for SOEL [69, 74, 77].

The lifetime of the electrolysis stack is defined by the voltage degradation over time. As introduced in subsection 2.4.3, the voltage applied to the system defines its efficiency (on stack level). Whenever the stack is operational, the stack degradation requires an overpotential to be applied, hence the name voltage degradation, to maintain the same hydrogen output. In other terms, the efficiency of the electrolysis stack degrades per hour it is used. The performance loss is caused by the degradation of the components within the stack, such as the catalyst, electrolyte, electrode and membrane. The degradation of these components leads to an increase in the resistance within the stack, inducing higher losses. Typical values for degradation are found to be in the range of $1 - 2\ \mu V\ h^{-1}$ for AEL, $3 - 5\ \mu V\ h^{-1}$ for PEMEL and $< 7.3\ \mu V\ h^{-1}$ for SOEL [56]. However, the SOEL system is only tested in laboratory environments as the technology is not commercialised and therefore might show deviations in reality.

To give an overview of what kind of effect this has on the stack performance, a calculation example is given. Assuming a cell voltage of $2.0\ V$ for an AEL stack ($\eta_{LHV} = 61.5\%$), with $90,000\ h$ as lifetime, operating at full-load ($8,497\ h$) and the aforementioned degradation values of $1 - 2\ \mu V\ h^{-1}$ the stack efficiency drops to $\eta_{LHV} = 56.4 - 58.8\%$.

Hereby a linear relationship is assumed. However, this linear relationship does not always apply, especially not in the case of cycling the stack. Exact numbers are not stated in the literature, but the relationship between stack degradation and cycling is often noted. Therefore, this technical parameter requires optimisation for cycling behaviour in the mathematical framework. An efficiency loss of 10% on the stack after its lifetime is deemed to be normal and requires an investment into the replacement of the stack.

Finally, it is noted that the system lifetime exceeds the stack lifetime at least twice (based on full-load operation) for all types of electrolysers, a minimum number of one replacement for the electrolysis stack during its lifetime is a necessity.

2.8. Optimisation of Electrolysis Processes

With the theoretical framework presented, the operational policies and technical parameters indicators of different electrolysis processes being discussed and the economic analysis of the technologies given, this can be summarised into the aim of this research. Namely, the optimisation of hydrogen electrolysis processes for the optimal investment and operational models.

As seen throughout the chapter, electrolysis and the electrochemical reaction for the splitting of water is a complex process, with multiple parameters of influence. These parameters are dictated for the electrolytic cell by but are not limited to: thermodynamic properties (e.g., temperature and pressure), material properties (e.g., conductivity and thickness), reaction kinetics, efficiency losses (e.g., activation, ohmic and diffusion overpotentials) and time to reach the optimal working conditions.

Then there is the overall electrolyser system, that is consisting of the electrolysis stack (performing the hydrogen production), the transformer and rectifier units, compressor units, hydrogen gas storage and the Balance of Plant (BoP). The BoP may consist of the hydrogen gas/lye separator, oxygen/lye separator, lye tank, lye cooler, feed water purification system, hydrogen scrubber, hydrogen gas tank, deoxidiser and twin tower dryer [100, 101]. The nuance is that all these elements depend on which of the aforementioned technologies for water electrolysis (i.e., AEL, PEMEL, SOEL) is used.

3

Methodology

This chapter contains a description of the methodology used in this research. The research contains both a mathematical framework for the optimal usage of hydrogen water electrolysis technologies and a case study. The case study is performed to assess the validity and sensitivity of the described mathematical framework. The chapter starts with the methods used to create the mathematical formulation and model, after which the case study is discussed. Lastly, the sensitivity analysis performed on the case study is explained.

3.1. Plan of Approach

The plan of approach for the research can be captured in the flowchart as given in Figure 3.1, whereby the modelling work is divided into seven sections. Firstly, the model is put on paper with the creation of the mathematical framework. Thereafter, the model is implemented into AIMMS (short for Advanced Interactive Multidimensional Modeling System), where the optimisation is performed and the objective function is solved. Thirdly, the case study data is defined and loaded, to obtain results from the optimisation performed.

The consecutive steps are the verification of the model results and the analysis of the results. These can be deemed as one singular step, however, are split into two parts on purpose. The simplification in the flowchart diagram shows one direction, however many iterations on the 'AIMMS Modelling' and 'Case Study Definition' follow based on the verification of the model results. This way any modelling errors are patched and the analysis of the results is based upon verified results. The step hereafter includes the sensitivity analysis, meaning that the effect of a change in input data is analysed over the obtained model results. Finally, the output is put through Excel and MATLAB to obtain visual data.

Figure 3.1: Plan of Approach for the research

3.2. Modelling and Mathematical Framework

Implementation of green hydrogen (hydrogen generated via electrolysis) into our future energy system depends on technological developments in terms of generation, storage and infrastructure. These technological developments can be defined as chemical, electrical and/or mathematical constraints on system operation and performance (e.g., efficiency, degradation, etc.) and also as economic constraints (i.e., costs). Within this research, these constraints are referred to as technical parameters and operational policies and form the constraints and decision variables for two optimisation models.

Optimisation modelling is expected to be a known theory to the reader, however, as a small refreshment, this paragraph introduces the essential concepts. Optimisation modelling (also referred to as mathematical programming) is a mathematical approach to defining the best possible set of solutions for a set of variables. With optimisation modelling the cohesion between these variables also becomes clear and the variables to be optimised are called the 'decision variables. An optimisation model has an 'objective function' (target) and in the case of this research, the objective is to minimise the costs for investments and operational models for the usage of hydrogen within the existing power systems. The decision variables are always to be found in the objective function. Furthermore, an optimisation model has a set of constraints, defining the boundaries for the set of solutions. Methods to find the best possible set of solutions varies, depending on the type of objective function or the type of constraints. In many cases, the solution can be found with software programs on computers. One such software programmes, AIMMS, is introduced in subsection 3.2.1.

The first model case is referred to as the reference (base case) model and includes an overly simplified version of the hydrogen pathway. The optimisation model is defined as a Linear Programming (LP) model, which means both the objective function and the constraints consider only linear relationships. Therefore, the technical parameters and operational policies, such as the minimum uptime, minimum downtime, unit commitment, etcetera are not implemented in this case. The model can be characterised in canonical form as stated in Equation 3.1.

$$\begin{aligned} &\textit{Objective Function:} && minimum_{\mathbf{x}}\ \mathbf{c}^T\mathbf{x} \\ &\textit{Subject to:} && \mathbf{A}\mathbf{x} = \mathbf{b} \\ & && \mathbf{x} \geq \mathbf{0} \in \mathbb{R}^{N_x} \end{aligned} \tag{3.1}$$

Hereby, (**c**) represent the cost vector that is associated with the continuous decision variable (**x**), (**A**) represents the matrix of constraints, (**b**) represent the known terms in the constraint and the dimension of the vector (**x**) is given by (N_x).

The system does include the following elements distilled from the performed literature review:

- Two constraints ensure the hydrogen balance and the electricity balance, with the addition of an extra set of constraints relating both balancing constraints to each other.
- Ramping constraints define the capability to ramp up and ramp down within a certain window of time for both the generation and reconversion technology.
- Capacity constraints for all the technologies within the mix (generation, storage, reconversion), as explained in more detail at the end of this section. Here also capacity constraints for the cables from and to the grid are defined, as well as the constraints ensuring the charging and discharging capacities for the storage system.
- The storage system is further specified, with a storage balance including a self-discharge component. Other constraints for the storage system include a definition for the first and last value obtained within the storage system (to prevent depletion of the system at the end of each simulation), as well as a constraint defining the upper and lower boundaries for the storage system.

The second model can be seen as a refined version of the previously introduced optimisation model. The level of detail in this model comes forth from the usage of mixed integer constraints (both binary variables and discrete variables are mixed within the constraint), meaning the model is called a Mixed Integer Programming (MIP) model. The binary variables indicate if the system is on or off. The model can be characterised in canonical form as stated in Equation 3.2 [102].

$$\begin{aligned} &\textit{Objective Function:} && \min_{\mathbf{x},\mathbf{y}} \ (\mathbf{c}^T\mathbf{x} + \mathbf{d}^T\mathbf{y}) \\ &\textit{Subject to:} && \mathbf{A}\mathbf{x} + \mathbf{B}\mathbf{y} = \mathbf{b} \\ & && \mathbf{x} \geq \mathbf{0} \in \mathbb{R}^{N_x}, \mathbf{y} \in \{0,1\}^{N_y} \end{aligned} \tag{3.2}$$

Hereby, additional elements are: the cost vector (**d**), representing the binary decision variable (**y**), for which (**B**) defines the matrix of constraints and the dimension of the vector (**y**) is given by (N_y).

The additional features of the second model are summarised as:

- An addition to the decision variables and thus the objective function, the binary decision variables are included for the start-up trajectory, non-load operation (idle) and degradation of the units.
- All capacity constraints change, as the inclusion of the binary variable, allows rewriting the constraints in such a way that partial-load operation is enforced, one of the technical parameters as introduced in subsection 2.7.1.
- Similarly, the storage constraints do also include part-load operation capabilities.
- Minimum uptime and downtime constraints are added, along with constraints defining the start-up and shutdown logic of the systems within the hydrogen pathway configuration, as introduced in subsection 2.7.3.
- Lastly, degradation of the units within the system is added to the mathematical framework as a constraint, to mathematically define wear and tear as described in Equation 4.2.2.

As solving a MIP model is often more time-consuming than an LP, the benefit of using a MIP model would be to obtain more realistic results. If this is not the case, the benefit of creating a computational heavier model becomes pointless. Therefore, this model is simulated with different configurations, to obtain the simulation time and optimisation results for each type of simulation. The components that can be present in the simulations are as follows:

- **L** - Minimum part-load
- **M** - Minimum uptime and minimum downtime
- **S** - Start-up costs
- **D** - Degradation due to cycling

3.2.1. AIMMS

'Advanced Interactive Multidimensional Modeling System', or AIMMS in short, is an analytics software company developing software with the same name for modelling and optimisation purposes. With AIMMS users can perform various mathematical optimisation problem types, amongst which Linear Programming (LP) and Mixed-Integer Programming (MIP) are used within this research. The software is coupled to various solvers, of which CPLEX version 20.1 is used in this research. The AIMMS software uses both declarative as well as imperative ways of programming [103].

3.2.2. MATLAB

MATrix LABoratory, or MATLAB in short, is a 'programming and numerical computing tool', as stated on [104]. The software is specifically designed to perform calculations with matrices and arrays, but can also be used to create graphical representations of data. In this case, the data output from AIMMS in 'Comma Separated Value'-files is put through both Excel and MATLAB, depending on the type of data (whereby Excel is deemed to be a known software).

3.3. System Description

Both optimisation models introduced in section 3.2, and discussed in more detail in section 4.1 and section 4.2, are an implementation of the hydrogen pathway as given in Figure 3.2. The hydrogen pathway thus forms the basis of all modelling and the 'Mathematical Framework' as given in Figure 3.1. This visual pathway for hydrogen can be split up into four clusters. The first element of the cluster includes all blocks and arrows that are coloured yellow, which represent the usage of electricity (either as input, output or generation). The second cluster considers the production (generation) of hydrogen, which is represented by the green-coloured block. Thirdly a cluster is defined for the fuel cell, which can convert hydrogen back into electrical energy and is represented by an orange-coloured block. Lastly, all elements within the cluster that represent the input, output, storage or demand for hydrogen are coloured blue. It is noted that this is an overly simplified representation of the hydrogen pathway. Elements that are left out in the representation or for instance the power grid, transmission lines, all electronic power converters, etcetera.

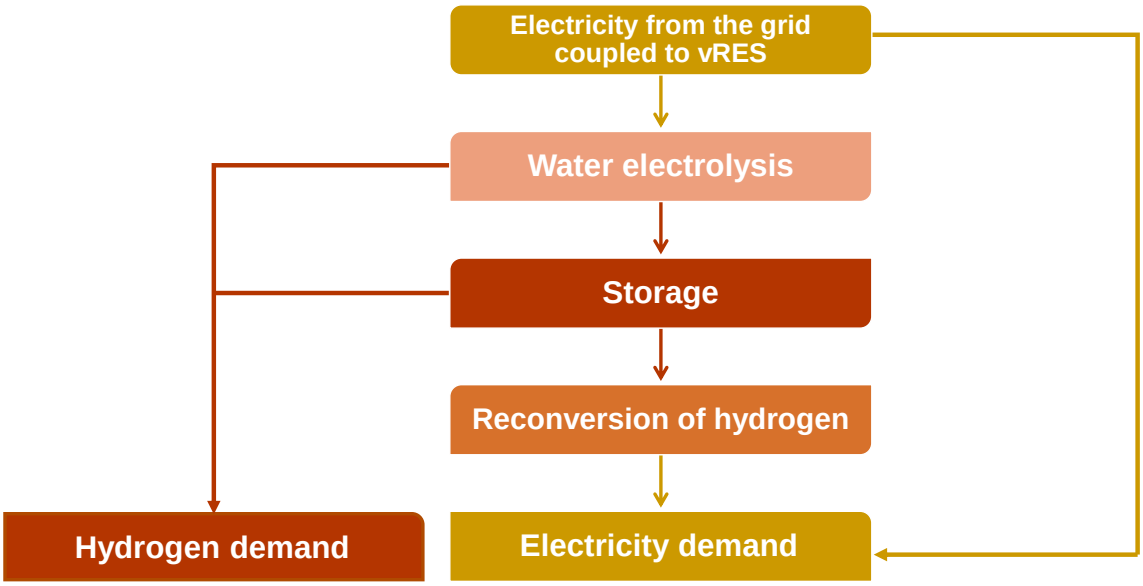

Figure 3.2: Schematic overview of the hydrogen pathway considered within the system

Additionally, the technology mix within the hydrogen pathway is defined as:

- The electrolysis technologies, consisting out of the three introduced technologies of Alkaline Electrolysers, Proton Exchange Membrane Electrolysers and Solid Oxide Electrolysers. The choice for these three technologies is made upon the commercialisation and technical parameters, as reflected within the respective Technology Readiness Levels. For further reasoning, the reader is referred to subsection 2.4.1.
- The storage technology, consisting of the compressed storage vessels, amongst others due to its relative easy implementation (no insulation required) and the matureness of the technology, as explained in more detail within section 2.5.
- Finally, the reconversion technology consists of the Proton Exchange Membrane Fuel Cell, due to its capability for dynamic operation amongst other reasons stated in section 2.6.

For the case study optimisation purposes, the system is coupled to the power grid. In future scenarios, the energy generated comes from vRES such as solar photovoltaic modules and wind turbines. This means that energy generation has an intermittent character and that there is a possibility to import or export electricity to/from the grid. The electricity price, both importing and exporting, is assumed for the entire year (known forecast). Lastly, the system considers flat demand for hydrogen.

The chosen industry has a demand for hydrogen and electricity, whereby electricity can be imported into the system, but both can be produced on-site. The produced electricity can be exported whenever spot prices are beneficial, as to minimise the total overall costs. The described system scope is further depicted in Figure 3.3. As can be seen in the figure, the rectifier and transformer for the electricity supply are deemed to be outside of the scope of the system, whilst the Balance of Plant for the functioning of the electrolyser unit, storage unit and fuel cell are considered within scope. The BoP, therefore, includes lye tanks, compressors, heat exchangers, etc. To reiterate, the BoP in this case, however, does not include any power conversion equipment.

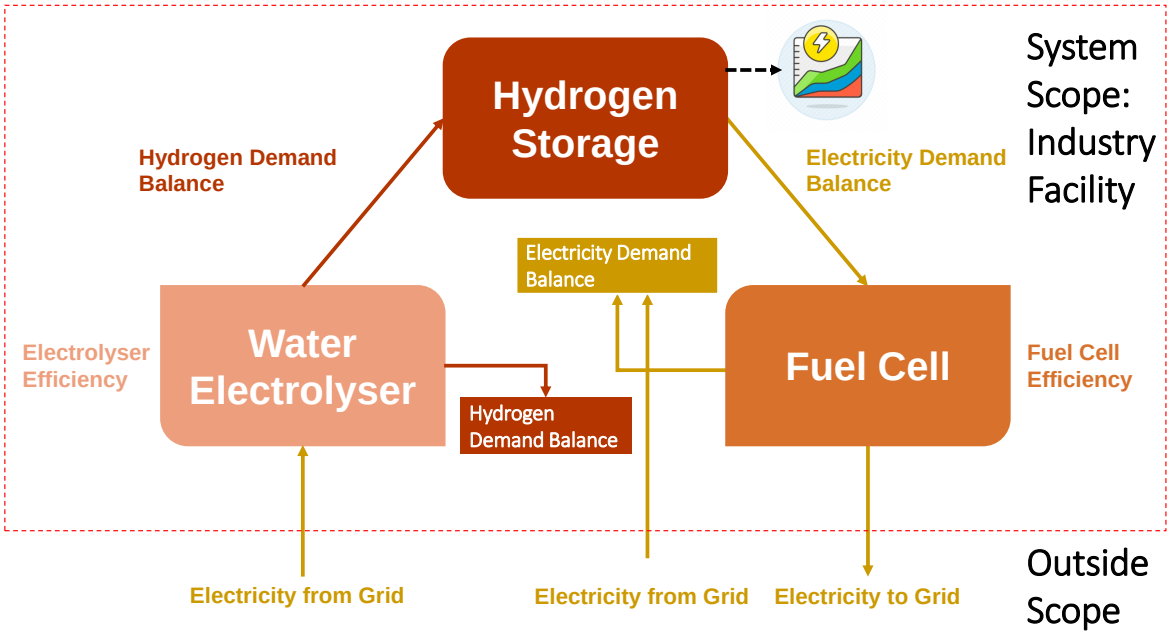

Figure 3.3: System scope considered for the system

3.4. Data Input

With the hydrogen pathway to be modelled and used in the case study introduced, the data input for the case studies becomes relevant. For the technologies that directly follow the hydrogen pathway, data was provided in tables at the end of each technology section in chapter 2. As observed in the tables the ranges of the technological parameters and operational policies are broad. This big range is caused by several reasons, like the fast pace of development, the number of definitions for certain parameters (like the efficiency the system can obtain), and most importantly the sheer amount of companies making hydrogen systems. Each company has a different expertise, manufacturing process or material, causing a huge amount of differences in the data that can be found in the literature. In Table 3.1 the data for the electrolysers is shown as will be used for the scenario of 2020 (later more explanation about the sensitivity towards simulation years).

Furthermore, the data provided within this research includes energy balances for electricity and hydrogen and also includes the day-ahead electricity prices (from the past, as well as a forecast for the future). The data for the electricity prices for 2030 and 2050 are composed by a research group at TNO, based on electrical energy trends [105]. These trends include amongst others the population growth (and thus growth in energy demand), the future power grids with more and more vRES coupled, but also the scarcity of fuels which results in higher fuel prices. Lastly, the data for the Steel Factory in IJmuiden comes from the work published by CBS [106] and the report of a steel-making factory in the region [107].

Table 3.1: Model data input for the electrolyser technologies for 2020 based on literature review as found in Table 2.3*, Table 2.4⁻ and Table 2.5ᵒ

Parameters for electrolysers 2020 - 'Base Case'	Units	Alkaline Electrolyser*	Proton Exchange Membrane Electrolyser⁻	Solid Oxide Electrolyserᵒ
System Capacity	MW	162	20	0.05
Stack Capacity	MW	24	3	0.05
CAPEX	€ MW_{el}^{-1}	750,000	1,400,000	2,000,000
Fixed O&M	€ MW_{el}^{-1} y^{-1}	34,000	13,600	35,139
System Efficiency	%	66	63	87
Lifetime System	y	25	20	3
Lifetime Stack	h	105,000	60,000	15,000
Ramping Up	%	7	40	0.5
Ramping Down	%	10	40	0.5
Load range (% of nominal load)	%	20-100	5-100	0-100

Similarly, in Table 3.2 the data input is presented for the fuel cell in the 2020 scenario and for the pressurised storage vessel in Table 3.3. Not all this data is used in all the simulations. Depending on the mathematical optimisation defined, the relevant data input changes. Furthermore, the storage table includes both the data input for the pressurised storage vessel itself, but also the relevant data for charging and discharging the storage vessel. Lastly, the storage efficiency is the round-trip efficiency for all components regarding the storage of hydrogen. This implies losses that occur with compression, cooling, the throughput of hydrogen, leakage, and such elements of the charging/discharging/storage cycle.

Table 3.2: Model data input for the fuel cell technology [92, 108, 109, 110, 111]

Parameters for Fuel Cell 2020 - 'Base Case'	Units	PEMFC
System Capacity	MW	10
CAPEX	€ MW_{el}^{-1}	1,320,000
Fixed O&M	€ MW_{el}^{-1} y^{-1}	13,400
Lifetime	y	9
Efficiency	%	60
Ramping up	%	0.4
Ramping down	%	0.4

Table 3.3: Model data input for the storage and charging/discharging technology [83, 109]

Parameter for Storage 2020 - 'Base Case'	Units	PEMFC
System capacity	MW	2
CAPEX	€ MW_{el}^{-1}	380,000
Fixed O&M	€ MW_{el}^{-1} y^{-1}	7,600
Lifetime	y	25
Round-trip efficiency	%	80
Hydrogen flow rate	$kg\ h^{-1}$	60

An example of the day-ahead prices for the year 2020 in The Netherlands is given in Figure 3.4, data obtained from ENTSO-E [112]. It can be observed that the electricity prices become negative at certain intervals (although for short periods) and that there is a seasonal increase in electricity prices, with a higher demand for energy in the autumn and winter seasons.

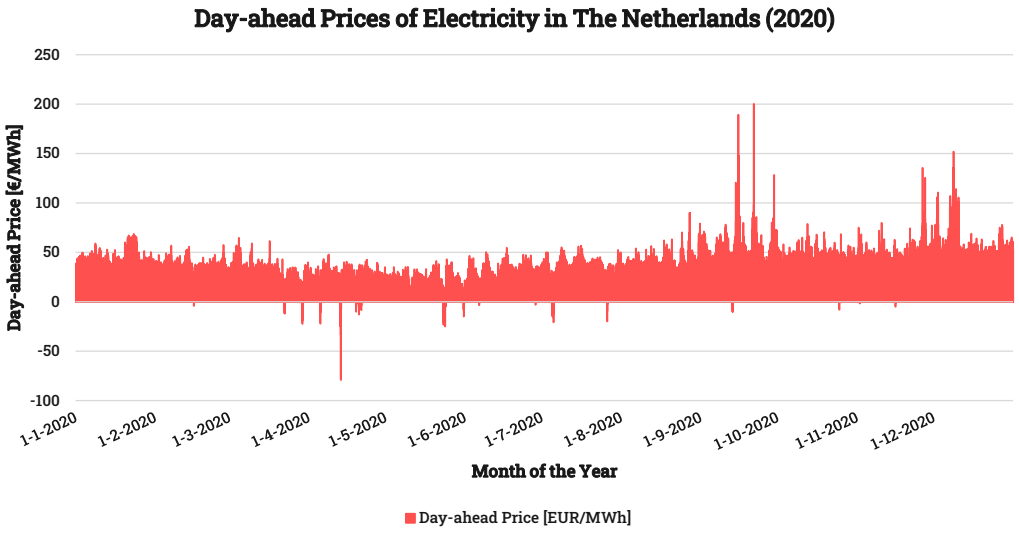

Figure 3.4: Day-ahead electricity prices on an annual basis for The Netherlands in 2020 [112]

To zoom in on the above-given profile, in Figure 3.5 a daily overview is given for a day in April in the same year (2020) in The Netherlands [112].

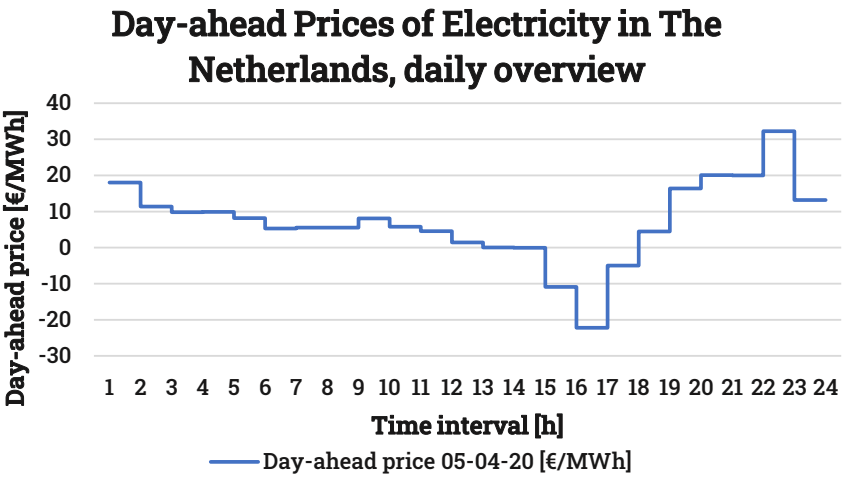

Figure 3.5: Day-ahead electricity prices on a daily basis for The Netherlands in April 2020 [112]

To conclude the data input, energy demand profiles for the case study location (steel industry around IJmuiden) is given in Figure 3.6 and Figure 3.7. The demand is split into two charts, as the characteristics of both are different. The electricity demand as referred to in this case is provided through a grid-coupled cable. The cables have a finite capacity, however, this is not dealt with in detail as it is outside the scope of this research. This electricity demand is based upon the real-life situation for the steel industry in IJmuiden, however, it is scaled down to a different demand size for the case study [107].

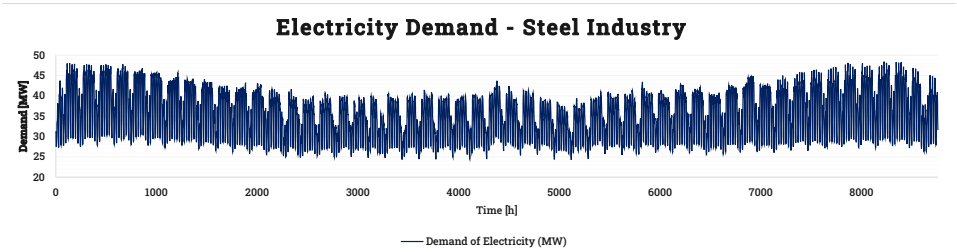

Figure 3.6: Electricity demand yearly profile

The demand for hydrogen is obtained from the work done by CBS and TNO in a joint report [113]. The analysis for 2020 and 2050 for the region 'IJmond' within the report is deemed to be one industry, namely the steel-making industry. As the steel-making industry requires both a tremendous amount of energy (in the forms of electricity and heat) and also makes use of hydrogen, this industry is deemed fit for a case study with on-site electrolysers. However, the data from the reference does not provide any details about the profile of the hydrogen demand. Therefore, the data is first spread out over the year in equal terms, where after the data is varied with a maximum variation of 10%. With the variation created, the model has a more dynamic demand for hydrogen as input, making it possible to see the effects of the storage and fuel cell systems in a more distinct manner. The obtained result still has the same average profile over the year, equalling $5\ PJ$ per annum.

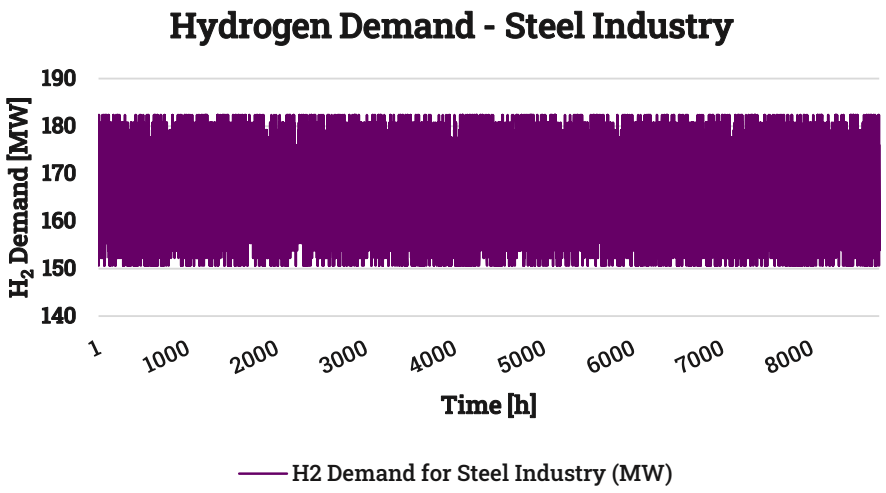

Figure 3.7: Hydrogen demand yearly profile

3.5. Sensitivity Analysis

Sensitivity analysis within optimisation modelling is meant the impact on the optimal solution due to an incremental change within one of the input parameters, variables or objectives. Sensitivity analysis is a useful way of assessing the impact on obtained optimisation results. The parameters or variables that are included in the sensitivity analysis are:

- ***Lifetime*** - The lifetime of the system is prone to improvement. Especially in the case of technologies that are yet to be commercialised. Therefore, the lifetime of the system (which has a big effect on the investments required) plays an important role in understanding the obtained optimisation results.
- ***Efficiency*** - The efficiency of all electrolysers is predicted to become higher (thus less loss of energy). The theoretical limit for electrolysers is $39.4\ kWh\ kg^{-1}$, however, this theoretical value is still far out of reach. Improvements are expected to be made on the system level especially, which considers the BoP, rectifiers, compressors and other equipment, which can be optimised for part-load efficiency. Before reaching that stadium, it is good to be aware of the sensitivity of this input parameter.
- ***CAPEX*** - As CAPEX incorporates the investments done, it has a huge influence on cost minimisation within the optimisation model. Which predictions in literature and surveys for price forecast ranging up from 70%-80% to 20%. Therefore, one of the most important features of the sensitivity analysis will be the analysis of the CAPEX.
- ***Ramping Rates*** - The ramping rates define how fast the system reacts to load changes. If this behaviour is relatively slow, especially in the case of larger system capacities, it might lead to an over-dimensioning of the whole system and thus a big cost component. Therefore, its impact is also verified with the sensitivity analysis.
- ***Interest Rates*** - Interest rates are not a fixed commodity over time. However, in the case studies performed, the interest rate is kept fixed (so as not to create too much variability). The influence of the interest rate on the optimisation results can however also be analysed, whereby the interest rate will have a lasting impact on return-on-investments and thus requires either lower CAPEX or higher turnovers to play breakeven in the same period.
- ***Future Scenarios*** - Future scenarios, hereby it is not meant what is already being analysed with other types of sensitivity analysis (e.g., improvements in the lifetime of systems or efficiency improvements due to more R&D). The scenarios here consider higher energy demand, both for hydrogen as for electricity, consider higher integration of hydrogen in the power grid (meaning hydrogen could also be imported), or consider the forecasted electricity prices (which are expected to increase, both due to inflation and an increase in demand). The scenarios implemented here will be adaptations of earlier introduced work from Segers et al. [106]

3.6. MIP Case Descriptions

The case description, similar to the modelling, is split into two. The base case is the situation in which the LP model is run, first with the data input found in the literature (as stated in Table 3.1). Thereafter, the case is run each time with differences for the input data, meaning a sensitivity analysis is performed. The goal of the sensitivity and the reasoning for the sensitivity are given in section 3.5.

Secondly, the MIP model, which is more refined will be used against the LP 'base case' simulation. The MIP model, however, will be simulated in all kinds of configurations. This can be considered as a sensitivity to the constraints, namely, to see what kind of computational burden they cause, compared to the detail of accuracy it adds when compared to the LP model simulation. An overview of all types of model configurations is given in Table 3.4.

Table 3.4: All possible model configurations based on four components (including Model 16 - 'Base Case')

Parameter	Minimum Part-Load *L*	Minimum Uptime & Downtime *M*	Start-up Costs *S*	Degradation Due to Cycling *D*
Model 1 / LMSD	X	X	X	X
Model 2 / LMS -	X	X	X	
Model 3 / LM - -	X	X		
Model 4 / LM - D	X	X		X
Model 5 / L - SD	X		X	X
Model 6 / - MSD		X	X	X
Model 7 / - - SD			X	X
Model 8 / - - - D				X
Model 9 / - - S -			X	
Model 10 / - M - -		X		
Model 11 / - MS -		X	X	
Model 12 / - M - D		X		X
Model 13 / L - - D	X			X
Model 14 / L - S -	X		X	
Model 15 / L - - -	X			
Model 16 / - - - -				

4

Mathematical Formulation of the Model

Implementation of green hydrogen (hydrogen generated via electrolysis) into our future energy system depends on technological developments in terms of generation, storage and infrastructure. These technological developments can be defined as chemical, electrical and/or mathematical constraints on system operation and performance (e.g., efficiency, degradation, etc.) and also as economic constraints (i.e., costs). Within this research, these constraints are referred to as technical parameters and operational policies and form the constraints and decision variables for an optimisation model.

The optimisation model is a mathematical formulation, in which the electrolysis, storage and reconversion technologies from chapter 2 are defined in terms of decision variables and whereby the cohesion between the decision variables is stated. The objective of this optimisation is to minimise the cost of hydrogen generation and electricity generation and storage of hydrogen. Numerous optimisation models are to be found in literature, of which the models found in ([16], [28] - [31], [102], [114] - [109]) have been an inspiration to create the mathematical formulation in this research.

The hydrogen reconversion pathway from Welder et al. [16] is used as inspiration for the definition of the decision variables for the modelled system. In the work of Gabrielli et al. (2020) [28], Petkov et al. [29], Weiman et al. [30], Gabrielli et al. (2018) [102], Morales-España et al. [114], Gusain et al. [115] and Lukszo et al. [116, 117, 118] optimisation models for different types of technologies are proposed. These all form an inspiration for the models created within this research.

This chapter presents the mathematical formulation for the optimisation models split into two, as described in section 3.2. The chapter starts with a section considering a Linear Programming (LP) formulation. Thereafter, the Mixed Integer Programming (MIP) formulation will be introduced. These formulations will later be used in the case study to compare the differences between the two formulations.

As stated in previous chapters of this research, the focus of both the mathematical formulations is on the technical parameters and operational policies. With these as the starting point, the models consider the following elements in the hydrogen chain: water electrolysis (AEL, PEMEL and SOEL), storage (compressed hydrogen) and reconversion (PEMFC) of hydrogen into electricity. This is called the 'system' as defined in the section 3.3. Ideally, the decision on the type of electrolyser units (within the technology mix) follows from the optimisation modelling.

Finally, the comparison between optimisation models by Wirtz et al. [31] has been an inspiration for the comparison of the Linear Programming and Mixed Integer Programming formulations performed in this research (to be shown in section 5.2).

4.1. Linear Programming Model

This section is devoted to the mathematical formulation of the linear programming part of the model. This model is used as a reference (base case) model, with a simplification of reality, and does not incorporate unit commitment or any non-linear behaviour. To start, a nomenclature is given. It is noted that this nomenclature is different from the nomenclature in the introductory part of this document, as this nomenclature is specifically intended for reader convenience within the Mathematical Framework.

Nomenclature

Indices and Sets

$g \in \mathcal{G}$	Electrolyser units, running from 1 to $\lvert\mathcal{G}\rvert$.	
$j \in \mathcal{J}$	Fuel cell units, running from 1 to $\lvert\mathcal{J}\rvert$.	
$s \in \mathcal{S}$	Storage units, running from 1 to $\lvert\mathcal{S}\rvert$.	
$t \in \mathcal{T}$	Hourly periods, running from 1 to $\lvert\mathcal{T}\rvert$ hours.	

Parameters

A_s	Capacity coefficient for the storage unit s.	$[-]$
C_x	Annualised investment cost for unit x (with x being ch for charging, dis for discharging, g for electrolysers, j for fuel cells and s for storage).	$[€/kW/y]$
CH_0	Initial charge capacity for storage units within system boundaries.	$[kWh]$
CRF_x	Capital recovery factor for unit x (with x being ch for charging and dis for discharging, g for electrolysers, j for fuel cells and s for storage).	$[-]$
DIS_0	Initial discharge capacity for storage units within system boundaries.	$[kWh]$
D_t	Demand at hour t for Y (with Y being E for electricity and H for hydrogen).	$[kWh]$
F_0	Initial electrical capacity for fuel cell units within system boundaries.	$[kWh]$
H_0	Initial hydrogen capacity for electrolyser units within system boundaries.	$[kWh]$
I_x	Investment cost for unit x (with x being ch for charging and dis for discharging, g for electrolysers, j for fuel cells and s for storage).	$[€/kW]$
L_x	Lifetime of the unit x (with x being ch for charging and dis for discharging, g for electrolysers, j for fuel cells and s for storage).	$[y]$
OM_x	Fixed operation and maintenance costs for unit x (with x being ch for charging and dis for discharging, g for electrolysers, j for fuel cells and s for storage).	$[€/kW/y]$
R_{xt}^{down}	Ramping down limit of unit x (with x being i for electrolysers and j for fuel cells) at hour t.	$[pu]$
R_{xt}^{up}	Ramping up limit of unit x (with x being i for electrolysers and j for fuel cells) at hour t.	$[pu]$
SOC_0	Initial storage capacity for the storage units within system boundaries.	$[kWh]$
Π_t	Electricity price via or to the grid at hour t.	$[€/kWh]$
η_x	Efficiency for the H2-to-Power and Power-to-H2 conversions x (with x being i for electrolysers and j for fuel cells).	$[-]$
η^{S}	Round-trip efficiency for the hydrogen storage.	$[-]$
Ω	Real discount rate.	$[pu]$

Variables

ch_t^{H}	Charge of the hydrogen storage facility at hour t.	$[kWh]$
$ch^{\mathrm{H,max}}$	Maximum hydrogen charge capacity to the hydrogen storage unit.	$[kW]$
dis_t^{H}	Discharge of the hydrogen storage facility at hour t.	$[kWh]$

$dis^{\text{H,max}}$	Maximum discharge capacity from the hydrogen storage unit.	$[kW]$
e_t	Buying or selling electricity via/to the grid at hour t.	$[kWh]$
$e^{\text{E,max}}$	Maximum electricity import capacity from the grid into the system.	$[kW]$
f_{jt}^{E}	Fuel cell electricity generation at hour t for unit j.	$[kWh]$
f_{jt}^{H}	Fuel cell hydrogen demand at hour t for unit j.	$[Nm3/h$ or $kWh]$
$f_j^{\text{E,max}}$	Maximum electricity capacity of fuel cell unit j.	$[kW]$
h_{gt}^{E}	Electrolyser electricity demand at hour t for unit g.	$[kWh]$
h_{gt}^{H}	Electrolyser hydrogen generation at hour t for unit g.	$[Nm3/h$ or $kWh]$
$h_g^{\text{H,max}}$	Maximum hydrogen capacity of electrolyser unit g.	$[kW]$
soc_{s1}	First State-of-Charge for storage unit s.	$[kWh]$
soc_t	State-of-Charge of the hydrogen storage facility at hour t.	$[kWh]$
$soc_s^{\text{H,max}}$	Maximum capacity of hydrogen storage for unit s.	$[kW]$

Subscripts

0	Initial value of technology.	$[-]$
ch	Charge unit.	$[-]$
dis	Discharge unit.	$[-]$
g	Electrolyser unit.	$[-]$
j	Fuel cell unit.	$[-]$
s	Storage unit.	$[-]$

Superscripts

ch	Charging the hydrogen storage.	$[-]$
dis	Discharging the hydrogen storage.	$[-]$
down	Ramping down.	$[-]$
E	Electricity.	$[-]$
H	Hydrogen.	$[-]$
min	Minimum.	$[-]$
max	Maximum.	$[-]$
S	Round-trip efficiency for the storage.	$[-]$
SD	Self-discharge.	$[-]$
up	Ramping up.	$[-]$

4.1.1. Objective Function LP Model

To compare the modelling of a basic and a detailed hydrogen model, first the basic model is defined. The objective function of the LP problem is to minimise the (operation) costs and investments required to implement the hydrogen into the system. This is defined as the sum of:
(i) expenditures for the electrolyser(s), (ii) expenditures for the fuel cell(s), (iii) expenditures for the storage technology, (iv) and (v) the expenditures for the charge and discharge of the hydrogen into storage and (vi) variable costs for the import/export of electricity from or to the grid.

Hereby, the expenditures are divided into the initial investments (capital expenditures) and the fixed operating costs. The electricity can freely be imported or exported from and to the power grid for a variable electricity price. Note, in case electricity is exported from within the system, the electricity price will be reflected as a negative price in the objective function (meaning the total cost will go down), as the optimisation objective is to minimise costs. This translates into the mathematical description of the objective function as described in (4.1).

$$\begin{aligned}\min \; & \underbrace{\sum_{g\in\mathcal{G}}(C_g + OM_g)h_g^{\mathrm{H,max}}}_{i} + \underbrace{\sum_{j\in\mathcal{J}}(C_j + OM_j)f_j^{\mathrm{E,max}}}_{ii} + \underbrace{\sum_{s\in\mathcal{S}}(C_s + OM_s)soc_s^{\mathrm{H,max}}}_{iii} \\ & + \underbrace{\sum_{s\in\mathcal{S}}(C_s^{\mathrm{ch}} + OM_s^{\mathrm{ch}})ch_s^{\mathrm{H,max}}}_{iv} + \underbrace{\sum_{s\in\mathcal{S}}(C_s^{\mathrm{dis}} + OM_s^{\mathrm{dis}})dis_s^{\mathrm{H,max}}}_{v} + \underbrace{\sum_{t\in\mathcal{T}}\Pi_t e_t}_{vi}\end{aligned} \tag{4.1}$$

The annualised cost for investment $(€/kW/y)$ for the electrolyser, fuel cell, storage, storage charging and storage discharging are given by: C_g, C_j and C_s, C_s^{ch} and C_s^{dis} respectively. The annualised cost follows from the following relationship:

$$C_x = CRF(\Omega, L_x)I_x \qquad \forall x \tag{4.2}$$

where the x in the equation can take the value of g for electrolysers, j for fuel cells, s for storage technology, I_x $(€/kW)$ is the initial investment cost per aforementioned units x, and CRF the Capital Recovery Factor. The CRF is a ratio that follows from:

$$CRF(\Omega, L_x) = \frac{\Omega}{1 - \frac{1}{(1+\Omega)^{Lx}}} \qquad \forall x \tag{4.3}$$

whereby, Ω (pu) is the discount rate and L_x (y) is the lifetime per aforementioned unit x.

4.1.2. Constraints

Energy Balances

To ensure electricity and hydrogen balance within the system, energy balance constraints are applied for both electricity and hydrogen generation and demand. Both equations are therefore of the form: supply = demand. Furthermore, the electricity and hydrogen balances have an interdependency in the form of their efficiencies.

Electricity Balance

The electricity balance is described in (4.4) governing both supply and demand. The equation can be stated in words as follows: electricity supplied by the grid and the electricity being generated by the fuel cell (left-hand side of the equation) is equal to the electricity demand by the consumers and/or the electricity demand of the electrolyser units.

$$e_t + \sum_{j\in\mathcal{J}} f_{jt}^{\mathrm{E}} = D_t^{\mathrm{E}} + \sum_{g\in\mathcal{G}} h_{gt}^{\mathrm{E}} \qquad \forall t \tag{4.4}$$

The constraint in (4.4) ensures that the electricity within the system boundaries is used to meet the electric load demand and to produce hydrogen. In that sense, it also implies that there is no ‘direct storage of electricity’.

Hydrogen Balance

Similarly, the hydrogen balance as described in (4.5), ensures that the difference between charging and discharging the hydrogen storage facility, plus the hydrogen produced (left-hand side of (4.5)), equals the hydrogen demand and the hydrogen required for the fuel cell (right-hand side).

$$\sum_{s\in\mathcal{S}} dis_{st}^{\mathsf{H}} - \sum_{s\in\mathcal{S}} ch_{st}^{\mathsf{H}} + \sum_{g\in\mathcal{G}} h_{gt}^{\mathsf{H}} = D_t^{\mathsf{H}} + \sum_{j\in\mathcal{J}} f_{jt}^{\mathsf{H}} \qquad \forall t \tag{4.5}$$

Relationship Between the Balances

There is a relationship between both balances previously described. Namely, the connecting technologies Power-to-Hydrogen (PtH2) and Hydrogen-to-Power (H2tP), and their efficiencies. This results in the constraints as described.

$$h_{gt}^{\mathsf{E}} = \frac{h_{gt}^{\mathsf{H}}}{\eta_g} \qquad \forall g,t \tag{4.6}$$

$$f_{jt}^{\mathsf{H}} = \frac{f_{jt}^{\mathsf{E}}}{\eta_j} \qquad \forall j,t \tag{4.7}$$

In the conversion step PtH2, some of the energy is lost, hence the hydrogen output of the electrolyser is lower than the electricity input to the electrolyser in (4.6). Similarly, the conversion step H2tP results in the loss of electricity in (4.7), therefore the ratio of hydrogen fed into the fuel cell is larger than the obtained electricity, as η_j is always lesser than 1.

Ramping Up and Ramping Down

The system, especially the electrolyser and the fuel cell has ramping limits when operational. These operational limits depend on several conditions, such as the system operating point, pressure and temperature. The maximum difference in output for two subsequent time steps can therefore be expressed as follows. An example is given for the electrolyser unit (h_g) in (4.8) and (4.9) for ramping down and ramping up respectively, whereby similar logic is used for the fuel cell units (f_j).

In case the hydrogen electrolyser is ramped down, the difference in hydrogen output between the last and current time step for the electrolyser unit should be less than or equal to a percentage of the maximum hydrogen generation capacity of the unit. Similar logic applies in case the electrolyser is ramped up. On both occasions, a percentage of the maximum capacity (pu) represents the upper boundary for the difference in consecutive time steps.

$$h_{g,t-1}^{\mathsf{H}} - h_{gt}^{\mathsf{H}} \leq R_g^{\mathsf{down}}(h_g^{\mathsf{H,max}} + H_0) \qquad \forall g, t > 1 \tag{4.8}$$

$$h_{gt}^{\mathsf{H}} - h_{g,t-1}^{\mathsf{H}} \leq R_g^{\mathsf{up}}(h_g^{\mathsf{H,max}} + H_0) \qquad \forall g, t > 1 \tag{4.9}$$

Capacity Constraints

The system needs to adhere to certain capacity conditions. These are minima and maxima, which are most often operationally driven. First off, the electricity price (which has a known forecast) is subject to change over the year. This change is dependent on factors such as day/night differences, seasonal fluctuations, etc.

The export and import capacity to and from the grid is determined by the capacity of the cable capacity and all auxiliary equipment (transformer capacity, rectifier capacity, etc.). Therefore, the import variable e_t is bound by an upper capacity constraint parameter $E^{\mathrm{E,max}}$, which is equal to the already available capacity within the industry location.

However, as the same capacity is also available in case the electricity is exported from the system to the grid, the lower boundary is the negative equivalent of the upper boundary, whereby the negative value indicates export. Since the investment into the cable capacity and auxiliary equipment is not a decision variable, but a parameter, the formulation is in capital letters.

$$-E^{\mathrm{E,max}} \leq e_t \leq E^{\mathrm{E,max}} \qquad \forall t \tag{4.10}$$

The capacity constraints for the generation of hydrogen with the water electrolyser are described in (4.11). This equation implies the electrolyser can be turned off since the lower boundary is zero. The upper capacity constraint implies a maximum generation capacity, however, as this is a variable, this will be the outcome of the optimisation modelling. Also worth noting: the maximum generated hydrogen is the sum of the maximum generation capacity of the electrolyser and the hydrogen that is initially present within system boundaries (from previous import and/or generation with different technology), presented as a parameter H_0. Most often this parameter will be equal to zero, but as the optimisation formulation is written out for a generic case, it is considered within the mathematical formulation.

$$0 \leq h_{gt}^{\mathrm{H}} \leq h_g^{\mathrm{H,max}} + H_0 \qquad \forall g, t \tag{4.11}$$

The fuel cell follows the same generation logic as the electrolyser, meaning the fuel cell can be turned off and the maximum depends on the electricity demand within system boundaries and the electricity that is initially present within system boundaries, as described with lower and upper capacity constraints respectively in (4.12).

$$0 \leq f_{jt}^{\mathrm{E}} \leq f_j^{\mathrm{E,max}} + F_0 \qquad \forall j, t \tag{4.12}$$

Finally, the same logic and capacity constraints are applied for the charge and discharge, as seen in (4.13) and (4.14). The lower capacity constraint in both formulations is once again zero, whilst the upper limit for both is defined by the maximum charge or discharge capacity of the cables plus any already existing capacity within the system boundary.
The State-of-Charge levels and capacity constraints are separately discussed for the storage units in the subsection 4.1.2.

$$0 \leq ch_{st}^{\mathrm{H}} \leq ch_s^{\mathrm{H,max}} + CH_0 \qquad \forall s, t \tag{4.13}$$

$$0 \leq dis_{st}^{\mathrm{H}} \leq dis_s^{\mathrm{H,max}} + DIS_0 \qquad \forall s, t \tag{4.14}$$

Storage

The storage capacity needs to be larger than the sum of the hydrogen stored per hour and cannot be negative. This is satisfied by the following equation and constraint for the storage facility, whereby the content of hydrogen storage is expressed in the form of State-of-Charge (SoC). Similarly, the charge and discharge depend on the State-of-Charge of the storage capacity, as the storage capacity cannot be overcharged or fully depleted. Therefore, the capacity constraints for storage and charging and/or discharging have a relationship. The relationship is described below.

Firstly to ensure that the optimal solution is not one whereby the storage is depleted at the end of the time horizon, the initial SoC (soc_{s1}) and the SoC at the end of the time horizon (soc_{sT}) for each unit s are equal to each other, as defined in (4.15).

$$soc_{s1} = soc_{sT} \tag{4.15}$$

Then, in (4.16) the SoC of time step t is defined as the sum of the State-of-Charge of the previous time step multiplied by a self-discharge coefficient and the charge and discharge into the system multiplied by a round-trip efficiency for storage.
Lastly, the SoC is bound to an upper and lower capacity constraint, with the upper constraint considering any previously installed capacity within system boundaries (soc_{s0}), as described in (4.17). The lower capacity constraint is hereby defined as a fraction of the maximum storage capacity, multiplied by a capacity coefficient A_s.

$$soc_{st} = soc_{s,t-1} SD + \eta_s^{\mathrm{S}} ch_{st}^{\mathrm{H}} - dis_{st}^{\mathrm{H}} \qquad \forall s, t > 1 \tag{4.16}$$

$$\mathrm{A}_s (soc_s^{\mathrm{H,max}} + SOC_0) \leq soc_{st} \leq soc_s^{\mathrm{H,max}} + SOC_0 \qquad \forall s, t \tag{4.17}$$

4.2. Mixed Integer Programming Model

This section is devoted to the mathematical formulation of the Mixed Integer Programming (MIP) part of the model. This model is used to extend the described base case model, whereby Unit Commitment (UC) is implemented into the model. This means that the units can be turned on or off if necessary. The usage of UC also implies that the unit can be dictated to work within a predefined working window (the operating window).

The section will build upon the used nomenclature and constraints in section 4.1. However, the nomenclature is extended with parameters and binary variables that will be introduced within this section for the MIP formulation.

Nomenclature

Parameters

C_g^{NL}	Non-load cost of electrolyser unit g for the production of hydrogen.	$[€/h/MWel]$
C_j^{NL}	Non-load cost of fuel cell unit j for the production of electricity.	$[€/h/MWel]$
C_x^{SU}	Start-up cost for unit x (with x being g for electrolysers and j for fuel cells).	$[€]$
PLR_x	Part-load ratio of unit x (with x being g for electrolysers and j for fuel cells).	$[pu]$
X_{cycles}	Degradation threshold amount of cycles after which the unit shows a decay of performance.	$[h]$
$\Psi_x t$	Degradation for unit x (with x being g for electrolysers, j for fuel cells).	$[\mu V/h]$

Binary Variables

u_{xt}	Commitment status of unit x (with x being g for electrolysers and j for fuel cells) for hour t, which is 1 when the unit is online and 0 otherwise.	$[-]$
v_{xt}	Start-up status of the unit x (with x being g for electrolysers and j for fuel cells) for an hour t, when the unit starts up this equals 1 and 0 when the unit was already in operation.	$[-]$
w_{xt}	Shutdown status of unit x (with x being g for electrolysers and j for fuel cells) for an hour t, when the unit starts up this equals 1 and 0 when the unit was already in operation.	$[-]$

Subscripts

k	Counting time steps for start-ups.	$[-]$
l	Counting time steps for shutdowns.	$[-]$

Superscripts

SU	Start-up.	$[-]$
SD	Shutdown.	$[-]$
TU	Minimum uptime.	$[-]$
TD	Minimum downtime.	$[-]$

4.2.1. Objective Function MIP model

The second model to be discussed is an elaboration of the previous model. The objective function of the Mixed Integer Programming (MIP) problem is to minimise the (operation) costs and investments required to implement the hydrogen into the system. This is defined as the sum of (i) expenditures for the electrolyser(s), (ii) expenditures for the fuel cell(s), (iii) expenditures for the storage technology and (iv) variable costs for the import/export of electricity from or to the grid. Hereby, the expenditures are split into the initial investments (capital expenditures) and the fixed operating costs. The electricity can freely be imported or exported from and to the power grid for a variable electricity price.

Note, in the case of the export of electricity, the electricity price is negative as the optimisation is done for costs. This translates in the mathematical formulation of the objective function in (4.18).

$$\min \underbrace{\sum_{g\in\mathcal{G}}\left((C_g + OM_g)h_g^{\mathrm{H,max}} + \sum_{t\in\mathcal{T}}\left(C_g^{\mathrm{SU}}v_{gt} + C_g^{\mathrm{NL}}u_{gt} + C_g\Psi_{gt}\right)\right)}_{i} + \underbrace{\sum_{j\in\mathcal{J}}\left(C_j + OM_j)f_j^{\mathrm{E,max}} + \sum_{t\in\mathcal{T}}\left(C_j^{\mathrm{SU}}v_{jt} + C_j^{\mathrm{NL}}u_{jt} + C_j\Psi_{jt}\right)\right)}_{ii}$$
$$+ \underbrace{\sum_{s\in\mathcal{S}}(C_s + OM_s)soc_s^{\mathrm{H,max}}}_{iii} + \underbrace{\sum_{s\in\mathcal{S}}(C_s^{\mathrm{ch}} + OM_s^{\mathrm{ch}})ch_s^{\mathrm{H,max}}}_{iv} + \underbrace{\sum_{s\in\mathcal{S}}(C_s^{\mathrm{dis}} + OM_s^{\mathrm{dis}})dis_s^{\mathrm{H,max}}}_{v} + \underbrace{\sum_{t\in\mathcal{T}}\Pi_t e_t}_{vi} \tag{4.18}$$

4.2.2. Constraints

Energy Balances

As is the case for the basic model described above, the electricity balance, hydrogen balance and relationship between the balances apply here in unchanged conditions as well. Since the balances are unchanged, no explanation is given, but for reading convenience only the balance formulation is restated per balance.

Electricity balance

$$e_t + \sum_{j\in\mathcal{J}} f_{jt}^{\mathrm{E}} = D_t^{\mathrm{E}} + \sum_{g\in\mathcal{G}} h_{gt}^{\mathrm{E}} \qquad \forall t \qquad \text{(4.4 revisited)}$$

Hydrogen balance

$$\sum_{s\in\mathcal{S}} dis_{st}^{\mathrm{H}} - \sum_{s\in\mathcal{S}} ch_{st}^{\mathrm{H}} + \sum_{g\in\mathcal{G}} h_{gt}^{\mathrm{H}} = D_t^{\mathrm{H}} + \sum_{j\in\mathcal{J}} f_{jt}^{\mathrm{H}} \qquad \forall t \qquad \text{(4.5 revisited)}$$

Relationship between the balances

$$h_{gt}^{\mathrm{E}} = \frac{h_{gt}^{\mathrm{H}}}{\eta_g} \qquad \forall g,t \qquad \text{(4.6 revisited)}$$

$$f_{jt}^{\mathrm{H}} = \frac{f_{jt}^{\mathrm{E}}}{\eta_j} \qquad \forall j,t \qquad \text{(4.7 revisited)}$$

Ramping Up and Ramping Down

The ramping limits applicable in the case of the extended model are unchanged with respect to the basic model described above. Therefore, only the equations are restated in this section for refreshing purposes.

In case the hydrogen electrolyser is ramped down, the difference in hydrogen output between the last and current time step for the electrolyser unit should be less than or equal to a percentage of the maximum hydrogen generation capacity of the unit. Similar logic applies in case the electrolyser is ramped up. On both occasions, a percentage of the maximum capacity (pu) represents the upper boundary for the difference in consecutive time steps.

$$h^{\mathrm{H}}_{g,t-1} - h^{\mathrm{H}}_{gt} \leq R^{\mathrm{down}}_{g}(h^{\mathrm{H,max}}_{g} + H_0) \qquad \forall g, t > 1 \qquad \text{(4.8 revisited)}$$

$$h^{\mathrm{H}}_{gt} - h^{\mathrm{H}}_{g,t-1} \leq R^{\mathrm{up}}_{g}(h^{\mathrm{H,max}}_{g} + H_0) \qquad \forall g, t > 1 \qquad \text{(4.9 revisited)}$$

Capacity Constraints

The system needs to adhere to certain capacity conditions. These are minima and maxima, which are most often operationally driven. First off, the electricity price (which has a known forecast) is subject to change over the year. Since there is a relationship between how much electricity is produced on-site, how much is exported and the electricity price, the variable that is affected by this change is the import and export of electricity as given in (4.10). This variable can take any value in between minus E and positive E, whereby E is unknown and a negative value indicates export.

$$-E^{\mathrm{E,max}} \leq e_t \leq E^{\mathrm{E,max}} \qquad \forall t \qquad \text{(4.10 revisited)}$$

The capacity constraints for the generation of hydrogen with the water electrolyser are described in (4.19), whereby the formulation is an extension of (4.11) with UC. This equation implies the electrolyser can be turned off since the lower boundary is zero. The upper capacity constraint implies a maximum generation capacity, however, as this is a variable, this will be the outcome of the optimisation modelling. Also worth noting: the maximum generated hydrogen is the sum of the maximum generation capacity of the electrolyser and the hydrogen that is initially present within system boundaries (from previous import and/or generation with different technology), presented as a parameter H_0. Most often this parameter will be equal to zero, but as the optimisation formulation is written out for a generic case, it is considered within the mathematical formulation.

$$u_{gt}(PLR_g h^{\mathrm{H,max}}_{g} + H_0) \leq h^{\mathrm{H}}_{gt} \leq u_{gt}(h^{\mathrm{H,max}}_{g} + H_0) \qquad \forall g, t \qquad (4.19)$$

The fuel cell follows the same generation logic as the electrolyser, meaning the fuel cell can be turned off and the maximum depends on the electricity demand within system boundaries and the electricity that is initially present within system boundaries, as described with lower- and upper capacity constraints respectively in (4.20), whereby the formulation is an extension of (4.12) with UC.

$$u_{jt}(PLR_j f^{\mathrm{E,max}}_{j} + F_0) \leq f^{\mathrm{E}}_{jt} \leq u_{jt}(f^{\mathrm{E,max}}_{j} + F_0) \qquad \forall j, t \qquad (4.20)$$

Finally, the same logic and capacity constraints are applied for the charge and discharge, as seen in (4.13) and (4.14). These balances are revisited here for reader convenience but are exactly the same as in the case of the LP formulation.
The State-of-Charge levels and capacity constraints are separately discussed for the storage units in the subsection 4.2.2.

$$0 \leq ch^{\mathrm{H}}_{st} \leq ch^{\mathrm{H,max}}_{s} + CH_0 \qquad \forall t \qquad \text{(4.13 revisited)}$$

$$0 \leq dis^{\mathrm{H}}_{st} \leq dis^{\mathrm{H,max}}_{s} + DIS_0 \qquad \forall t \qquad \text{(4.14 revisited)}$$

Storage

The hydrogen capacity is similar to the basic model and therefore only the governing equations have been restated.

Firstly, the initial SoC (soc_{s0}) and the SoC at the end of the time horizon (soc_{sT}) are equal to each other for each storage unit s, as defined in (4.15).

$$soc_{s0} = soc_{sT} \qquad \text{(4.15 revisited)}$$

Then, in (4.16) the SoC at time step t is defined and the SoC is bound to an upper and lower capacity constraint, as described in (4.17).

$$soc_{st} = soc_{s,t-1} SD + \eta_s^{\mathrm{S}} ch_{st}^{\mathrm{H}} - dis_{st}^{\mathrm{H}} \qquad \forall s, t > 1 \qquad \text{(4.16 revisited)}$$

$$\mathrm{A}_s (soc_s^{\mathrm{H,max}} + SOC_0) \leq soc_{st} \leq soc_s^{\mathrm{H,max}} + SOC_0 \qquad \forall s, t \qquad \text{(4.17 revisited)}$$

Minimum Uptime and Minimum Downtime & Start-up Costs

As is the case with many energy technologies, also in the case of hydrogen production and hydrogen reconversion into electricity, the units are influenced by cycling behaviour. This cycling behaviour will cause wear and tear within the unit. The degradation of unit performance can be described mathematically by a penalty for each start-up. On the other hand, many systems have minimum uptime and minimum downtime requirements. These requirements are of importance for the safe and technically feasible operation of the electrolyser and fuel cell technologies. Mathematically the constraints defining the minimum up and downtime with the addition of a commitment logic constraint describe the behaviour for both the minimum up and downtime of the unit as well as the start-up costs incurred with each start-up. Therefore, this subsection is devoted to both of these constraints.

The operational conditions discussed in the introduction for the minimum up and downtime are a consequence of technical requirements and safety measures, having an impact on the start-up and shutdown procedures. Examples of technical requirements that cannot be reached instantaneously are the pressure and temperature levels within the respective units. Similarly, some parameters and procedures will influence the safe operation of the units. The unit will follow slower start-up and shutdown trajectories, to follow the procedures or reach the optimal value for these parameters. Examples of such are the current levels within the unit, the temperature of the safety sensors and the procedures to check for any hydrogen leakages. Contributing most to this delay in the start-up phase are the pressurisation procedures of all components within the unit (stacks, piping, separators and purification system). As this delay is dependent on the volume and operating pressure of the unit, it is prone to the size of the unit.

The start-up costs discussed in the introduction can be divided into two categories: either the system starts up from a cold status or a warm status. Whereby, the first implies that the system has been shut down completely and the latter that the unit is kept running at a minimal operational condition. Both the start-up trajectories will incur a loss of revenue, as the system will not be operational until the system has reached the conditions defined. This cost is monetised for each consecutive time the start-up takes place.

In this research, the modelling approach of Morales-España et al. [114] is used to model the minimum uptime and downtime constraints. Firstly, two binary variables are introduced, being v_{xt} for a start-up sequence of unit x at time step t and w_{xt} for a shutdown sequence of unit x at time step t. Hereby the x represents either the units of the electrolyser technology or the units of the fuel cell technology. These binary variables v and w take the value of 1 if the respective unit is turned on, or turned off at time step t, otherwise, the value is 0.

The constraint for the minimal uptime in the case of a unit start-up is defined as; the sum over t for the start-up variable is less than or equal to the unit commitment status of the unit, with t within the time domain in between two start-ups, as described in (4.21). Similarly, the minimal downtime is defined in (4.22) for the shut-down variable.

$$\sum_{k=1}^{TU_x} v_{x,t-k} \leq u_{xt} \qquad \forall x, t \in [TU_x, T] \tag{4.21}$$

$$\sum_{l=1}^{TD_x} w_{x,t-l} \leq 1 - u_{xt} \qquad \forall x, t \in [TD_x, T] \tag{4.22}$$

Furthermore, the commitment logic constraint described in (4.23) ensures that the unit cannot shut down/start up simultaneously, governing the appropriate values for start-up and shutdown procedures for all x and t.

$$u_{xt} - u_{x,t-1} = v_{xt} - w_{xt} \qquad \forall x, t \tag{4.23}$$

Degradation of the Units

The performance of the electrolyser and fuel cell units heavily depends on operating characteristics. For instance, electrolysers are designed to operate at full load conditions, as discussed in subsection 2.7.1. However, in the use case with vRES, the energy supply will have an intermittent character. Therefore, the units will decay more (will have more degradation) when compared to normal operating conditions, whenever the system is switched on and off. This behaviour is described in (4.24 - 4.25) for electrolysers.

$$\Psi_{(gt)} \geq 0 \qquad \forall g, t \tag{4.24}$$

$$\Psi_{(gt)} \geq \left(\frac{\sum_{t \in \mathcal{T}} v_{(gt)} - X_{cycles}}{X_{cycles}} \right) \qquad \forall g, t \tag{4.25}$$

To understand these constraints, it is first and foremost important to define what 'X_{cycles}' (#) refers to in the constraints. Each electrolyser unit can be switched on and off, this is part of normal operation for the technology. With X_{cycles} meant, the number of cycles does not correspond to this normal operation. It is noted that the exact amount for cycles is not defined, either in literature or by industry. Therefore, the normal operation is considered to have an on-off cycle on daily basis, corresponding to 365 every year, the time horizon in the model.

According to this formulation, the degradation ($\Psi_{(gt)}$) of an electrolyser unit g at time t is at least greater than or equal to 0, as ensured in (4.24). In case the sum of $v_{(g,t)}$ (indicating the unit start-up status) is greater than X_{cycles} (which is the parameter for the 'normal yearly cycles' as defined earlier to 365), the degradation is equal to the normalised amount of yearly cycles, as stated in (4.25).

Note that the binary start-up variable is only 1, whenever the unit is turned on, meaning that the unit has performed a full on-off cycle. Therefore, the minimum threshold X_{cycles} that needs to be exceeded, is the minimum amount of on-off cycles. However, if this threshold is not exceeded, there will be no extra degradation (first constraint), thus the lifetime of the system will be regular.

5

Optimisation Results

The focus of this chapter is to discuss and analyse the results obtained from the case studies performed. As introduced in chapter 3 the case study focuses on different types of models, each performed at different extents of detail. The results are started with the reference model, which is referred to as the 'Linear Programming Optimisation'. Thereafter, the levels of detail are added per layer in the 'Mixed Integer Programming Optimisation' section, whereby a discussion is added on the sensitivity of the different types of models.

5.1. Linear Programming Optimisation

In Table 5.1, Table 5.2 and Table 5.3 the parameters that are used within the optimisation framework are restated for reader convenience. It is worth mentioning that with the optimisation framework presented the system capacity (rating or size) is not incorporated into the formulation. This means, that the capacities defined in the table are indicative sizes, which are used afterwards to analyse the results. In this case, however, as results will show for the majority of cases, the system capacities that result from the LP optimisation modelling are within the boundaries defined. However, not covering the system capacity in the formulation has implications for the implementation of the obtained optimisation result, this argument is further addressed in chapter 7.

Furthermore, all results (except when specified otherwise) in this section of the case study are obtained with data input for the 'Base Case', referring to 2020. This includes the electricity prices, hydrogen demand and electricity demand as well.

Table 5.1: Model data input for the electrolyser technologies for 2020 based on literature review as found in Table 2.3*, Table 2.4⁻ and Table 2.5º

Parameters for electrolysers 2020 - 'Base Case'	Units	Alkaline Electrolyser*	Proton Exchange Membrane Electrolyser⁻	Solid Oxide Electrolyserº
System Capacity	MW	162	20	0.05
Stack Capacity	MW	24	3	0.05
CAPEX	$€\ MW_{el}^{-1}$	750,000	1,400,000	2,000,000
Fixed O&M	$€\ MW_{el}^{-1}\ y^{-1}$	34,000	13,600	35,139
System Efficiency	%	66	63	87
Lifetime System	y	25	20	3
Lifetime Stack	h	105,000	60,000	15,000
Ramping Up	%	7	40	0.5
Ramping Down	%	10	40	0.5
Degradation	$\%_{\eta_{LHV\ Stack}}\ y^{-1}$	0.25-1.5	0.5-2.5	3-50
Load range (% of nominal load)	%	20-100	5-100	0-100

Table 5.2: Model data input for the fuel cell technology [92, 108, 109, 110, 111]

Parameters for Fuel Cell 2020 - 'Base Case'	Units	PEMFC
System Capacity	MW	10
CAPEX	€ MW_{el}^{-1}	1,320,000
Fixed O&M	€ MW_{el}^{-1} y^{-1}	13,400
Lifetime	y	9
Efficiency	%	60
Ramping up	%	0.4
Ramping down	%	0.4

Table 5.3: Model data input for the storage and charging/discharging technology [83, 109]

Parameter for Storage 2020 - 'Base Case'	Units	PEMFC
System capacity	MW	2
CAPEX	€ MW_{el}^{-1}	380,000
Fixed O&M	€ MW_{el}^{-1} y^{-1}	7,600
Lifetime	y	25
Round-trip efficiency	%	80
Hydrogen flow rate	$kg\ h^{-1}$	60

In Figure 5.1 the total energy overview for the industry location is given in three different plots. In the first plot are incorporated all loads (both for the hydrogen and electricity demand), the generation of hydrogen by all the electrolysers (AEL, PEMEL and SOEL) and the reconversion of hydrogen in electricity (by the PEMFC). In the second plot is visible in the positive y-axis the charge of the pressurised storage vessel, whereas the negative axis displays the discharge of the pressurised storage vessel. Lastly, in the third plot is visible what kind of interaction with the grid occurs through the import and export of electricity (negative values indicate export to the grid, whilst positive values indicate import from the grid).

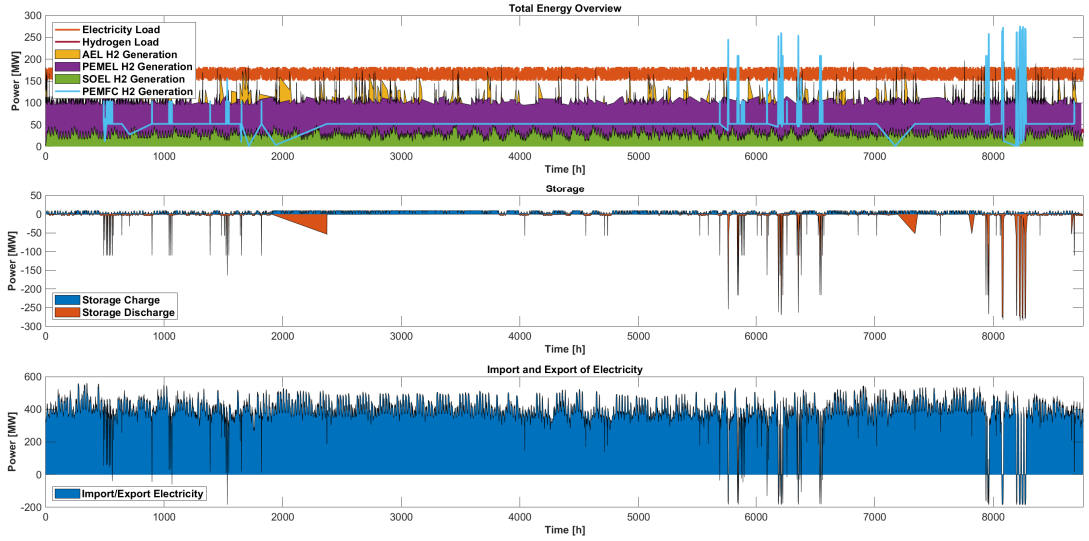

Figure 5.1: Total Energy Overview - LP Simulation

From the figure the following observations are made:

- The optimisation model chooses a large investment in AEL, as the spike at the beginning of the chart to over $1000\ MW$ production is caused by the utilisation of the maximum capacity of AEL. This immediately leads to the fulfilment of the hydrogen demand. This type of investment is caused by the fact no limiting constraints apply in the LP case, such as minimum up and downtime constraints or start-up costs (which is amongst others the penalisation of start-up costs). Therefore, the cheapest technology (with relatively high efficiency) is the most beneficial one to invest in. This overcapacity is then used whenever the prices for electricity surge or immediately after prices spike. In the case of a surge in electricity price, the AEL produces 'extra' hydrogen for storage. The hydrogen that is replenished from the storage vessel during electricity price spikes is filled-up at more convenient times thereafter (visible as yellow triangles in the first area plot).
- Investments in the technologies seem to be made according to the following logic: firstly based on the CAPEX, then the efficiency, then the ramping rates and lastly the lifetime of the system. This becomes apparent when the overall investment for SOEL is observed more closely. Despite SOEL having an $11\ \%$ and $14\ \%$ more efficient system concerning AEL and PEMEL, the investments for those two technologies are relatively higher. With a CAPEX of 2.67 times the AEL and 1.42 times the PEMEL, this is not a curious investment strategy outcome. However, as the CAPEX of the PEMEL is still almost double the CAPEX of AEL, it is interesting to see the PEMEL is also invested highly (although still less than AEL). Although the OPEX and lifetime of the PEMEL are also disadvantageous, the ramping possibilities are 4/5 times higher than the AEL. With dynamic operations, the system has opted for this investment, to fulfil hydrogen demand on the spot, rather than hydrogen from storage. This can be caused by the losses induced in the round-trip (nearly $\sim 68\ \%$ of the energy is lost for the route electricity-hydrogen-electricity with AEL), making it beneficial to directly produce and use the hydrogen generated. Another possible explanation is that the electricity prices are fluctuating too much, making it not possible to generate enough hydrogen to store it at a specific time interval.

With the case study results provided for the LP Case, the case study is thereafter put through several sensitivity analyses, to assess the effects of different parameters.

5.1.1. Sensitivity Analysis of the LP Case

The sensitivity analysis is divided into sections. In each section, the sensitivity is performed on one parameter and only on one type of electrolyser. So for example, the sensitivity analysis concerning the CAPEX is performed firstly on the AEL, whereby the CAPEX for the AEL is increased/decreased with a fixed number, within a pre-defined range. The CAPEX for the PEMEL and the SOEL are untouched while performing this part of the analysis, as well as all the other parameters. This condition is called 'ceteris paribus' in Latin and roughly translates to: 'all other things equal'. Hereby, the input data such as the hydrogen demand, electricity demand and electricity prices all follow from the same year, as introduced in section 3.4. The sensitivity analysis will be performed on the parameters as introduced in section 3.5, whereby 'Base Case' values and respective ranges are displayed in Table 5.4.

Table 5.4: Sensitivity analysis, 'Base Case' and the reference ranges per type of electrolyser

Type of Electrolyser		**CAPEX** [€ MW^{-1}]	**Lifetime** [y]	**Efficiency** [%]	**Ramping Rates** [%]	**Interest Rates** [%]	**Time Horizon** [-]
AEL	*'Base Case'*	750,000	25	66	7	2.5	2020
	Range	500,000	10	51	2	0	2030
		950,000	40	81	32	10.5	2050
PEMEL	*'Base Case'*	1,400,000	20	63	40	2.5	2020
	Range	1,115,000	5	48	25	0	2030
		1,600,000	35	78	55	10.5	2050
SOEL	*'Base Case'*	2,000,000	5	87	0.05	2.5	2020
	Range	1,500,000	5	72	0.05	0	2030
		2,400,000	25	102	25.05	10.5	2050

Sensitivity to CAPEX

The sensitivity analysis for the Total Annualised Costs as an effect of the changing CAPEX shows three atypical plots at first glance. In Figure 5.2 it can be observed that although the CAPEX increases and decreases around the initial value of $€750,000\ MW^{-1}$ for the AEL, the Total Annualised Costs (TAC) are not directly increasing nor decreasing. However, especially whenever the CAPEX change is over $€100,000$, the TAC severely drops and increases. The range of AEL CAPEX in literature for 2020 is as wide as $€400,000\ MW^{-1}$ to $€1,100,000\ MW^{-1}$, so the range shown in the figure is not unthinkable. In that sense, the change of the TAC to the right-hand side is also interesting. As in the optimisation, the result obtained from the investment into the electrolysers is heavily on AEL, a CAPEX increase has a bigger influence on the rise of the TAC than compared to the rise in TAC for PEMEL and SOEL.

With that said, in Figure 5.3 the plot shows a smooth decline/incline with a favourable effect on the price decline. This beneficial behaviour has to do with the mix of characteristics for the PEMEL, it is a decent efficiency performance, the ramping rates are the best out of the three types of electrolysers and its lifetime is also performing not quite far away from that of the AEL. The combination makes it beneficial to invest in this type of technology. The increase in CAPEX on the other side also has a relatively big impact on the TAC, as the technology was second in investment in the 'base case' scenario of this chapter.

In the case of the CAPEX for the SOEL, it is first good to note that the delta is not set on $€50,000\ MW^{-1}$ as was the case for AEL and PEMEL, but on a scale of $€100,000\ MW^{-1}$. When looking at the SOEL plot in Figure 5.4 not many changes are apparent, till the lower CAPEX zone of $< 1,700,000\ MW^{-1}$. This can be explained by the investment into the SOEL technology, which is not heavily invested in the LP case, meaning a price decrease or increase does not have a big influence on the TAC. The explanation for the decrease at lower CAPEX is to be found in the high efficiency of the SOEL. As the SOEL is highly efficient, the difference in CAPEX with AEL and SOEL technologies is covered by the higher productivity. This means that the shift in investment is towards SOEL technology.

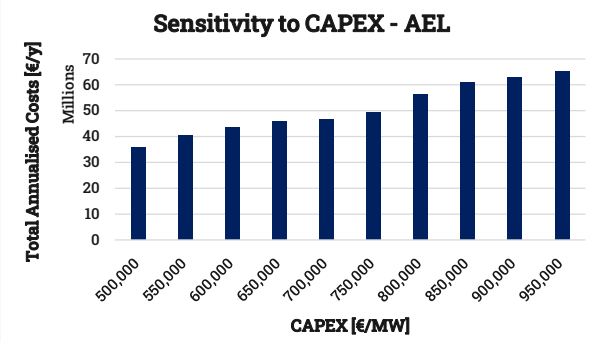

Figure 5.2: Sensitivity analysis on TAC to changing AEL CAPEX

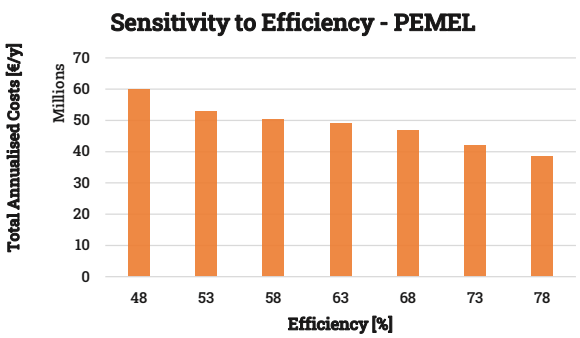

Figure 5.3: Sensitivity analysis on TAC to changing PEMEL CAPEX

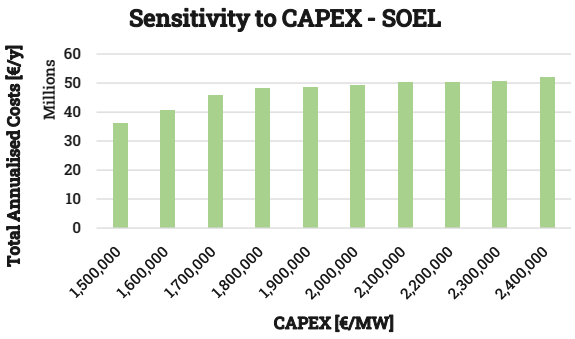

Figure 5.4: Sensitivity analysis on TAC to changing SOEL CAPEX

Sensitivity to Lifetime

In this subsection, the sensitivity analysis is performed on the lifetime of each electrolyser. To start, the 'base case' as introduced at the beginning of this chapter for each of the electrolysers is as follows: $25\ y$ - AEL, $20\ y$ - PEMEL and $3\ y$ - SOEL. In Figure 5.5, Figure 5.6 and Figure 5.7 the resulting sensitivity analysis is shown. In the case of the SOEL, it can be observed the sensitivity is covering fewer data points than the sensitivity analysis performed on the other two products. With no possibility to go analyse below the 5 years mark in terms of the lifetime, as investments would not be recovered at all.

When taking a look at the plots, the situation for the SOEL shows dissimilarities from the two other plots. The SOEL stack cannot operate for longer periods than $3\ y$ due to stack failure under high operating temperatures, unless material improvements take place in the close future. The SOEL becomes more beneficial with the extension of its lifetime, especially with the SOEL's relatively high efficiencies. However, the TAC does not decrease as expected. This is caused by the high CAPEX of SOEL, meaning that the shift in investments and operational models into SOEL does lead to lower operational costs (mainly due to a more efficient system consuming less energy), but not to an overall decrease in the objective value.

The AEL and PEMEL cases show the result in line with expectations, with a decrease in TAC whenever the lifetime is increased. Curiously enough, the effect over the PEMEL is higher. An explanation for this occurrence is given in the difference in mutation concerning the annualised investment costs. In the case of the PEMEL technology, the mutation is higher (in absolute terms), as the initial CAPEX is also higher. Therefore, the gap between the two technologies is made smaller on yearly basis and thus investments in PEMEL are more interesting. The more expensive CAPEX is therefore not disadvantageous in the case of the PEMEL and lifetime sensitivity like was for SOEL.

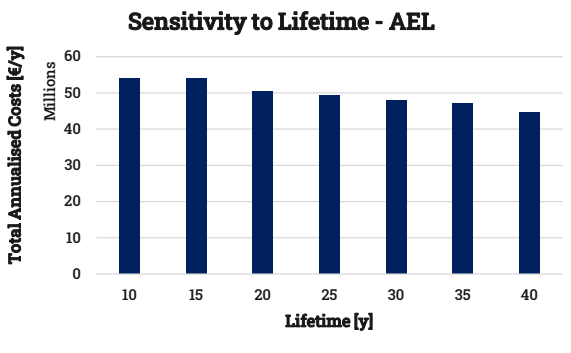

Figure 5.5: Sensitivity analysis on TAC to changing AEL Lifetime

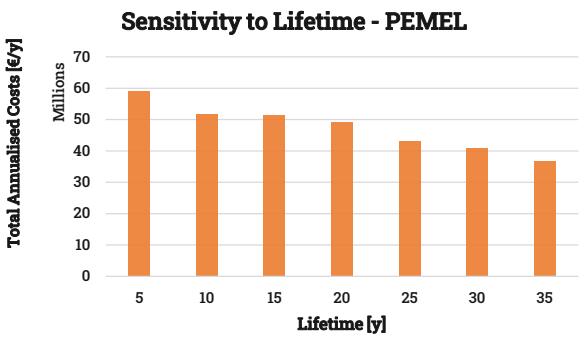

Figure 5.6: Sensitivity analysis on TAC to changing PEMEL Lifetime

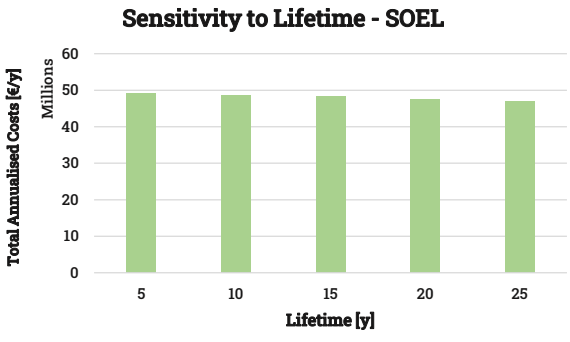

Figure 5.7: Sensitivity analysis on TAC to changing SOEL Lifetime

Sensitivity to Efficiency

In this subsection, the sensitivity analysis is performed on the efficiency of each electrolyser. To start, the 'base case' as introduced at the beginning of this chapter for each of the electrolysers is as follows: $66\ \%$ - AEL, $63\ \%$ - PEMEL and $87\ \%$ - SOEL. In Figure 5.8, Figure 5.9 and Figure 5.10 the respective plots are shown for AEL, PEMEL and SOEL. What pops out is that the efficiency for AEL and PEMEL behave similar, meaning that the efficiency decrease leads to an over effect on the TAC, as these two technologies are technologies with higher investments from the start. Vice versa, an increase in efficiency leads to a sharp decrease in TAC as they can play a vital role in the investment and operational strategies with long lifetimes, lower CAPEX, etc.

More interesting is the plot for the SOEL. In the decrease in efficiency, this plot does not show much change, as it is not one of the major technologies being invested in. Vice versa, however, with an increase in efficiency, the TAC almost surpasses the best-case scenario for the PEMEL. This is a noticeable change and the only reason it does not exceed the PEMEL in performance is the fact that the CAPEX is still ~ 1.5 times as much. However, the reduction in operational costs (electricity feed-in from the grid) results in a very sharp decrease in TAC.

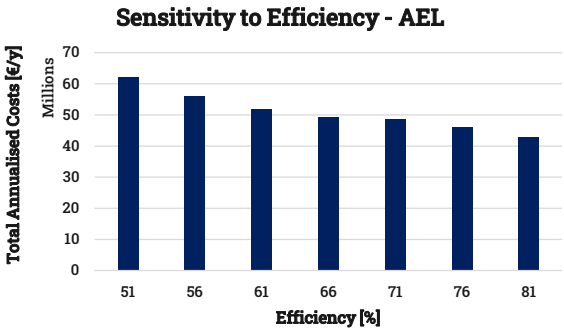

Figure 5.8: Sensitivity analysis on TAC to changing AEL Efficiency

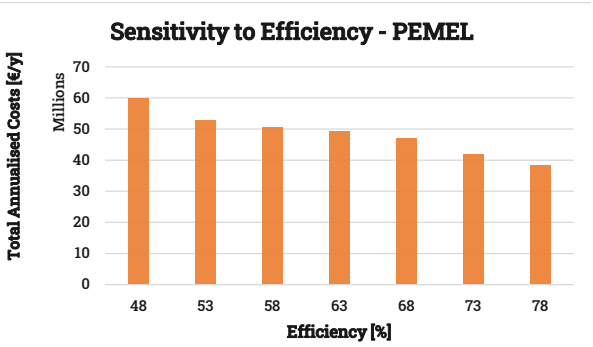

Figure 5.9: Sensitivity analysis on TAC to changing PEMEL Efficiency

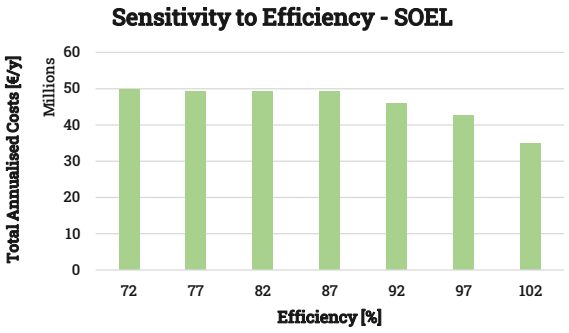

Figure 5.10: Sensitivity analysis on TAC to changing SOEL Efficiency

The effect of the efficiency is also clearly visible in the Total Energy Overview. Since the efficiency is near the $100\ \%$ and in one case of the case study even above that mark, the round-trip efficiency for electricity-hydrogen-electricity becomes $\sim 16\ \%$ more efficient than was the case for AEL. In other words, the price has to change by twice the amount to overcome this loss in the system, whilst previous cases a minimum price change of $300\ \%$ was required to overcome the loss. This makes it more beneficial to store hydrogen and this can be seen in Figure 5.11, where the clear increase in SOEL production is visible (green area plot) in the first plotbox and the increase in storage is visible in plot two (blue area plot). Similarly, the earlier mentioned decrease in electricity import is visible in plot 3. This does not necessarily mean the TAC decreases enormously (with the high CAPEX), however, there is a clear shift in investment and operational strategies apparent.

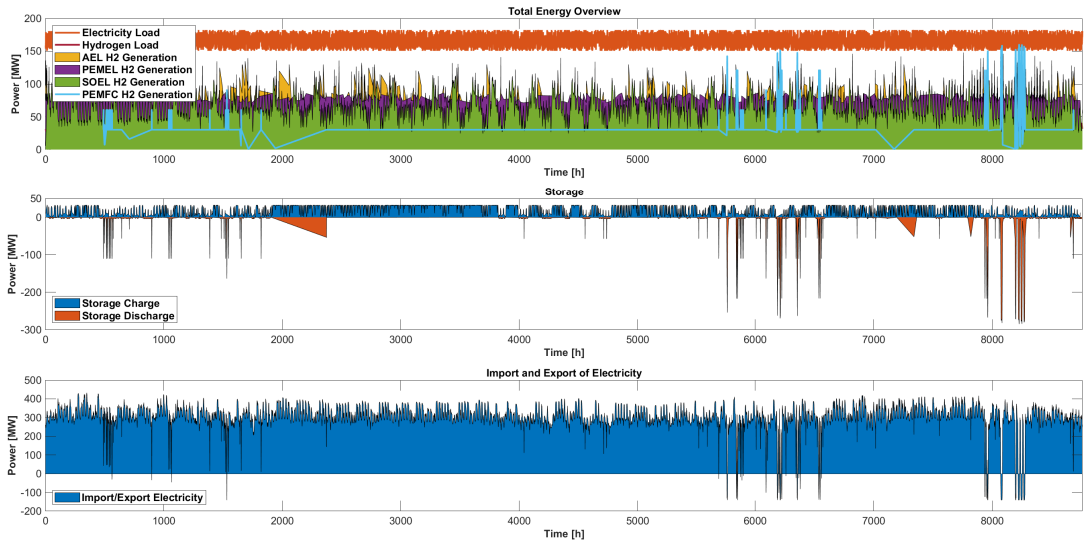

Figure 5.11: Total Energy Overview sensitivity to changing efficiency

Sensitivity to Ramping Rates

The ramping rates are defined in the base case as follows: $7-10$ % - AEL, 40 % - PEMEL and 0.05 % - SOEL. The ramping rate is different for ramping up and ramping down specifically for the AEL, as is indicated with the double value. In the sensitivity analysis, each of the In Figure 5.12, Figure 5.13 and Figure 5.14 the respective plots are shown for AEL, PEMEL and SOEL.

First, behaviour for all types of sensitivity is flat for all three models. Ramping is either crucial when the ramping is very limited over time, or whenever the capacity of the system that needs to be ramped up and ramped down is very large. Logically, in the latter case, it will require more time to solve the model. Therefore, the ramping constraint does not directly become dominant in the investment or operational model.

There seems to be a sweet spot when all sensitivity plots show radical changes for the obtained TAC. This spot is found earlier with the AEL and is below the PEMEL parameter value reached (so before the 40 % ramping rate is reached). The reason for this switch in investment towards the AEL and the resulting lower TAC can be justified when the parameters are analysed. In such a scenario the AEL outperforms PEMEL on all parameters or is nearly as good (i.e., better efficiency, better lifetime, better CAPEX and then ramping rates in the comparable zone).

This sweet spot occurs also in the sensitivity analysis for PEMEL and SOEL, albeit differently. PEMEL is already advantageous, making it possible to ramp up and down quickly. So, there is no switch in investment or operational model seen in the first situation, up until the difference in ramping constraint is of added value, making the optimisation model invest more into the PEMEL.

The SOEL on the other hand is not competitive with the other two models, with low commercialisation, the ramping rates are only $1/8oth$ the ramping capacities of PEMEL for instance. Therefore, the sensitivity of SOEL is different from the other two models, with a percentage change which is above realistic developments in near future. Even though this is not directly a sensitivity analysis, it shows where the sweet spot is for SOEL, above 20 % of ramping rates.

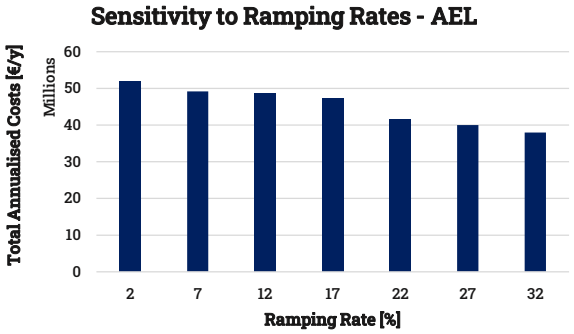

Figure 5.12: Sensitivity analysis on TAC to changing AEL Ramping Rates

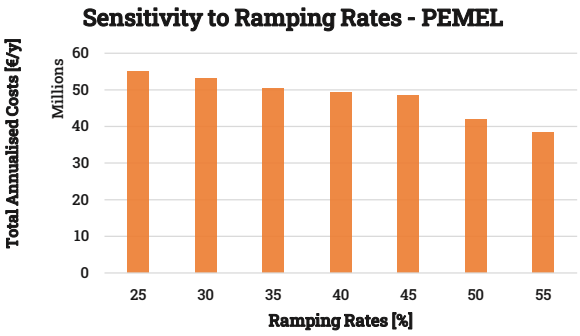

Figure 5.13: Sensitivity analysis on TAC to changing PEMEL Ramping Rates

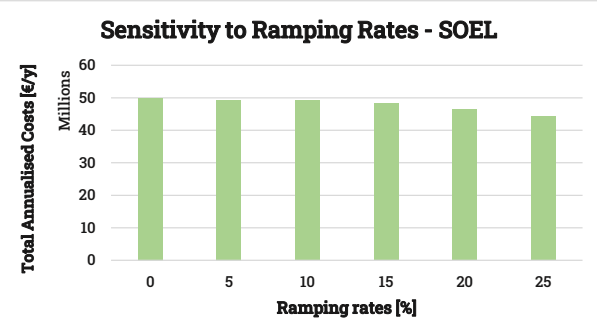

Figure 5.14: Sensitivity analysis on TAC to changing SOEL Ramping Rates

Sensitivity to Interest Rates

In the case of the change of interest rate, all three plots show similar behaviour, therefore only one of the three is displayed in Figure 5.15. What strikes is that the increase in interest rates leads to a merely linear increase in TAC. There is not much shift in the investment behaviour for all three technologies, because of this linear relationship.

However, two elements worth noting: the TAC increases relatively more for PEMEL and SOEL as both have higher CAPEX, meaning the Annualised Costs as introduced in chapter 4 with its relationship towards lifetime and interest rates is more influenced (numerically) then the AEL case shown. Similarly, the TAC decreases more than linear for the 0 % interest rate case, this is not deemed a realistic scenario. Despite the historically low-interest rates in recent years, the interest rate is increasing again and above all is always higher for companies with investments with a long return on investment.

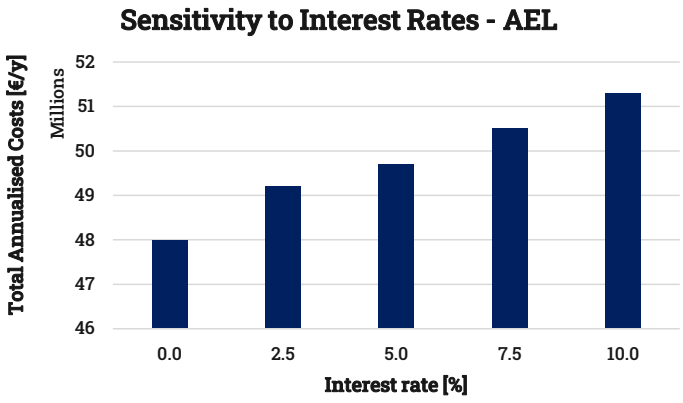

Figure 5.15: Sensitivity analysis on TAC for different interest rates

Sensitivity to Time Horizon

With the sensitivity towards the time horizon meant, incorporating R&D on the technologies (the whole hydrogen pathway), considering the growth of world population (and thus the energy demand), the switch from fossil fuels to more and more vRES, what kind of impact would that have on the model. This is a different type of sensitivity analysis than the ones previously done throughout the chapter, as this includes the change of multiple parameters at once, let alone the fact that the change in parameters is highly uncertain. In Table 5.5 and Table 5.6 the data input as being used in this section and assessed from the literature (see chapter 2 for further reference) can be obtained. It is noted that the 'Fixed O&M' is taken to be a value of 2% of the CAPEX, as this is found in different literature to be an acceptable approach ([66, 56]).

Table 5.5: Model data input for the electrolyser technologies for 2030 [66, 68, 69, 74, 77]

Parameters for electrolysers 2030	Units	Alkaline Electrolyser	Proton Exchange Membrane Electrolyser	Solid Oxide Electrolyser
System Capacity	MW	200	50	0.1
Stack Capacity	MW	50	10	0.1
CAPEX	€ MW_{el}^{-1}	580,000	760,000	1,060,000
Fixed O&M	€ MW_{el}^{-1} y^{-1}	11,600	15,200	21,200
System Efficiency	%	70	74	93
Lifetime System	y	25	20	5
Lifetime Stack	h	115,000	80,000	25,000
Ramping Up	%	17	40	0.5
Ramping Down	%	17	40	0.5
Load range (% of nominal load)	%	15-100	5-100	0-100

Table 5.6: Model data input for the electrolyser technologies for 2050 [66, 68, 69, 74, 77]

Parameters for electrolysers 2030	Units	Alkaline Electrolyser	Proton Exchange Membrane Electrolyser	Solid Oxide Electrolyser
System Capacity	MW	300	200	3
Stack Capacity	MW	100	100	3
CAPEX	€ MW_{el}^{-1}	360,000	680,000	530,000
Fixed O&M	€ MW_{el}^{-1} y^{-1}	7,200	13,600	35,139
System Efficiency	%	70	80	97
Lifetime System	y	30	30	10
Lifetime Stack	h	120,000	120,000	100,000
Ramping Up	%	10	40	3
Ramping Down	%	10	40	2
Load range (% of nominal load)	%	5-300	5-300	0-200

With the aforementioned data, the figures in Figure 5.16 and Figure 5.17 are simulation outcomes for the cases in 2030 and 2050 respectively. A few observations can be made on both figures simultaneously. For example, the general hydrogen load and electricity load is more than in the scenario of 2020, in both the 2030 and the 2050 scenarios. This is expected due to population growth, the implementation of more vRES in the power grid (requiring more storage), but also an increase in hydrogen due to a more mainstream adaptation of hydrogen, as explained in the reference papers for the demand [105]. However, the increase is not reflected one on one caused by an increase in system efficiencies. Therefore, the import of electricity from the grid into the system scope is reduced, as the higher efficiency leads to a decrease in electricity requirement in the overall system.

Further, in both the figures, it can be observed that the efficiencies of the fuel cell are expected to increase. This requires some logic before it can be understood. The differences between the fuel cell operation and hydrogen dispatch in plots 'Total Energy Overview' and 'Storage' are not reflected directly in the 'Import and Export of Electricity' plot. Each time, the exported electricity is less than the hydrogen converted back into electricity in terms of power (MW). Hereby, the export of electricity, the spikes below 0 are to be analysed and as can be seen, this value increases from the Base Case in

Figure 5.1 to the 2030 and 2050 scenarios. The difference is the loss occurring in the fuel cell, with efficiencies expected to increase in the upcoming years.

From the scenario in 2020 to the scenarios in 2030 and 2050, there is also an apparent shift in the used technologies. The AEL is less and less used, whereby the investments (and thus capacity) in PEMEL and SOEL are increased. This is along the expectations, as the PEMEL and SOEL show a sharp decrease in CAPEX and an increase in lifetime, whereby the AEL levels for these two technical parameters are reached. The improvement in terms of AEL technology is limited, as the TRL is at 9 and further increases and developments are not staggering.

Lastly, the behaviour of the storage of the system also is impacted by the change in efficiencies for the round-trip (electricity-hydrogen-electricity). The round-trip efficiencies are increased with higher efficiencies yielded for all technologies involved, meaning the storage of hydrogen is increased.

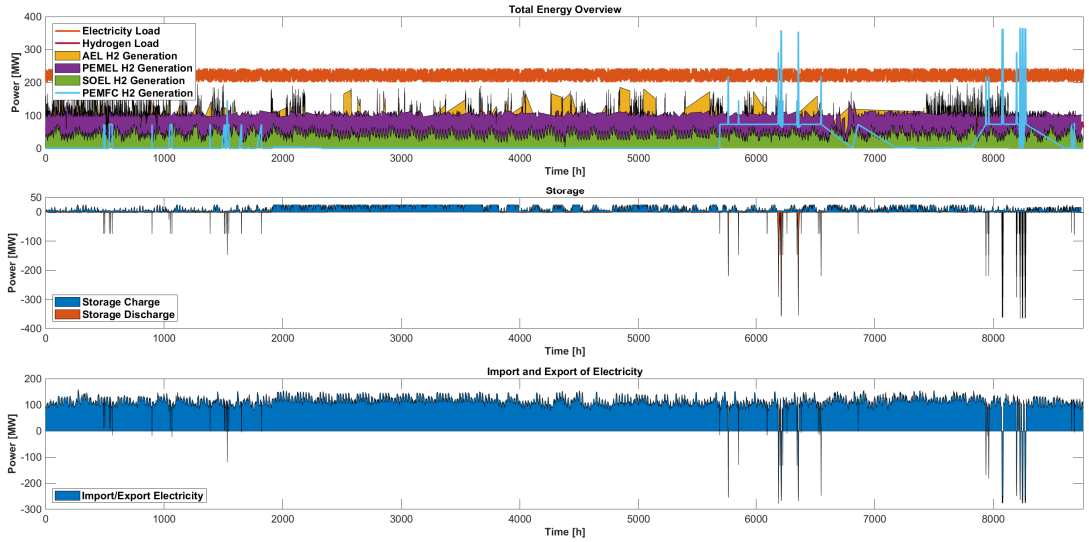

Figure 5.16: Total Energy Overview - 2030 scenario

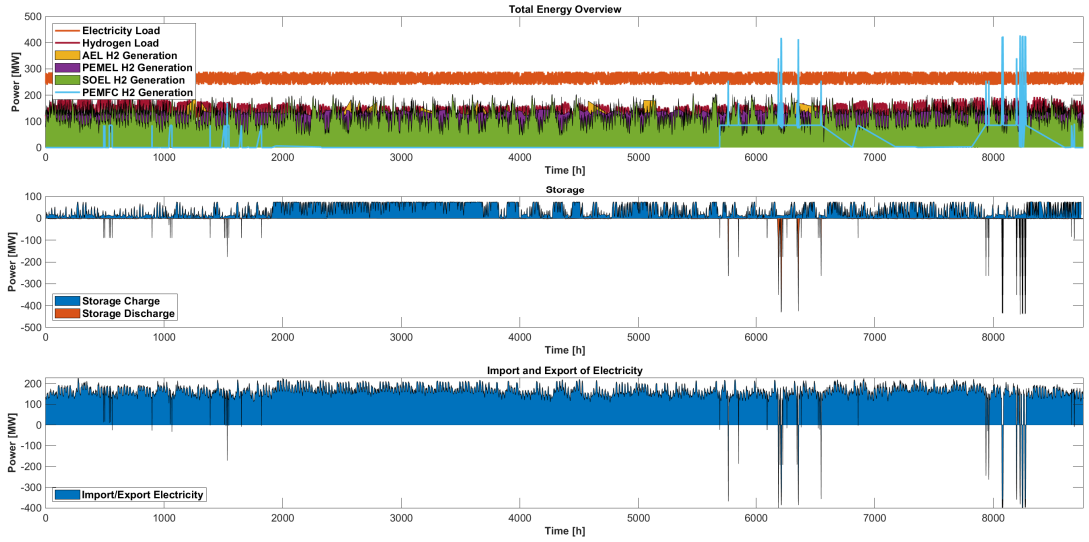

Figure 5.17: Total Energy Overview - 2050 scenario

5.2. Mixed Integer Programming Optimisation

In this section, the detailed optimisation formulation is put through different scenarios. The approach is to test every possible configuration of the detailed model, such that the influence of the four constraints can be assessed individually and whenever the constraints are activated in a combined manner. The four constraints in the case are:

- *Minimum Part-Load* - Constraint that defines at which load the system needs to run idle or be turned off. With this constraint non-linear loads are a possibility (e.g., once the system switches on, the part-load operation is at $20\ \%$)
- *Minimum Uptime & Downtime* - Constraint that defines how long it takes for the system to undergo all necessary operational procedures before it is up and running again (once it is switched off), or once the system is switched on, how long it needs to maintain the same pressure and temperature before it can be switched off.
- *Start-up Costs* - This constraint is an accompaniment for the previous constraint and defines if there are any losses in the system at start-up that need to be penalised. Examples of losses are: left-over hydrogen and oxygen in the tank whenever the system is turned off (the system needs flushing) or the loss in efficiency (performance) at lower part-load operation.
- *Degradation Due to Cycling* - As discussed elaborately throughout the research, there is a significant effect of cycling behaviour on the degradation of the electrodes and other materials in the electrolysis cell. This constraint enforces the replacement of the stack whenever the degradation exceeds a certain threshold within a predefined timeframe.

An overview of all possible combinations can be consulted in Table 5.7. This approach can be considered as a form of sensitivity analysis to all the results obtained.

Table 5.7: All possible model configurations based on four components (including Model 16 - 'Base Case')

Parameter	Minimum Part-Load *L*	Minimum Uptime & Downtime *M*	Start-up Costs *S*	Degradation Due to Cycling *D*
Model 1 / LMSD	X	X	X	X
Model 2 / LMS -	X	X	X	
Model 3 / LM - -	X	X		
Model 4 / LM - D	X	X		X
Model 5 / L - SD	X		X	X
Model 6 / - MSD		X	X	X
Model 7 / - - SD			X	X
Model 8 / - - - D				X
Model 9 / - - S -			X	
Model 10 / - M - -		X		
Model 11 / - MS -		X	X	
Model 12 / - M - D		X		X
Model 13 / L - - D	X			X
Model 14 / L - S -	X		X	
Model 15 / L - - -	X			
Model 16 / - - - -				

The overall optimisation results can be obtained in Table 5.8. The term MIP GAP is introduced within this table. The MIP GAP is a term used in optimisation solvers, literally meaning the gap that still exists to the best possible solution for the MIP model, whenever the predefined simulation time is exceeded. So in the case of 'Model 1', the Total Annualised Costs are calculated to be $366\ M€\ y^{-1}$, however, this value is the best value approach in the order of 4.6% (above or under) the best solution, since the MIP GAP is stated to be 4.6%. The predefined simulation time in this research is defined as $10\ min$. This limit is a scaled-down computational limit, as the system modelled in this research is smaller than the possible use case of the mathematical framework.

To clarify the last sentence, an example can be considered where the data points include a model considering the whole of The Netherlands or even Europe. The necessity for the introduction of a MIP GAP becomes clear, as the data points increase exponentially and thus take a computational toll on the model. This computational burden will not make it more beneficial to finish each simulation, as long as the results are within a certain margin (say 5 %) of the precise result. This is an arbitrary process, as both the MIP GAP margin has to be predefined as a boundary condition, as well as the simulation time. However, the implementation of both is a trade-off whereby it can still be more beneficial than waiting for the simulation to finish as long as the expected result is giving enough indication of the outcome.

Despite the presence in the table, *Model Type 1 / L M S D* and *Model Type 2 / L M S -* has also been simulated for the complete length. For Model type 1 this resulted in a computational time of $2,155\ s$ ($36\ min.\ 55\ s$) and a TAC of $65.7\ M€\ y^{-1}$ and for Model Type 2 the following results where obtained: computational time of $1,531\ s$ ($25\ min.\ 31\ s$) and a TAC of $63.3\ M€\ y^{-1}$.

Table 5.8: Optimisation results for all configurations, defining both the computational time and the Total Annualised Costs

Model	Type				Computational Time [s]	MIP GAP [%]	Total Annualised Costs [$M€\ y^{-1}$]
1	L	M	S	D	600	4.6	63.7
2	L	M	S	-	600	3.7	61.2
3	L	M	-	-	363	≤0.1	54.4
4	L	M	-	D	499	≤0.1	57.8
5	L	-	S	D	523	≤0.1	58.9
6	-	M	S	D	45	≤0.1	54.7
7	-	-	S	D	39	≤0.1	51.4
8	-	-	-	D	22	≤0.1	49.6
9	-	-	S	-	35	≤0.1	51.6
10	-	M	-	-	29	≤0.1	50.0
11	-	M	S	-	46	≤0.1	53.3
12	-	M	-	D	31	≤0.1	50.3
13	L	-	-	D	303	≤0.1	51.5
14	L	-	S	-	241	≤0.1	52.6
15	L	-	-	-	166	≤0.1	50.3
16	-	-	-	-	16	-	49.2

What is furthermore noted around the simulation configurations in Table 5.8 is:

- The effect caused by the separate constraints over the LP (Model Type 16) either in terms of computational time or in terms of extra TAC is not always reflected one-on-one when constraints are combined. For instance, in the case of the minimum uptime and downtime constraint and start-up combination (Model Type 11 / - M S -), the length of the combined constraints is less than the difference caused between the separate constraints and the base case. This reasoning also upholds the resemblance in the TAC. Therefore, it can be assumed that the computational burden is not only caused by the complexity of the constraints, but also by the configuration of the model.

- In all the cases with at least one constraint (Model Types 1-15) the Total Annualised Costs increase. Although the increase is dependent on the type of configuration, it is interesting to note that a more accurate model leads to an increase in the objective value. One could assume that an increase in accuracy leads to fewer oversized systems, meaning fewer investments and thus a lower TAC. However, the increase can be explained by the tight grip a constraint has over the model. Either way, a constraint implemented requires the model to slow down (for example the system cannot shut down immediately after its start-up due to minimum uptime). These types of constraints make the system less dynamic and thus less efficient.

In Figure 5.18 the same results are visualised in a graphical manner. What becomes apparent in this figure is that there is a clear impact of the electricity costs on the TAC (here referred to as 'objective value' on the y-axis, as the term are interchangeable in this case). Almost in all cases, this operational cost is $\sim$ 70 % of the TAC. Further is noticed that the start-up costs are having the least impact in terms of TAC. However, there is an extra computational burden the start-up trajectories add to the optimisation model, to be precise, when comparing *Model 9 / - - S -* and *Model 16 / - - - -* the difference is $19\ s$ in the disadvantage of the model with the start-up trajectory. Although $19\ s$ is a relatively small addition of time, the overall time is increased by double the amount of time. The difference in TAC is not negligible with $€2.4M$ on an overall TAC of $€49.2M$, however, depending on the size of the case, the start-up costs constraint can be neglected.

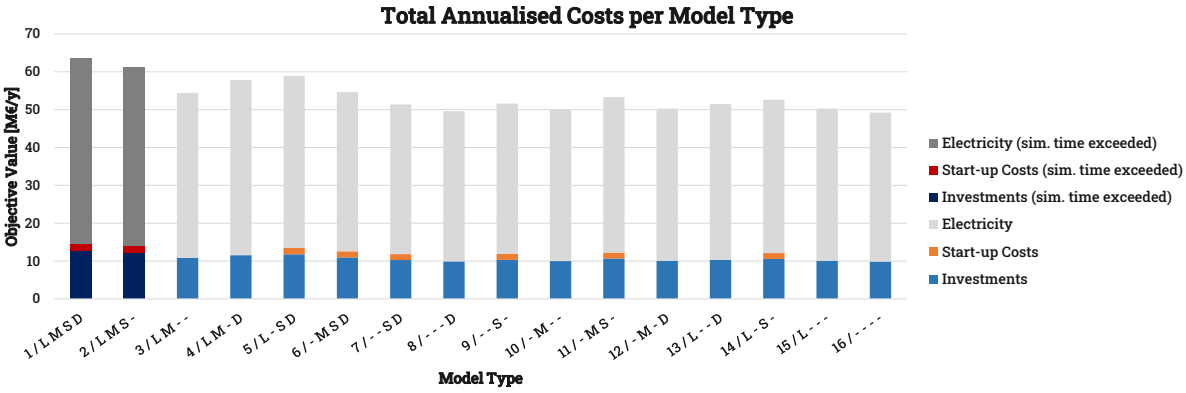

Figure 5.18: Sensitivity analysis on TAC for different constraint configurations

6

Conclusions

Within this research, a novel hydrogen optimisation and scheduling model is presented for water electrolysis, storage and fuel cells. The water electrolysis technologies consist of Alkaline Electrolyser (AEL), Proton Exchange Membrane Electrolyser (PEMEL) and Solid Oxide Electrolyser (SOEL), whilst the fuel cell is the Proton Exchange Membrane Fuel Cell (PEMFC) and the storage consists of a pressurised $200\ bar$ hydrogen storage vessel. With a structured approach, two models have been created to compare the effects of technical parameters and operational policies within the optimisation framework to assess the following research goal:

Asses the optimal level of detail for modelling the hydrogen reconversion pathway with electrolysis and the effects of different levels of detail on the computational time.

After a literature review of technical parameters and operational policies regarding the technologies, two models were created in a mathematical framework. The two models proposed were Linear Programming (LP) and a Mixed-Integer Programming (MIP) Model. Within the LP model 6 different sensitivity analysis has been performed, to be precise on *Capital Expenditures (CAPEX), efficiency, lifetime, ramping rates, interest rates* and finally *different time horizons*. The outcome of these analyses is that the technology mix can best be used in a combined manner, whereby each component of the mix contributes towards minimising the objective value: the Total Annualised Cost.

Furthermore, the optimisation results obtained due not change swiftly to the sensitivity analysis, as most parameters influence the obtained result. To clarify this with an example, in Figure 6.1 the figure for the sensitivity analysis to CAPEX on the Total Annualised Costs (TAC) for the SOEL is shown. As the high CAPEX prevents any investment into this electrolyser, at higher CAPEX' the TAC is relatively unchanged. Up until it reaches the point at around $< €1,700,000\ MW^{-1}$. Despite the CAPEX still being higher than the other two technologies in the mix (AEL at $€750,000\ MW^{-1}$ and PEMEL at $€1,400,000\ MW^{-1}$), the TAC starts decreasing, as there is an investment into SOEL. This investment is initiated by the fact that the efficiency of the SOEL is $12-14\ \%$ higher than respectively the AEL and PEMEL. With this higher efficiency, the difference in CAPEX is overcome and less electricity is needed to be imported, resulting in a decreasing TAC.

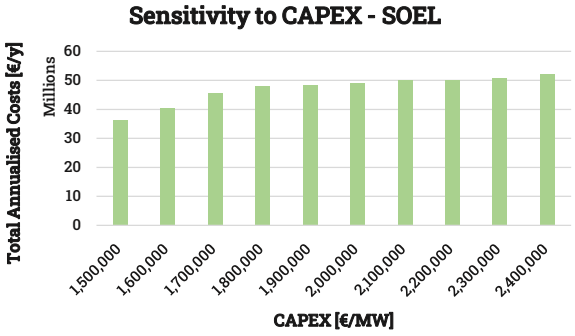

Figure 6.1: Sensitivity analysis on Total Annualised Costs for changing SOEL CAPEX

The LP and MIP combined framework led to the configuration of 16 different types of constraints. The constraints to be modelled were: minimum uptime and downtime, start-up costs, degradation due to cycling and finally the part-load operation. The most outstanding findings of the sensitivity analysis towards the MIP model and the 16 different configurations were:

- The impact of the start-up cost on the obtained results is limited. However, there is an extra computational complexity added to the optimisation model. Therefore, the start-up cost can be neglected when modelling bigger data sets. Similarly, this advice does not uphold when the start-up trajectories have to be split in two, namely: warm and cold start-up trajectories, as this was not part of this research. The effects of such on the model and the obtained results are not assessed.
- Although the model becomes more precise and realistic with the implementation of the additional constraints, the TAC does not decrease, but on the contrary increases. Therefore, the constraints added do add to the TAC as defined within the research.

Finally, the optimisation framework and the work that lead to the proposition of this framework have also led to insights regarding the process. These insights are discussed in chapter 7, where also recommendations for future research have been stated.

7

Discussion & Research Recommendations

7.1. Discussion

Within this research, the optimal investments and operational models for the usage of hydrogen have been researched. While performing this research assumptions were made, either it was not part of the scope or a simplification of the optimisation model was required. These simplifications and their respective effect on the obtained optimisation results are discussed in this section.

- Within this research modelling has been done over an hourly time horizon and for a single year (no multi-year resolution). Especially the first assumption can be critical for constraints such as the start-up trajectory or ramping up and down. These constraints have data input that has a resolution on a $15\ min.$, $10\ min.$, $5\ min.$ or sometimes even $seconds$ interval. Whenever the model considers an hourly time horizon, these constraints become redundant. Therefore, the constraints for the start-up trajectory and minimum uptime and downtime are not claimed to be redundant in the research, despite comments made the impact of both is limited on obtained Total Annualised Cost (TAC).
- During the optimisation modelling the system capacity (in other words, the rating or size) is not incorporated in the model framework. The site for implementation of the hydrogen pathway system (electrolyser, fuel cell and storage) is not checked upon the available square meters. Especially in the case of Solide Oxide Electrolyser (SOEL), which has a bigger footprint when compared to Alkaline ELectrolyser (AEL) and especially to Proton Exchange Membrane Electrolyser (PEMEL), this is a consideration to be made. In the work of IRENA [68] and Jens [119], the following footprints and electrode areas are stated:

Table 7.1: Electrolyser Footprint and Electrode Area [68, 119]

Parameter	Units	AEL	PEMEL	SOEL
Electrolyser Footprint	$m^2\ MW^{-1}$	100	60	150
Electrode Area	cm^2	10,000-30,000	1,500	200

This implies the following: the electrode footprint of the SOEL is very small compared to the other two technologies. However, as the auxiliary equipment and BoP are very large, the total area occupied is 1.5 to 2.5 times as large as the other two technologies. Although this might seem like a disadvantage, the benefit of such a system is that all the components have room for improvement, rather than only one component that requires further finetuning. Therefore, this aspect gives hope for further implementation of SOEL in areas where there is not much space.

However, for this research, noting that the SOEL electrodes are comparatively small in size (i.e., capacity), the SOEL will require more systems installed on-site. Depending on the number of systems installed, the system with all its auxiliary equipment will cover a tremendous amount of space on the industry site. These limitations are not covered within this research, as the goal is to find the optimal mix of technologies, however, are put up as food for thought.

- During the creation of the optimisation model framework a thorough literature review has taken place. One of the often implemented methods for start-up trajectories includes a start-up from a warm state and one from a cold state. The difference between these two implies what status the system was in the previous period (idle/stand-by or entirely shutdown). Especially shutting down the electrolyser might have serious consequences (e.g., degradation of the electrodes, catalyst, etc.). However, as specified under the first item, the model resolution is chosen on an hourly timescale. Aside, the quantification of the degradation after such a form of cycling is still in public debate and the quantification is something to be researched. Combining both reasons, the research continued with the assumption that the minimum uptime and downtime constraint, together with the defined start-up constraint was enough to replace the warm and cold start-up constraints. This assumption is to be researched in future research.
- During this research the COVID-19 pandemic still played a major role in all markets and the Russian-Ukrainian war broke out. Due to these circumstances, the gas prices increased to record heights [120]. A welcome side effect of the increased gas price and oil price is that the usage of fossil fuel-based hydrogen production routes becomes economically less viable compared to water electrolysis techniques. A strengthening development in favour of water electrolysis is that many countries have intensified their search for alternatives for natural gas and other fossil fuels, investing in alternative technologies. Therefore, the time horizon sensitivity analysis in this research might become outdated at a rather fast pace, with these developments and investments ramping up the viability of electrolyser units sooner than expected.
- The economies of scale are not deemed applicable within this research for electrolyser units and fuel cell units, due to the modular nature of sizing the capacity of these technologies. However, this assumption only holds for an industry which does not have a monopoly position on the market. With a monopoly position or with a position whereby the installed capacity will be big enough to influence the market price, economies of scale might be applicable as stated by Morgan et al. [121]. However, as the article states, the benefit of the economies of scale is still not applicable to the electrolysis stacks, but rather to the auxiliary equipment (such as transformers, rectifiers, compressors) and the BoP. This assumption is left out of the equation.
- Although also stated as a benefit for the future realisation of green hydrogen pathways, the fact that R&D development on electrolysers and similar technologies seems to be lacking on most of the forecasts is also a point of concern. The future is unpredictable (to an extent), however and in retrospect, the assumptions made in 2005, 2010 and 2015 for the latter 2010, 2015 and 2020 are not met in terms of electrolyser technical parameters and operational strategies. For a breakthrough in this technology, a leap has to be made.

7.2. Research Recommendations

Due to the nature and size of this research, the scope of the project is limited. However, as an outcome of this research, several topics of interest have been identified for future research in light of the future hydrogen economy.

- First and foremost, the design of the current electrolysers is focused on 'full-load' operation. In practice, full-load is not met, especially not with vRES, fluctuating demand, limited storage facilities and fluctuating electricity prices. Therefore, the system needs to be remodelled in such a way that the performance peaks at partial-load. The remodelling of a system as delicate as the electrolyser is not simply made, therefore, this requires a serious commitment to R&D, both from the industry as well as academia. The reader is also pointed to the usage of the word 'system' and not just the electrolysis stack, as commonly the terms are mistaken for each other, leading to the misconception of the performance and efficiency of electrolysis.
- As proposed in the discussion section, the quantification of the degradation of electrolysis components (such as the electrode, catalysts, electrolyte, and membrane) is of utmost importance for further developments of the dynamic operation of electrolysis units. TNO and TU Delft, both academic institutions with a focus on applied sciences could be frontrunners in this topic. With the degradation quantified, the research can be extended into the mechanisms causing the degradation and thereafter possible solutions. Here the sidenote can be made, if after all the degradation is quantified and deemed to be within an acceptable range, this argument that blocks the dynamic operation of AEL and SOEL technologies can be cleared. Either way, the outcome can provide a step forward in the development of electrolysis technologies.
- The research is focused on the optimisation of hydrogen production with electrolysis. Within the scale of technologies, three electrolysis technologies were chosen, as they have a proven track record, the highest Technology Readiness Level (TRL) or are assumed to be chosen for future implementation (e.g. the SOEL). The research, however, could be extended with the implementation of fossil fuel-oriented hydrogen production routes and alternative electrolysis technologies (such as Anion Exchange Membrane Electrolyser). Especially, the fossil fuels-oriented route suddenly is less advantageous as gas prices spike (making the comparison with green hydrogen more beneficial for the 'green' route), but there is still a huge price advantage for the fossil fuel-oriented route. Until this disadvantage disappears, there will be no incentive to change to alternative methods, therefore also requiring continuous effort and R&D into the fossil fuel-oriented routes.
- Similarly, the research is limited to one storage technology of choice (compressed hydrogen storage) and one type of fuel cell (Proton Exchange Membrane Fuel Cell - PEMFC). The choice for hydrogen storage is based on the hydrogen demand on-site for the case study, whereby regional or national hydrogen storage options such as salt caverns or salt mines are deemed competitive storage alternatives. Similarly, the PEMFC option is based on dynamic operation within the system, however, alternatives could also be added for completeness.
- The two models proposed in the mathematical framework are a Linear Program (LP) model and a Mixed-Integer Program (MIP) model. These do not include any constraints that extend the advanced model in non-linearity in terms of constraints or the objective to be obtained. In addition, this framework can be done by focusing only on these segments and combining both into a renewed hydrogen pathway model.

Bibliography

[1] Intergovernmental Panel on Climate Change. *Climate Change 2014: Mitigation of Climate Change. Contribution of Working Group III to the Fifth Assessment Report of the Intergovernmental Panel on Climate Change*. Cambridge University Press, Cambridge, United Kingdom and New York, NY, USA, 2015.

[2] T.A. Boden, G. Marland, and R.J. Andres. Global, Regional, and National Fossil-Fuel CO2 Emissions (1751 - 2014) (V. 2017), 2017. United States.

[3] Centre for Climate and Energy Solutions. History of UN Climate Talks, n.d. https://www.c2es.org/content/history-of-un-climate-talks. Accessed: 21-06-2021.

[4] United Nations Framework Convention on Climate Change. The Paris Agreement, Paris, France, 2015. https://unfccc.int/process-and-meetings/the-paris-agreement/the-paris-agreement. Accessed: 22-06-2021.

[5] P. Friedlingstein, M.W. Jones, M. O'Sullivan, and R.M. Andrew ... S. Hauck Zaehle. Global Carbon Budget 2019. *Earth System Science Data*, 11(4):1783–1838, 2019.

[6] US Energy Information Administration. International Energy Outlook 2019, 2019. https://www.eia.gov/outlooks/ieo/pdf/ieo2019.pdf.

[7] H. Ritchie and M. Roser. Electricity mix. *Our World in Data*, 2020. https://ourworldindata.org/electricity-mix, Modified from source.

[8] The International Renewable Energy Agency. Energy Transition, 2020. https://www.irena.org/energytransition. Accessed: 30-06-2021.

[9] The International Renewable Energy Agency. *Renewable Power Generation Costs in 2020*. IRENA, Abu Dhabi, Jun. 2021.

[10] International Energy Agency. *Renewables 2021*. IEA, Paris, 2021.

[11] Energy-Charts.info and ENTSO-E. Total net electricity generation in Netherlands in July 2021, 2021. https://www.energy-charts.info. Accessed: 26-10-2021.

[12] F. Mulder and H. Geerlings. Hydrogen Technology, May. 2021. Delft University of Technology.

[13] National Grid. The hydrogen colour spectrum, n.d. https://www.nationalgrid.com/stories/energy-explained/hydrogen-colour-spectrum#:~:text=Black%20and%20brown%20hydrogen&text=Just%20to%20confuse%20things%2C%20any,%2Dto%2Dhydrogen%20project%20recently.. Accessed: 03-07-2021.

[14] International Energy Agency. *The Future of Hydrogen*. IEA, Paris, 2020. https://www.iea.org/reports/the-future-of-hydrogen.

[15] International Energy Agency. *Global average levelised cost of hydrogen production by energy source and technology, 2019 and 2050*. IEA, Paris, 2020. https://www.iea.org/data-and-statistics/charts/global-average-levelised-cost-of-hydrogen-production-by-energy-source-and-technology-2019-and-2050.

[16] L. Welder, P. Stenzel, N. Ebersbach, and P. Markewitz ... D. Stolten. Design and evaluation of hydrogen electricity reconversion pathways in national energy systems using spatially and temporally resolved energy system optimization. *International Journal of Hydrogen Energy*, 44(19):9594–9607, 2019. Special Issue on Power To Gas and Hydrogen applications to energy systems at different scales - Building, District and National level.

[17] K. Górecki, M. Górecka, and P. Górecki. Modelling Properties of an Alkaline Electrolyser. *Energies*, 13(12), 2020.

[18] J. Milewski, G. Guandalini, and S. Campanari. Modeling an alkaline electrolysis cell through reduced-order and loss-estimate approaches. *Journal of Power Sources*, 269:203–211, 2014.

[19] K. Zeng and D. Zhang. Recent progress in alkaline water electrolysis for hydrogen production and applications. *Progress in Energy and Combustion Science*, 36(3):307–326, 2010.

[20] R. García-Valverde, N. Espinosa, and A. Urbina. Simple PEM water electrolyser model and experimental validation. *International Journal of Hydrogen Energy*, 37:1927–1938, Jan. 2012.

[21] F. Marangio, M. Santarelli, and M. Calì. Theoretical model and experimental analysis of a high pressure PEM water electrolyser for hydrogen production. *International Journal of Hydrogen Energy*, 34:1143–1158, Feb. 2009.

[22] P. Choi, D.G. Bessarabov, and R. Datta. A simple model for solid polymer electrolyte (SPE) water electrolysis. *Solid State Ionics*, 175:535–539, Nov. 2004.

[23] Z. Abdin, C.J. Webb, E. Mac, and A. Gray. Modelling and simulation of a proton exchange membrane (PEM) electrolyser cell. *International Journal of Hydrogen Energy*, 40(39):13243–13257, 2015.

[24] Y. Guo, G. Li, J. Zhou, and Y. Liu. Comparison between hydrogen production by alkaline water electrolysis and hydrogen production by pem electrolysis. In *IOP Conference Series: Earth and Environmental Science*, volume 371. Institute of Physics Publishing, Dec. 2019.

[25] B. Guenot, M. Cretin, and C. Lamy. Clean hydrogen generation from the electrocatalytic oxidation of methanol inside a proton exchange membrane electrolysis cell (PEMEC): Effect of methanol concentration and working temperature. *Journal of Applied Electrochemistry*, 45:1–9, 06 2015.

[26] J. Stempien, Q. Sun, and S.H. Chan. Solid Oxide Electrolyzer Cell Modeling: A Review. *Journal of Power Technologies*, 93:216, Mar. 2013.

[27] J.P. Stempien, O. Lian Ding, Q. Sun, and S. Hwa Chan. Energy and exergy analysis of Solid Oxide Electrolyser Cell (SOEC) working as a CO2 mitigation device. *International Journal of Hydrogen Energy*, 37(19):14518–14527, 2012. HYFUSEN.

[28] P. Gabrielli, A. Poluzzi, G.J. Kramer, and C. Spiers ... M. Gazzani. Seasonal energy storage for zero-emissions multi-energy systems via underground hydrogen storage. *Renewable and Sustainable Energy Reviews*, 121:109629, Apr 2020.

[29] I. Petkov and P. Gabrielli. Power-to-hydrogen as seasonal energy storage: an uncertainty analysis for optimal design of low-carbon multi-energy systems. *Applied Energy*, 274:115197, 2020.

[30] L. Weimann, P. Gabrielli, A. Boldrini, G.J. Kramer, and M. Gazzani. Optimal hydrogen production in a wind-dominated zero-emission energy system. *Advances in Applied Energy*, 3:100032, May. 2021.

[31] M. Wirtz, M. Hahn, T. Schreiber, and D. Müller. Design optimization of multi-energy systems using mixed-integer linear programming: Which model complexity and level of detail is sufficient? *Energy Conversion and Management*, 240:114249, Jul. 2021.

[32] Royal Society of Chemistry. Periodic Table, Hydrogen, n.a. https://www.rsc.org/periodic-table/element/1/hydrogen, Accessed: 07-09-2021.

[33] U.S. Department of Energy. Safety, Codes, and Standards. Technical report, Fuel cell Technologies Program, 2011. https://cameochemicals.noaa.gov/report?key=CH8729, Accessed: 06-06-2021.

[34] F. Mulder. Hydrogen use aspects, Aug. 2021. Delft University of Technology.

[35] A. Godula-Jopek (ed.). *Hydrogen Production by Electrolysis*. Wiley-VCH Verlag GmbH & Co., KGaA, Boschstr. 12, 69469 Weinheim, Germany, 2015.

[36] International Energy Agency. *Current policy support for hydrogen deployment*. IEA, Paris, 2018. https://www.iea.org/data-and-statistics/charts/current-policy-support-for-hydrogen-deployment-2018.

[37] McKinsey & Company. *Hydrogen Insights, A perspective on hydrogen investment, market development and cost competitiveness*. Hydrogen Council, 2021. https://hydrogencouncil.com/en/hydrogen-insights-2021/.

[38] M. Conte. Hydrogen economy. *Encyclopedia of Electrochemical Power Sources*, pages 232–254, 2009.

[39] International Energy Agency. *Global hydrogen demand by sector in the Net Zero Scenario, 2020-2030*. IEA, Paris, 2021. Edited by Yavuz Cinek from https://www.iea.org/data-and-statistics/charts/global-hydrogen-demand-by-sector-in-the-net-zero-scenario-2020-2030.

[40] International Electrotechnical Storage. Electrical Energy Storage. Technical report, IEC, White Paper, 2011.

[41] L. Wei, L. Jiheng, G. Junhong, B. Zhe, F. Lingbo, and H. Baodeng. The Effect of Precipitation on Hydropower Generation Capacity: A Perspective of Climate Change. *Frontiers in Earth Science*, 8, 2020.

[42] J.M. Eyer and J.J. Iannucci and G.P. Corey. A Study for the DOE Energy Storage Systems Program. Technical report, Sandia National Laboratories, Albuquerque, New Mexico, 87185 and Livermore, California 94550, Dec. 2004.

[43] F. Crotogino, S. Donadei, U Bünger, and H. Landinger. Large-Scale Hydrogen Underground Storage for Securing Future Energy Supplies. In D. Stolten and T. Grube (eds.), editors, *Parallel Sessions Book 4 Storage Systems / Policy Perspectives, Initiatives and Co-operations*, volume 78 of *4*, pages 37–45. Institute of Energy Research - Fuel Cells (IEF-3), Forschungszentrum Jülich GmbH, Jan. 2010.

[44] Air Liquide, CEMTEC, Neas Energy, EMD, Aalborg University. Power2Hydrogen - WP1 report - Potential of hydrogen in energy systems. Technical report, HyBalance - Fuel Cells and Hydrogen 2 Joint Undertaking, 2016.

[45] Y. Zhang, A. Lundblad, P.E. Campana, and J. Yan. Comparative Study of Battery Storage and Hydrogen Storage to Increase Photovoltaic Self-sufficiency in a Residential Building of Sweden. *Energy Procedia*, 103:268–273, Dec. 2016.

[46] M.A. Pellow, C.J.M. Emmott, C.J. Barnhart, and S.M. Benson. Hydrogen or batteries for grid storage? A net energy analysis. *Energy and Environmental Science*, 8:1938–1952, Jul. 2015.

[47] P.D. Cavaliere, A. Perrone, and A. Silvello. Water electrolysis for the production of hydrogen to be employed in the ironmaking and steelmaking industry. *Metals*, 11, Nov. 2021.

[48] H. Thomas and F. Armstrong and N. Brandon and B. David ... B. Koppelman. Options for producing low-carbon hydrogen at scale. Technical report, The Royal Society, 2017.

[49] R. De Levie. The electrolysis of water. *Journal of Electroanalytical Chemistry*, 476:92–93, Oct. 1999.

[50] M. Lehner, R. Tichler, H. Steinmüller, and M. Koppe. *Power-to-Gas: Technology and Business Models*. SpringerBriefs in Energy, 2014.

[51] M. Schalenbach, A.R. Zeradjanin, O. Kasian, S. Cherevko, and K.J.J. Mayrhofer. A perspective on low-temperature water electrolysis - Challenges in alkaline and acidic technology, 2018.

[52] U.K. Chakraborty. Reversible and Irreversible Potentials and an Inaccuracy in Popular Models in the Fuel Cell Literature. *Energies*, 11(7), 2018.

[53] K.W. Harrison, R. Remick, G.D. Martin, and A. Hoskin. Hydrogen Production: Fundamentals and Case Study Summaries. Technical report, National Renewable Energy Laboratory, May. 2010. https://www.nrel.gov/docs/fy10osti/47302.pdf.

[54] C. Lamy and P. Millet. A critical review on the definitions used to calculate the energy efficiency coefficients of water electrolysis cells working under near ambient temperature conditions. *Journal of Power Sources*, 447:227350, 2020.

[55] F. Mulder and H. Geerlings. Electrolysis for Hydrogen Production 1, May. 2021. Delft University of Technology.

[56] A. Buttler and H. Spliethoff. Current status of water electrolysis for energy storage, grid balancing and sector coupling via power-to-gas and power-to-liquids: A review. *Renewable and Sustainable Energy Reviews*, 82:2440–2454, 2018.

[57] X. Li. *Principles of Fuel Cells*. CRC Press, first edition, 2005.

[58] A.J. Bard and L.R. Faulkner. *Electrochemical Methods: Fundamentals and Applications*. John Wiley & Sons, Inc, Hoboken, NJ, second edition, 2001.

[59] M. Carmo and D. Stolten. Energy Storage Using Hydrogen Produced From Excess Renewable Electricity: Power to Hydrogen. *Science and Engineering of Hydrogen-Based Energy Technologies: Hydrogen Production and Practical Applications in Energy Generation*, pages 165–199, Jan. 2019.

[60] S. Krishnan, M. Fairlie, P. Andres, T. de Groot, and G.J. Kramer. Power to gas (h2): alkaline electrolysis. *Technological Learning in the Transition to a Low-Carbon Energy System: Conceptual Issues, Empirical Findings, and Use, in Energy Modeling*, pages 165–187, Jan. 2020.

[61] M. Holst, S. Aschbrenner, T. Smolinka, C. Voglstätter, and G. Grimm. COST FORECAST FOR LOW TEMPERATURE ELECTROLYSIS-TECHNOLOGY DRIVEN BOTTOM-UP PROGNOSIS FOR PEM AND ALKALINE WATER ELECTROLYSIS SYSTEMS. Technical report, Fraunhofer Institute for Solar Energy Systems ISE, Heidenhofstraße 2, 79110 Freiburg, Germany, Oct. 2021.

[62] A.M. Bazzanella and F. Ausfelder. Low carbon energy and feedstock for the European chemical industry. Technical report, DECHEMA, Theodor-Heuss-Allee 25, 60486 Frankfurt am Main, Jun. 2017.

[63] M. Little, M. Thomson, and D. Infield. Electrical integration of renewable energy into standalone power supplies incorporating hydrogen storage. *International Journal of Hydrogen Energy*, 32(10):1582–1588, 2007.

[64] C.A Schug. Operational characteristics of high-pressure, high-efficiency water-hydrogen-electrolysis. *International Journal of Hydrogen Energy*, 23(12):1113–1120, 1998.

[65] T. de Groot, A. Zarghami, R. Lira Barros, B. Vreman, and N. Deen. Alkaliflex: vergroting van de flexibiliteit en productiecapaciteit van alkalische waterelektrolyse, Apr. 2021. https://www.rvo.nl/sites/default/files/2021/04/Powerpoint-6-april-Waterstof-elektrolyse-ter-publicatie.pdf. Accessed: 02-08-2021.

[66] L. Bertuccioli, A. Chan, D. Hart, F. Lehner, B. Madden, and E. Standen. Study on Development of Water Electrolysis in the European Union, Feb. 2014. Fuel Cells and Hydrogen Joint Undertaking.

[67] O. Schmidt, A. Gambhir, I. Staffell, A. Hawkes, J. Nelson, and S. Few. Future cost and performance of water electrolysis: An expert elicitation study. *International Journal of Hydrogen Energy*, 42(52):30470–30492, 2017.

[68] The International Renewable Energy Agency. *Green Hydrogen Cost Reduction: Scaling up Electrolysers to Meet the 1.5° Climate Goal*. IRENA, Abu Dhabi, 2020.

[69] M. Marsidi. LARGE-SCALE ALKALINE-ELECTROLYSIS HYDROGEN INSTALLATION, Technology Factsheet. Technical report, Nederlandse Organisatie voor Toegepast Natuurwetenschappelijk Onderzoek - TNO & Energieonderzoek Centrum Nederland - ECN, Dec. 2018. https://energy.nl/wp-content/uploads/final-factsheet-large-scale-h2-alkalische-elektrolyse-7.pdf.

[70] M. Carmo, D.L. Fritz, J. Mergel, and D. Stolten. A comprehensive review on PEM water electrolysis. *International Journal of Hydrogen Energy*, 38(12):4901–4934, 2013.

[71] Battery University. BU-210: How does the Fuel Cell Work?, Oct. 2021. https://batteryuniversity.com/article/bu-210-how-does-the-fuel-cell-work. Accessed: 10-09-2021.

[72] S. Adelung, E. Kurkela, F. Habemeyer, and M. Kurkela. Review of electrolysis technologies and their integration alternatives. Technical Report 3, VTT Technical Research Centre of Finland Ltd, 2018. Project for the EU FCHJU - FLEXCHX.

[73] DNV. Energy Transition Outlook 2021 - Technology Progress Report. Technical report, DNV, NO-1322 Høvik, Norway, 2021. https://eto.dnv.com/technology-progress-report-2021#TPR2021-top.

[74] M. Marsidi. POLYMER ELECTROLYTE MEMBRANE (PEM) HYDROGEN INSTALLATION - LARGE-SCALE, Technology Factsheet. Technical report, Nederlandse Organisatie voor Toegepast Natuurwetenschappelijk Onderzoek - TNO, Jun. 2019. https://energy.nl/wp-content/uploads/polymer-electrolyte-membrane-pem-hydrogen-installation-large-scale-7.pdf.

[75] F.M. Sapountzi, J.M. Gracia, C.J. Weststrate, H.O.A. Fredriksson, and J.W. Niemantsverdriet. Electrocatalysts for the generation of hydrogen, oxygen and synthesis gas. *Progress in Energy and Combustion Science*, 58:1–35, Jan. 2017.

[76] S. Shiva Kumar and V. Himabindu. Hydrogen production by PEM water electrolysis – A review. *Materials Science for Energy Technologies*, 2(3):442–454, 2019.

[77] B. Koirala. SOLID-OXIDE ELECTROLYSIS, Technology Factsheet. Technical report, Nederlandse Organisatie voor Toegepast Natuurwetenschappelijk Onderzoek - TNO, Nov. 2020. https://energy.nl/media/data/Technology-Factsheets_SOElectrolysis.pdf.

[78] R. von Helmolt and U. Eberle. Fuel cell vehicles: Status 2007. *Journal of Power Sources*, 165:833, Mar. 2007.

[79] J. Andersson and S. Grönkvist. Large-scale storage of hydrogen. *International Journal of Hydrogen Energy*, 44(23):11901–11919, 2019.

[80] U.S. Department of Energy. Hydrogen storage, n.d. https://www.energy.gov/eere/fuelcells/hydrogen-storage, Accessed: 09-10-2021.

[81] S.S. Makridis. *Chapter 1 – Hydrogen storage and compression*, pages 1–28. IET Digital Library, first edition, Jun. 2016. In book: Methane and Hydrogen for Energy Storage.

[82] S. Papavinasam. Chapter 5 – Mechanisms. *Corrosion Control in the Oil and Gas Industry*, pages 249–300, Jan. 2014.

[83] G. Janssen. COMPRESSED HYDROGEN STORAGE, Technology Factsheet. Technical report, Nederlandse Organisatie voor Toegepast Natuurwetenschappelijk Onderzoek - TNO, Oct. 2020. https://energy.nl/wp-content/uploads/compressed_hydrogen_storage-1-9.pdf.

[84] M. Li, Y. Bai, C. Zhang, and Y. Song ... D. Grouset. Review on the research of hydrogen storage system fast refueling in fuel cell vehicle. *International Journal of Hydrogen Energy*, 44, Mar. 2019.

[85] B. Sakintuna, F. Lamari-Darkrim, and M. Hirscher. Metal hydride materials for solid hydrogen storage: A review. *International Journal of Hydrogen Energy*, 32:1121–1140, Jun. 2007.

[86] DEMACO. What to do with hydrogen boil-off gas?, n.d. https://demaco-cryogenics.com/blog/what-to-do-with-hydrogen-boil-off-gas/. Accessed: 27-12-2021.

[87] Gasunie. Hydrogen Network Netherlands. Technical report, n.d. https://www.gasunie.nl/en/projects/hydrogen-network-netherlands, Accessed: 15-11-2021.

[88] F. Mulder and H. Geerlings. Hydrogen use aspects, May. 2021. Delft University of Technology.

[89] A. van den Noort and W. Sloterdijk and M. Vos and J. Lieffering and J. Knijp. Verkenning waterstofinfrastructuur - Ministerie van Economische Zaken. Technical report, P.O. Box 2029, 9704 CA Groningen, Nov. 2017. https://eto.dnv.com/technology-progress-report-2021#TPR2021-top.

[90] J.L. Gillette and R.L. Kolpa. Overview of interstate hydrogen pipeline systems. Technical report, Argonne National Labratory, United States, California, 9700 South Cass Avenue, Argonne, Illinois 6043, Feb. 2008. https://publications.anl.gov/anlpubs/2008/02/61012.pdf.

[91] J. Larminie and A. Dicks. *Fuel Cell Systems Explained*. John Wiley & Sons Ltd, The Atrium, Southern Gate, Chichester, West Sussex PO19 8SQ, England, second edition, 2003.

[92] U.S. Department of Energy. Fuel Cells, n.d. https://www.energy.gov/eere/fuelcells/fuel-cells, Accessed: 29-10-2021.

[93] F. Mulder and H. Geerlings. Fuel Cell Introduction, May. 2021. Delft University of Technology.

[94] Ø. Ulleberg. Modeling of advanced alkaline electrolyzers: a system simulation approach. *International Journal of Hydrogen Energy*, 28(1):21–33, 2003.

[95] S.A. Grigoriev, V.I. Porembskiy, S.V. Korobtsev, V.N. Fateev, F. Auprêtre, and P. Millet. High-pressure PEM water electrolysis and corresponding safety issues. *International Journal of Hydrogen Energy*, 36(3):2721–2728, 2011. The Third Annual International Conference on Hydrogen Safety.

[96] U. Babic, M. Suermann, F. Büchi, L. Gubler, and T. Schmidt. Critical Review — Identifying Critical Gaps for Polymer Electrolyte Water Electrolysis Development. *Journal of The Electrochemical Society*, 164:F387–F399, Jan. 2017.

[97] T. Smolinka, M. Günther, and J. Garche. Stand und Entwicklungspotenzial der Wasserelektrolyse zur Herstellung von Wasserstoff aus regenerativen Energien. Technical report, Fraunhofer Institute for Solar Energy Systems ISE & FCBAT, 2011. https://www.now-gmbh.de/wp-content/uploads/2020/09/now-studie-wasserelektrolyse-2011.pdf.

[98] J.O. Jensen, V. Bandur, N. Bjerrum, and S. Jensen ... M. Mogensen. Pre-investigation of water electrolysis. Technical report, PSO-F&U, Jan. 2012. https://www.yumpu.com/en/document/read/4104988/pre-investigation-of-water-electrolysers, Accessed: 01-02-2022.

[99] J. Eichman, K. Harrison, and M. Peters. Novel Electrolyzer Applications: Providing More Than Just Hydrogen. Technical report, National Renewable Energy Lab. (NREL), 15013 Denver West Parkway, Golden CO 80401, United States, Sep. 2014. https://www.nrel.gov/docs/fy14osti/61758.pdf.

[100] T. Ramsden, D. Steward, and J. Zuboy. Analyzing the levelized cost of centralized and distributed hydrogen production using the H2A production model, version 2. Technical report, National Renewable Energy Lab. (NREL), 15013 Denver West Parkway, Golden CO 80401, United States, Sep. 2009. https://www.nrel.gov/docs/fy09osti/46267.pdf.

[101] T. Ramsden and M. Ruth. Current (2005) hydrogen production from central grid electrolysis. Technical report, National Renewable Energy Lab. (NREL), 15013 Denver West Parkway, Golden CO 80401, United States, 2008.

[102] P. Gabrielli, M. Gazzani, E. Martelli, and M. Mazzotti. Optimal design of multi-energy systems with seasonal storage. *Applied Energy*, 219:408–424, Jun. 2018.

[103] Wikimedia Foundation. AIMMS, n.d. https://en.wikipedia.org/wiki/AIMMS. Accessed: 17-12-2021.

[104] MathWorks. MATLAB, n.d. https://nl.mathworks.com/products/matlab.html. Accessed: 10-08-2022.

[105] M. Scheepers, S. Gamboa Palacios, E. Jegu, and L. Pupo ... K. West. Towards a sustainable energy system for the Netherlands in 2050 Sponsor Ministry of Economic Affairs and Climate Policy Project name Sustainable Energy Scenario for the Netherlands, May. 2020.

[106] R. Segers, K. Keller, and K. Geertjes. Disaggregation of the Statistics on final energy consumption in the industry sector in the Netherlands, 2017. Centraal Bureau voor de Statistiek - CBS.

[107] A. Feta, M. Van Den Broek, W. Crijns-Graus, and G. Jägers. Technical demand response potentials of the integrated steelmaking site of Tata Steel in IJmuiden, 2018.

[108] V. Cigolotti, M. Genovese, and P. Fragiacomo. Comprehensive review on fuel cell technology for stationary applications as sustainable and efficient poly-generation energy systems, Aug. 2021.

[109] K. Mongird, V. Viswanathan, J. Alam, and Ch. Vartanian ... Richard Baxter. 2020 Grid Energy Storage Technology Cost and Performance Assessment, Dec. 2020.

[110] J.R. Meacham, F. Jabbari, J. Brouwer, J.L. Mauzey, and G.S. Samuelsen. Analysis of stationary fuel cell dynamic ramping capabilities and ultra capacitor energy storage using high resolution demand data. *Journal of Power Sources*, 156(2):472–479, 2006.

[111] Y. Luo, Y. Shi, and N. Cai. Chapter 3 - bridging a bi-directional connection between electricity and fuels in hybrid multienergy systems. In Yu Luo and Yixiang Shi and Ningsheng Cai, editor, *Hybrid Systems and Multi-energy Networks for the Future Energy Internet*, pages 41–84. Academic Press, 2021.

[112] ENTSO-E. Transmission - Day-ahead Prices - Dashboard, 2020. https://transparency.entsoe.eu/dashboard/show. Accessed: 26-03-2022.

[113] M. Weeda and R. Segers. The Dutch hydrogen balance, and the current and future representation of hydrogen in the energy statistics, Jun. 2020. Centraal Bureau voor de Statistiek - CBS & Nederlandse Organisatie voor Toegepast Natuurwetenschappelijk Onderzoek - TNO.

[114] G. Morales-España, J.M. Latorre, and A. Ramos. Tight and Compact MILP Formulation for the Thermal Unit Commitment Problem. *IEEE Transactions on Power Systems*, 28:4897–4908, 2013.

[115] D. Gusain, M. Cvetković, R. Bentvelsen, and P. Palensky. Technical Assessment of Large Scale PEM Electrolyzers as Flexibility Service Providers. pages 1074–1078. 2020 IEEE 29th International Symposium on Industrial Electronics (ISIE): Proceedings, Jun. 2020.

[116] Z. Lukszo and S. Pfenninger. Energy System Optimisation - Lecture 'Economic Dispatch and Linear Programming', Sep. 2021. Delft University of Technology.

[117] Z. Lukszo and S. Pfenninger. Energy System Optimisation - Lecture 'Non-Linear Programming with constraints & unit commitment', Sep. 2021. Delft University of Technology.

[118] Z. Lukszo and S. Pfenninger. Energy System Optimisation - Lecture 'Market Clearing & Demand Response', Oct. 2021. Delft University of Technology.

[119] J. Jens. *Assessing the potential of Green Hydrogen using learning curves from expert elicitation and the implications for the Port of Rotterdam*. PhD thesis, Erasmus School of Economics, Nov. 2020. https://www.google.com/url?sa=t&rct=j&q=&esrc=s&source=web&cd=&ved=2ahUKEwjKhMDNmNr5AhVGOewKHYUkB0MQFnoECAgQAQ&url=https%3A%2F%2Fthesis.eur.nl%2Fpub%2F55598%2FFinal-version_v2_JaroJens.pdf&usg=AOvVaw3IrAWHm47ID4oUXrADR_oJ.

[120] T. Paraskova. Europe's Gas Price Is Now Equivalent To $410 Per Barrel Of Oil, Aug. 2022. https://oilprice.com/Energy/Natural-Gas/Europes-Gas-Price-Is-Now-Equivalent-To-410-Per-Barrel-Of-Oil.html Accessed: 21-08-2022.

[121] E.R. Morgan, J.F. Manwell, and J.G. McGowan. Opportunities for economies of scale with alkaline electrolyzers. *International Journal of Hydrogen Energy*, 38:15903–15909, Dec. 2013.

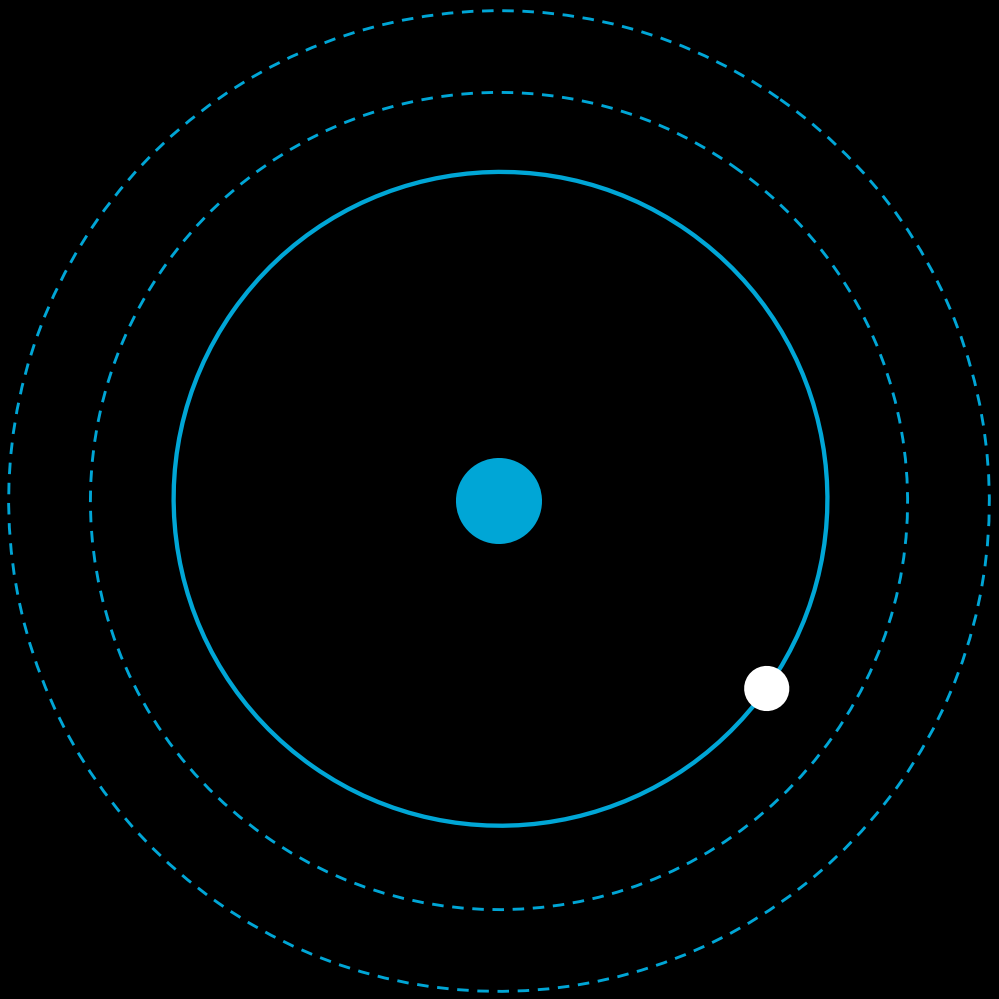

TU Delft